Exploring Different Approaches to Improve the Analytical Performance of Inductively Coupled Plasma Optical Emission Spectrometry with Pneumatic Nebulization or Electrothermal Vaporization

by

Ahmed Al Hejami

A thesis submitted to the Department of Chemistry

In conformity with the requirements for

the degree of Doctor of Philosophy

Queen's University

Kingston, Ontario, Canada

January, 2019

Abstract

This thesis is aimed at exploring new diverse approaches for improving the analytical performance of inductively coupled plasma (ICP) optical emission spectrometry (OES) with pneumatic nebulization (PN) or electrothermal vaporization (ETV).

First, a new infrared (IR)-heated PN system was developed to enhance sample transport efficiency and concurrently improve sensitivity, detection limit and plasma robustness of ICPOES. A cyclonic spray chamber was modified so as to insert an IR lamp heater inside it. The modified cyclonic (MC) spray chamber was heated up to 150 °C. Using a pre-evaporation tube (PET) between the MC spray chamber and the plasma torch was also investigated. Under optimum operating conditions, a 2-5 fold improvement in sensitivity and 2-7 fold improvement in detection limit were achieved for 26 elements compared to conventional PN at room temperature.

Second, the analytical performance of ICPOES was improved by IR heating of commercially available spray chambers using different types of IR heaters, namely ceramic block and ceramic beaded IR heaters. For 29 elements, the detection limit improved by, on average, 2-3 fold with the rope heater and 5-10 fold with the block heater. All IR-heated systems enabled the accurate analysis of a certified reference material (CRM) of waste water.

Third, the effect of IR heating of the top surface of a cyclonic spray chamber on the analytical performance of ICPOES was investigated. Upon IR heating (up to 150 °C), sensitivity and detection limit improved by 3-5 fold and 4-12 fold, respectively compared to those with the same system at room temperature. The IR-heated system allowed the accurate multi-elemental analysis of two CRMs.

Finally, addition of H_2, N_2 or water vapour to the central gas flow of the plasma was assessed to enhance the analytical performance of solid sampling (SS) ETV-ICPOES. Sensitivity and

detection limit were significantly improved upon sheathing the sample aerosol with H_2, N_2 or water vapour for 11 elements compared to those with conventional SS-ETV-ICPOES. To the best of the author's knowledge, this is the first published study of the effect of adding N_2 to the central gas flow of the plasma on the analytical performance of SS-ETV-ICPOES.

Co-Authorship

All the work done in this thesis was accomplished by the author under the supervision of Prof. Diane Beauchemin in the Department of Chemistry at Queen's University, Kingston, Ontario, Canada. Portions of this thesis are published in a peer-reviewed scientific journal. In all cases, data were acquired and processed by A. Al Hejami. The results were interpreted and discussed by A. Al Hejami with input from Prof. D. Beauchemin.

1. A. Al Hejami and D. Beauchemin, "New infrared-heated sample introduction system for enhanced analytical performance of inductively coupled plasma optical emission spectrometry", *J. Anal. At. Spectrom.*, 33, **2018**, 738-744.

This paper is reproduced in Chapter 2.

2. A. Al Hejami and D. Beauchemin, "Infrared heating of commercially available spray chambers to improve analytical performance of inductively coupled plasma optical emission spectrometry", *J. Anal. At. Spectrom.*, 33, **2018**, 2008-2014.

This paper is reproduced in Chapter 3.

3. A. Al Hejami and D. Beauchemin, "Infrared heating of the top surface of a cyclonic spray chamber to improve analytical performance of inductively coupled plasma optical emission spectrometry", *J. Anal. At. Spectrom.*, 34, **2019**, 232-238.

This paper is reproduced in Chapter 4.

4. A. Al Hejami and D. Beauchemin, "Effect of sheathing the sample aerosol with hydrogen, nitrogen or water vapour on the analytical performance of solid sampling electrothermal vaporisation coupled to inductively coupled plasma optical emission spectrometry", *J. Anal. At. Spectrom.*, **2019**, DOI: 10.1039/c8ja00266e.

This paper is reproduced in Chapter 5.

Acknowledgements

I would like to thank, first and foremost, my supervisor, Dr. Diane Beauchemin for her guidance, encouragement and support during my research. I gratefully appreciate her open door policy that smoothened my studies. I would also like to thank my supervisory committee, Dr. Stephen Brown and Dr. Gregory Jerkiewicz, for their valuable feedback.

I am grateful to the Beauchemin lab members, past and present, for their friendship and help. I would like to acknowledge with gratitude the financial assistance from the Natural Sciences and Engineering Research Council of Canada and Queen's University School of Graduate Studies and Research as well as the Department of Chemistry at Queen's University.

Finally, special thanks go to my family, my wife Halla, my daughter Sura and my son Hussain for their constant love, care, support and patience throughout my studies.

Table of Content

List of Figures

List of Tables

List of Abbreviations

BC	Baffled cyclonic spray chamber
CRM	Certified reference material
CVG	Chemical vapour generation
DDW	Doubly deionized water
DL	Detection limit
DP	Double-pass spray chamber
ETV	Electrothermal vaporization
FC	Flip single-pass spray chamber
FI	Flow injection
ICPOES	Inductively coupled plasma optical emission spectrometry
ICPMS	Inductively coupled plasma mass spectrometry
ID	Internal diameter
IR	Infrared
IRZ	Initial radiation zone
LA	Laser ablation
MC	Modified cyclonic spray chamber
MSIS	Multimode sample introduction system
NAZ	Normal analytical zone
PET	Pre-evaporation tube
PHZ	Preheating zone
PN	Pneumatic nebulization

PN-PTSC	Pneumatic nebulization in a programmable temperature spray chamber
RF	Radio frequency
RSD	Relative standard deviation
RT	Room temperature
SRM	Standard reference material
SS	Solid sampling
TISIS	Torch integrated sample introduction system
USN	Ultrasonic nebulizer

Chapter 1

General Introduction

1.1 Introduction

Inductively coupled plasma (ICP) optical emission spectrometry (OES) and mass spectrometry (MS) are powerful multi-elemental analysis techniques because pretty much every sample is atomized and most elements in the periodic table can be ionized in an ICP source. ICPOES is usually preferred for major (1-100%, m/v), minor (0.01-1%, m/v) and trace (1 µg L^{-1} to 100 mg L^{-1}) elemental analysis whereas ICPMS is typically used for ultra-trace (< 1 µg L^{-1}) analysis of different types of samples such as environmental, geological and biological samples. ICPOES is vastly used in routine trace multi-elemental analysis because of its robustness and low maintenance cost compared with ICPMS [1-3]. The most attractive features of ICPOES are its ability to perform multi-elemental analysis, wide linear dynamic ranges of up to six orders of magnitude, low detection limits, high sample throughput, simplicity and less matrix interferences compared to other techniques, such as flame-based ones [4-7].

1.2 Inductively coupled plasma

The ICP is an effective atomization/excitation source for OES. A standard Fassel-type ICP torch is usually used for plasma generation. The torch consists of three concentric quartz tubes, namely outer, intermediate and inner tubes. Argon (Ar) gas usually flows through these tubes because, of all the noble gases, it offers the best compromise in terms of ionization efficiency and cost. The outer (coolant or plasma) gas flow (10-20 L min^{-1}) is utilized to sustain the plasma and to protect the torch from melting by the very hot

plasma. The intermediate (auxiliary) gas flow (0-2 L min^{-1}) assists in the formation of the plasma and positions the plasma above the tip of the inner tube (the injector) to prevent it from melting. Furthermore, the auxiliary gas is helpful in avoiding accumulation of salt or carbon on the tip of the injector. The inner (nebulizer) gas flow (0.5-1 L/min), also called the aerosol carrier gas, is used to inject the sample aerosol into the plasma [8, 9].

Surrounding the top end of the ICP torch is a two- or three-turn water- or gas-cooled copper coil (load or induction coil), which is connected to a radio frequency (RF) power (1-1.7 kW) generator. Upon application of RF power to the load coil, an alternating current is generated, which oscillates at a rate corresponding to the frequency (typically 27 or 40 MHz) of the RF power, resulting in electromagnetic fields at the top of the torch. To initiate the plasma, a Tesla spark is applied to produce electrons from argon atoms inside the torch. These electrons are accelerated by the electromagnetic RF field causing collisions between these high-energy electrons and other argon atoms. As a result, more argon atoms are ionized and this chain reaction continues until a plasma is formed, which consists of argon atoms, electrons and ions. Once the plasma is formed, it is self-sustaining as long as RF power is applied to the load coil [6, 8, 9].

The high-temperature (7000-10000 K) plasma has sufficient energy to efficiently and reproducibly vaporize, atomize, excite and ionize a wide range of elements in different sample matrices. When the excited atoms or ions relax, they emit electromagnetic radiation at wavelengths characteristic of each element in the sample. The emission lines can be separated by a spectrometer and measured by detectors. The intensity of atomic or ionic emission lines are directly proportional to the concentration of the elements present in the samples [10].

The light emitted by the plasma can be viewed laterally or axially (Figure 1.1). Lateral or radial (side-on) viewing provides the highest upper linear analytical working range. On the other hand, axial (end-on) viewing offers better detection limits than lateral viewing because the sample path for axial viewing is longer than for lateral viewing [11-13]. Combining both lateral and axial viewing (dual view) is commercially available, allowing the plasma to be viewed in both configurations in a single analysis [14].

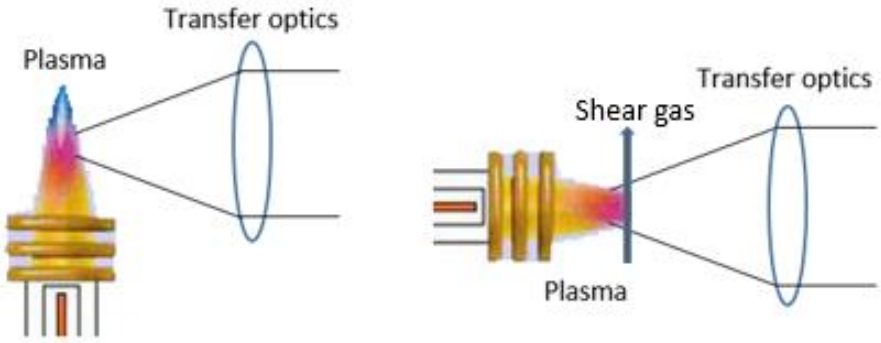

Figure 1.1 Schematic diagram of the two viewing modes for the ICP. Lateral (side-on) viewing (left) and axial (end-on) viewing (right); modified from [15].

Figure 1.2 depicts the temperature profile of the plasma, which consists of different zones or regions namely induction region, preheating zone (PHZ), initial radiation zone (IRZ) and normal analytical zone (NAZ). The transfer of inductive energy from the load coil to the plasma occurs in the induction region, which has the highest temperature, up to 10000 K. Desolvation, vaporization and atomization of the sample take place predominantly in the PHZ, while excitation and ionization of the analyte occur predominantly in the IRZ and the NAZ. Because it is often most sensitive, analyte emission is usually measured from the NAZ. The region located at the top of the plasma is called the tail plume [15].

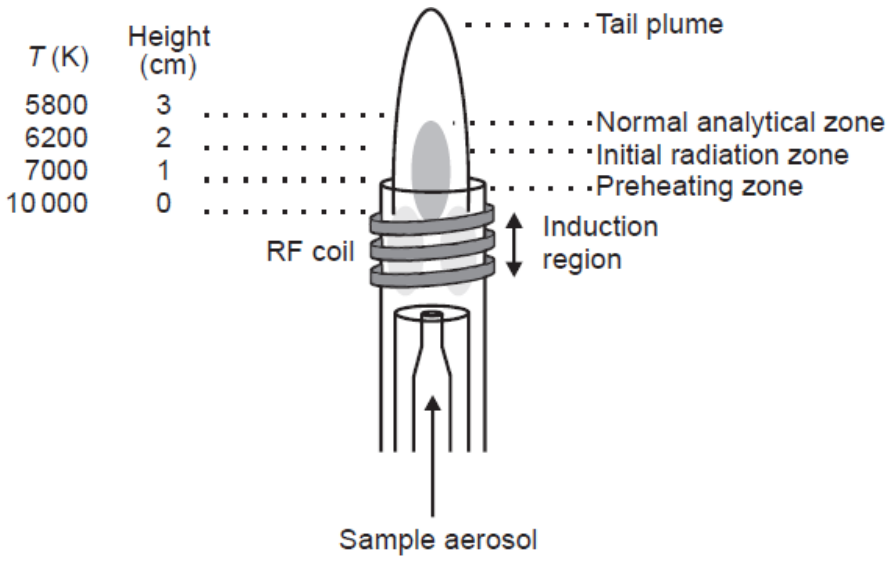

Figure 1.2 Schematic diagram of the ICP, describing the different zones of the plasma, with their temperature profile at varying heights above the RF coil [10].

Different mechanisms have been proposed to explain how the ionization processes occur [3]. The first mechanism is electron-impact ionization, where analyte (X) ionization occurs upon its collision with free electrons (Equation 1.1) if the kinetic energy of the free electrons is greater than the ionization energy of the analyte.

$$X + e^- \rightarrow X^+ + 2e^- \qquad \ldots\ldots\ldots\ldots\ldots\ldots\ldots\ldots \quad (1.1)$$

The second possible mechanism involves charge transfer reactions between argon ions and the analyte (Equation 1.2).

$$Ar^+ + X \rightarrow Ar + X^+ \qquad \ldots\ldots\ldots\ldots\ldots\ldots\ldots\ldots \quad (1.2)$$

The other possible mechanism is Penning ionization in which ionization of the analyte occurs through collision of metastable argon atoms (Ar^m) with the analyte (Equation 1.3).

$$Ar^m + X \rightarrow Ar + X^+ + e^- \qquad \ldots\ldots\ldots\ldots\ldots\ldots\ldots \quad (1.3)$$

The excess energy remaining from the three aforementioned mechanisms may promote the analyte ion to an excited state, in which case emission from ionic lines characteristic of the analyte can be measured after the relaxation processes.

1.3 Sample introduction system

The purpose of a sample introduction system is to deliver the sample into the central channel of the plasma in an adequate form. The overall analytical performance depends strongly on the efficiency and reproducibility of the sample introduction system [16, 17]. All types of sample forms (gas, liquid and solid) can be introduced into the plasma provided an appropriate sample introduction system is used. However, the most popular one is a nebulization system because it is simple, reproducible and enables easy-handling of liquid solutions. Moreover, it is easy to calibrate the instrument by preparing a number of standard solutions [17]. In order to introduce a liquid sample into the plasma, the sample should be converted into an aerosol of fine droplets through the use of a nebulization process.

Pneumatic nebulization (PN) is most widely employed in ICPOES and consists of a pneumatic nebulizer and a spray chamber. The pneumatic nebulizer converts the liquid sample into an aerosol of polydispersed droplets through gas-liquid interaction using a high-speed gas flow. Common types of pneumatic nebulizers used in ICPOES include the concentric nebulizer (where the gas-liquid interaction occurs concentrically; Figure 1.3A) and the cross-flow nebulizer (where the gas-liquid interaction occurs perpendicularly; Figure 1.3B) [17].

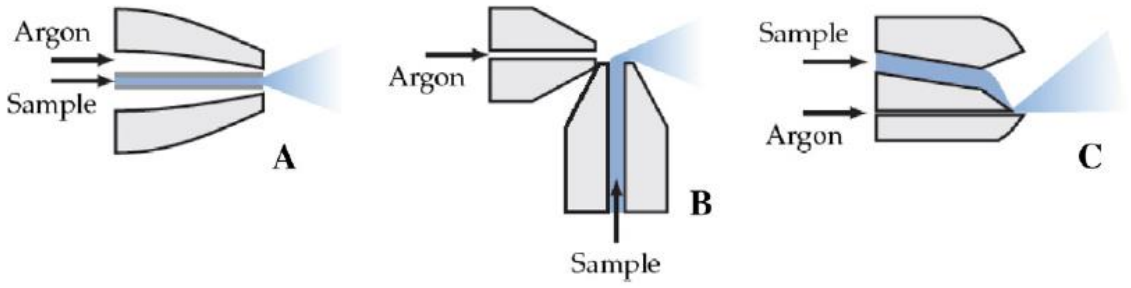

Figure 1.3: Schematic diagrams of three types of nebulizers. **A**: concentric nebulizer, **B**: cross-flow nebulizer and **C**: Burgener parallel path nebulizer [1].

The cross-flow nebulizer is designed to tolerate solutions with a high concentration of dissolved solids without inducing clogging problems. For a sample uptake rate below 100 µL/min, a microconcentric nebulizer [18, 19] can be used, but this type of nebulizer is prone to clogging, limiting its application to sample solutions with a low concentration of dissolved salts. A Burgener nebulizer (a parallel path nebulizer; Figure 1.3C) can be utilized to reduce the risk of clogging [20, 21].

A spray chamber is usually used in combination with a pneumatic nebulizer. The main purpose of the spray chamber is to filter the large droplets (coarse droplets), allowing just very fine droplets to pass into the plasma. Therefore, the spray chamber helps to avoid plasma overloading and reduces the noise associated with the nebulization process, including dampening the pulsations from the peristaltic pump. A variety of spray chambers is commercially available, but the most common ones used in ICPOES are the Scott-type double-pass spray chamber and the cyclonic spray chamber (Figure 1.4). Large droplets are filtered out to the drain by gravity and collision with the walls. The Scott-type double-pass spray chamber produces a finer tertiary aerosol than the cyclonic spray chamber. However, the cyclonic spray chamber provides a higher transport efficiency (*i.e.*, the ratio of the amount of analyte reaching the plasma to the amount of analyte delivered by the

nebulizer) and lower washout time (*i.e.*, the time required by the system to drop the analyte signal to 1% of the maximum) than the Scott-type double-pass spray chamber [22, 23].

Figure 1.4: Photographs of two commercially available spray chambers: Scott double-pass spray chamber (left) and cyclonic spray chamber (right).

The sample transport efficiency for conventional pneumatic nebulization is typically less than 5%. Hence, over 95% of the sample goes to the drain, affecting the analytical performance such as sensitivity and detection limit. For this reason, pneumatic nebulization remains the weakest part of ICPOES [1]. However, pneumatic nebulization is still the standard device for routine analysis because of its stability, simplicity and relatively low cost. Direct injection nebulization, where the torch injector is replaced by a nebulizer and no spray chamber is used, which essentially translates into 100% sample transport efficiency) has been used, but is susceptible to clogging [3].

An alternative nebulization system is the ultrasonic nebulizer (USN), which creates an aerosol of fine droplets through interaction of the sample solution with the ultrasonic waves generated by a piezoelectric transducer. The USN is usually equipped with a desolvation system (consisting of a heater and condenser) to minimize the solvent load in the plasma and even to prevent extinguishing or cooling of the plasma. The sample transport efficiency with a USN is up to 20%, and is not controlled by the nebulizer gas flow rate. The USN

can be operated at a low gas flow rate because the droplet production process is not relying on the nebulizer gas flow. Therefore, the residence time of the analyte in the plasma can be extended, resulting in enhanced analytical performance (sensitivity and detection limit). Nevertheless, a USN system has many drawbacks, including matrix effects, memory effects, long washout time and high cost. Furthermore, it is not compatible with hydrofluoric acid [10, 17].

Alternative sample introduction techniques to pneumatic nebulization are electrothermal vaporization (ETV) and laser ablation (LA). The later technique involves ablation of the sample surface using a laser, with the resulting sample plume being carried into the plasma by a carrier gas of Ar or He. Depth profile analysis of solid samples can be performed with LA in addition to bulk elemental analysis [24]. However, LA is mostly used for the analysis of solids, whereas ETV can be applied to the analysis of both liquid and solid samples. The next section will focus on the ETV technique.

1.3.1 Electrothermal vaporization

ETV offers several advantages, which make it an attractive alternative to conventional pneumatic nebulization. These advantages include high transport efficiency (up to 100%), direct analysis of very small volume or mass of sample with different matrices, ability to remove the sample matrix during the pyrolysis step and low detection limit. Direct sample analysis provides many features, such as minimal sample pre-treatment requirements, high sample throughput, low contamination risk and minimal analyte loss. As a result, ETV-ICP spectrometry is a versatile analysis tool because of its ability to analyze different sorts of samples with complex matrices, including non-aqueous solutions, solutions with high dissolved salt or acid concentration, slurries and solid samples [24, 25]. However, the

limited sample mass can have a negative impact on precision in ETV-ICP spectrometry if the sample is inherently inhomogeneous, such as soil.

Nixon *et al*. [26] were the first to use a tantalum filament vaporization device for sample introduction in ICPOES. Kikbright *et al*. [27] used a graphite furnace as a sample introduction system for ICPOES. Since then, ETV-ICPOES has been developed for the elemental analysis of a variety of samples, including biological, environmental, high-purity materials and forensic samples [28-31]. Figure 1.5 depicts a schematic diagram of the only commercially available ETV unit. The main part of this system is the ETV furnace, where the sample is resistively heated in steps to desolvate the sample, ash the matrix and vaporize the analyte. The analyte vapour is then transported into the ICP by a carrier gas.

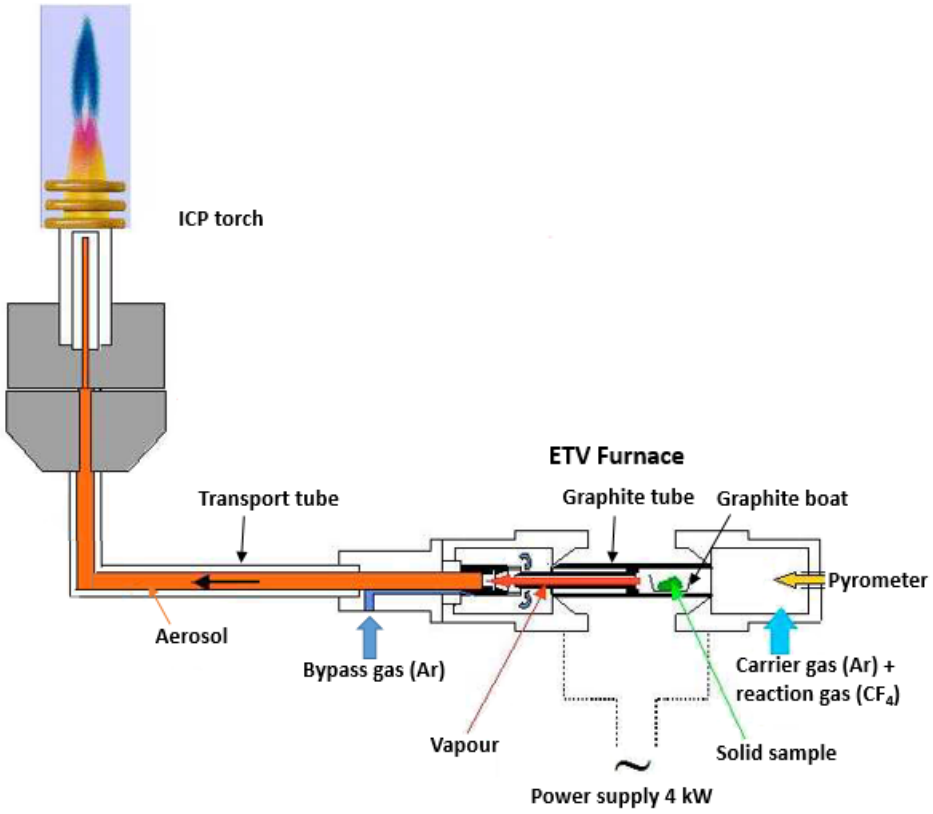

Figure 1.5: Schematic diagram of an electrothermal vaporization system (modified from [32]).

A bypass gas (Figure 1.6) plays an important role to cool down the analyte vapour, which is converted into a stable dry aerosol, thereby minimizing vapour condensation and deposition in the transfer tube, which ultimately minimizes analyte loss [33, 34]. Different modifiers (including reaction gases), such as CC_2F_2, CHF_3, CCl_4, CF_4, NF_3 and polytetrafluoroethylene, can be used to improve analyte vaporization [35-40]. The matrix effect that is associated with the high transport efficiency of ETV-ICP spectrometry can be alleviated by judicious selections of the ETV temperature program and chemical modifiers [41, 42]. Moreover, the plasma load in ETV-ICPOES can be compensated using an argon emission line (such as Ar 763.511 nm) as an internal standard [43-46].

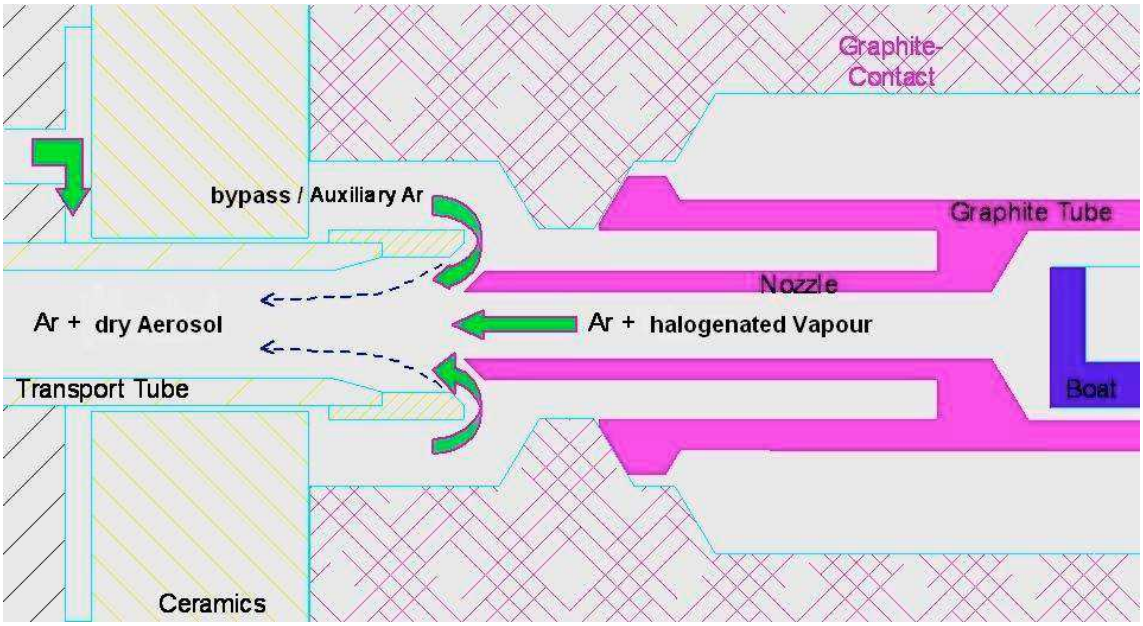

Figure 1.6: Schematic diagram of the transition zone, showing aerosol formation as a result of merging gas flows [32].

1.4 Mixed-gas plasma

A mixed-gas (Ar-N_2 or Ar-H_2) plasma can be employed to enhance robustness in ICP spectrometry. A foreign gas is added into one or more of the main Ar plasma gas flows (outer, auxiliary or carrier gas) [47, 48]. Introduction of 2% N_2 to the outer gas flow of the plasma in ETV-ICPMS alleviated matrix effects at the expense of analyte sensitivity [49]. Shrinking of plasma volume upon addition of N_2 to the outer plasma gas flow and the higher thermal conductivity of N_2 compared to that of Ar enhance sample-plasma interactions as well as increase plasma temperatures and electron densities [47, 50-54]. Mitigation of matrix effects was also achieved when a small flow rate of N_2 (20 mL min^{-1}) was added to the carrier gas in ICPOES with ultrasonic nebulization [55] and with pneumatic nebulization coupled to a desolvation system [56]. No study has yet investigated the effect of adding N_2 to the central gas flow of a dry plasma in ETV-ICP spectrometry. Nevertheless, sensitivity was improved for most of analytes when a small amount of N_2 was added to the central gas in laser ablation ICPMS [57]. Addition of a small amount of H_2 to the carrier gas in ETV-ICPOES improved sensitivity and detection limit. This was attributed to H_2 enhancing the thermal energy transfer between the plasma bulk and the central channel where the sample is introduced [58]. The analytical performance of ETV-ICPMS was also improved upon addition of a small amount of H_2 to the carrier gas [59].

1.5 Pre-evaporation of the aerosol

Pre-evaporation, which involves converting the solvent into vapor prior to introduction of the aerosol into the plasma without removing the solvent (usually water) from the system, saves energy from the plasma. It is an effective way to improve sensitivity,

detection limit and plasma robustness. The sample transport efficiency is significantly increased and analyte sensitivity is consequently enhanced. Moreover, the noise level of the background normally resulting from the signal fluctuating during the desolvation and vaporization steps in the plasma is greatly minimized because the sample aerosol is already converted into vapor [60-62]. Indeed, pre-evaporation of the sample minimizes or eliminates the desolvation and vaporisation steps in the plasma. Accordingly, the drying period of the droplets is reduced and more energy is available for the atomization, excitation and ionization processes.

The first attempt to perform pre-evaporation was by Greenfield and Smith [63] who determined trace elements in oil, organic compounds and blood. A spray chamber was heated by convective heating, providing total consumption of microliter samples. As a result, sensitivity of ICPOES was improved by up to one order of magnitude. A different approach involves the installation of a pre-evaporation tube (PET) between the spray chamber and the plasma torch, which was heated up to 400 °C with heating tape [64-67]. Sensitivity and detection limit were improved for ICPMS and this was ascribed to a reduction in the noise level from a decrease in the mean droplet size of the sample aerosol reaching the plasma. It was noticed that elements (such as V, Mo and La) forming strong oxides showed a significant improvement in sensitivity [64].

Replacing the whole desolvation system of the ultrasonic nebulizer system by a pre-evaporation tube, which was heated to 400 °C using heating tape, also improved sensitivity, detection limit and plasma robustness in ICPOES [68]. Further enhancement in the analytical performance of ICPOES using the same aforementioned setup of the USN with

the PET was obtained by applying infrared (IR) heating instead of solely convective heating (heating tape), which also reduced the washout time [69]. IR heating provides a more efficient and uniform heating than convective heating [70, 71]. A PET has also been employed in combination with a multimode sample introduction system (MSIS) to improve the analytical performance of ICPOES [72].

A significant improvement in sensitivity of ICPOES was reported when the so-called torch integrated sample introduction system (TISIS) was heated up to 100 °C [73, 74]. This was attributed to an increase in sample transport efficiency and to a reduction in droplet sizes. The excitation conditions of the plasma are also enhanced, leading to a more robust plasma. The TISIS was developed by Todoli and Mermet [75-77] to minimize the analyte washout time without sacrifice in sensitivity and detection limit. The TISIS consists of a pneumatic micro-nebulizer linked to a single-pass spray chamber that is placed at the torch base, providing very high sample introduction efficiency (close to 100%) at very low sample uptake rate (20 µL min^{-1}).

The ICPOES analysis of samples containing petroleum derivatives was successfully performed using the TISIS heated to 350 °C without matrix effects [78]. Coupling the heated TISIS with ICPMS was carried out to analyze various samples including environmental, biological and clinical samples [79-81]. However, the TISIS has some drawbacks, such as the analysis speed being limited by the very low sample uptake rate. Additionally, the TISIS is not tolerant to samples with high salt content because it uses a micro-nebulizer, which is prone to clogging.

Pneumatic nebulization in a programmable temperature spray chamber (PN-PTSC) coupled with chemical vapour generation (CVG) significantly improved the analytical performance of ICPOES without deterioration in plasma thermal characteristics [82-85]. A significant improvement in sensitivity and detection limit of ICPOES was also achieved when different spray chambers, such as a single-pass flip spray chamber (FC) coupled with a Burgener nebulizer were heated with ceramic block IR heaters, although the sample uptake rate for the IR-heated system was 10 times lower than with the PN system at room temperature [86].

Recently, a new IR heater so-called ceramic beaded rope IR heater, which provides both IR and convective heating, was utilized to heat a PET for USN [87] and MSIS [88] systems. This heater is flexible and can be wrapped around the spray chamber and the base of the torch providing more effective heating and compact design than the ceramic block type that has been used so far.

Table 1.1 summarizes some features and limitations of the aforementioned pre-evaporation sample introduction systems for ICPOES. Although several pre-evaporation approaches have been investigated, so far, a commercialized pre-evaporation system is not yet available. This could be because several limitations (Table 1.1) of the pre-evaporation approaches still need to be addressed. In particular, there is a need for a compact pre-evaporation system providing acceptable analysis speed.

Table 1.1 Features and limitations of different heated systems for ICPOES.

Sample introduction system	Features	Limitations
USN-PET(IR) [69]	• 10-25 fold improvement in sensitivity and detection limit • Ability to determine Hg and B • Working at 1.5 mL min^{-1} sample uptake rate • Using efficient IR heating	• Cumbersome design due to using a PET and bulky ceramic IR heaters • Expensive due to using USN
TISIS [73]	• 3-15 fold improvement in sensitivity and detection limit • Working at 20 µL min^{-1} sample uptake rate • Total consumption of sample	• Limited analysis speed due to working at very low sample uptake rate • Clogging issue due to using micro-nebulizer • Inefficient heating (heating tape)
FC(IR) [86]	• 2-13 fold improvement in sensitivity and detection limit • Working at 0.1 mL min^{-1} sample uptake rate • Total consumption of sample • Using efficient IR heating	• Cumbersome design due to using bulky ceramic IR heaters • Limited analysis speed due to working at low sample uptake rate
MSIS-PET(IR) [88]	• Significant improvement in sensitivity and detection limit, especially for hydride forming analytes • Working at 1-2 mL min^{-1} sample uptake rate. • Using efficient IR heating	• Cumbersome design due to using a PET

1.6 Thesis objectives

This thesis aims at exploring different approaches to improve the analytical performance of ICPOES and solid sampling (SS) ETV-ICPOES. The goals are to develop simple alternatives to the current sample introduction systems for ICPOES and better robust plasma condition for SS-ETV-ICPOES that could offer improved analytical performance in terms of sensitivity, detection limit, plasma robustness as well as sample

throughput and could be utilized to do a routine multi-elemental analysis in a commercial or industrial labs. This thesis will cover the following objectives:

a) To develop a simple, compact, low-cost IR-heated sample introduction system for ICPOES. The cumbersome design, or very small sample uptake rate in the case of the TISIS, is a major impediment to using the pre-evaporation systems in Table 1.1 for routine multi-elemental analysis. In Chapter 2, an IR heating lamp will be used to eliminate the need for bulky ceramic block heaters.

b) To apply a ceramic beaded rope IR heater to commercially available spray chambers to improve the analytical performance of ICPOES. In one report, replacing the ceramic IR block heaters of a USN-PET(IR) system by an IR rope heater provided similar ICPOES analytical performance at a lower heating temperature [87]. To assess the efficiency of the rope heater, the sensitivity and detection limit obtained with the rope heater on commercially available spray chambers will be compared to those obtained while heating the same spray chambers with IR block heaters in Chapter 3.

c) To optimize an IR-heated PN system for ICPOES at a conventional sample uptake rate (*i.e.* close to 1 mL min^{-1}). The analysis speed is directly dependent on the sample uptake rate. With total sample consumption (such as when using the TISIS in Table 1.1), the sample uptake rate must be minimized to avoid plasma extinction, which significantly decreases the analysis speed. Thus, in Chapter 4, the analytical performance of ICPOES will be improved at a regular sample uptake rate (close to 1 mL min^{-1}) by heating only the top of a baffled cyclonic spray chamber along with

its side arm, the elbow connection to the torch and the torch base with the IR rope heater.

d) To improve the analytical performance of SS-ETV-ICPOES. Addition of H_2, N_2 or water vapour to the central channel of the plasma has been used to enhance plasma excitation conditions in ICP spectrometry [46, 55, 58]. Thus, Chapter 5 will investigate the effect of sheathing the sample aerosol with H_2, N_2 or water vapour on sensitivity, detection limit and plasma robustness for SS-ETV-ICPOES.

1.7 References

[1] N. H. Bings, J. O. Orlandini von Niessen and J. N. Schaper, Liquid sample introduction in inductively coupled plasma atomic emission and mass spectrometry – critical review, *Spectrochim. Acta B.*, 100, **2014**, 14-37.

[2] G. L. Donati, R. S. Amais and C. B. Williams, Recent advances in inductively coupled plasma optical emission spectrometry, *J. Anal. At. Spectrom*., 32, **2017**, 1283-1296.

[3] J. H. Steve, Inductively coupled plasma spectrometry and its applications, 2nd ed., Blackwell: Oxford, **2007**.

[4] J. D. Winefordner, I. B. Gornushkin, T. Correll, E. Gibb, B. W. Smith and N. Omenetto, Comparing several atomic spectrometric methods to the super stars: special emphasis on laser induced breakdown spectrometry, LIBS, a future super star, *J. Anal. At. Spectrom*., 19, **2004**, 1061-1083.

[5] G. L. Moore, Introduction to inductively coupled plasma atomic emission spectrometry, Elsevier: New York, **1989**.

[6] M. Thompson and J. N. Walsh, Handbook of inductively coupled plasma spectrometry, 2nd ed., Blackie: New York, **1989**.

[7] S. Ghosh, V. L. Prasanna, B. Sowjanya, P. Srivani, M. Alagaraja and D. Banji, Inductively coupled plasma–optical emission spectroscopy: a review, *Asian J. Pharm. Ana*. 3, **2013**, 24-33.

[8] A. Montaser and D. W. Golightly, Inductively coupled plasmas in analytical atomic spectrometry, 2nd ed., VCH: New York, **1992**.

[9] H. E. Taylor, Inductively coupled plasma-mass spectrometry, Academic Press: California, **2001**.

[10] X. Hou and B. T. Jones, Inductively coupled plasma/optical emission spectrometry, in encyclopedia of analytical chemistry, R. A. Meyers, Ed., John Wiley & Sons, Chichester, **2000**.

[11] C. Dubuisson, E. Poussel and J. M. Mermet, Comparison of axially and radially viewed inductively coupled plasma atomic emission spectrometry in terms of signal-to-background ratio and matrix effects, *J. Anal. At. Spectrom.*, 12, **1997**, 281-286.

[12] I. B. Brenner, A. Zander, M. Cole and A. Wiseman, Comparison of axially and radially viewed inductively coupled plasmas for multi-element analysis: effect of sodium and calcium, *J. Anal. At. Spectrom*., 12, **1997**, 897-906.

[13] J. C. Ivaldi and J. F. Tyson, Performance evaluation of an axially viewed horizontal inductively coupled plasma for optical emission spectrometry, *Spectrochim. Acta, Part B*, 50, **1995**, 1207-1226.

[14] Y. Morishige and A. Kimura, Ionization interference in inductively coupled plasma-optical emission spectroscopy, *Sei. Tech. Rev*., 66, **2008**, 106-111.

[15] C. B. Boss, and K. J. Fredeen, Concepts, Instrumentation and Techniques in Inductively Coupled Plasma Optical Emission Spectrometry, 3rd ed.; Perkin-Elmer, Inc., Third Edition, USA, **2004**.

[16] S. Maestre, J. Mora, J. L. Todoli, and A. Canals, Evaluation of several commercially available spray chambers for use in inductively coupled plasma atomic emission spectrometry, *J. Anal. At. Spectrom.*, 14, **1999**, 61-67.

[17] J. Mora, S. Maestre, V. Hernandis and J. L. Todoli, Liquid-sample introduction in plasma spectrometry, *Trends Anal. Chem.*, 22, **2003**, 123-132.

[18] J. L. Todoli, V. Hernandis, A. Canalsa and J. M. Mermet, Comparison of characteristics and limits of detection of pneumatic micronebulizers and a conventional nebulizer operating at low uptake rates in ICP-AES, *J. Anal. At. Spectrom.*, 14, **1999**, 1289-1295.

[19] T. D. Hettipathirana and D. E. Davey, Evaluation of a microconcentric nebuliser–cyclonic spray chamber for flow injection simultaneous multielement inductively coupled plasma optical emission spectrometry, *J. Anal. At. Spectrom.*, 13, **1998**, 483-488.

[20] E. G. Yanes and N. J. Miller-Ihli, Parallel path nebulizer: Critical parameters for use with microseparation techniques combined with inductively coupled plasma mass spectrometry, *Spectrochim. Acta B.*, 60, **2005**, 555–561.

[21] E. G. Yanes, N. J. Miller-Ihli, Use of a parallel path nebulizer for capillary-based microseparation techniques coupled with an inductively coupled plasma mass spectrometer for speciation measurements, *Spectrochim. Acta B.*, 59, **2004**, 883-890.

[22] J. L. Todoli and J. M. Mermet, Liquid sample introduction in ICP spectrometry: a practical guide. Elsevier: Oxford, **2008**.

[23] J. A. C. Broekaert, Analytical Atomic Spectrometry with Flames and Plasmas, Wiley-VCH: Weinheim, **2002**.

[24] A. Limbeck, M. Bonta and W. Nischkauer, Improvements in the direct analysis of advanced materials using ICP-based measurement techniques, *J. Anal. At. Spectrom*., 32, **2017**, 212-232.

[25] B. Hu, S. Li, G. Xiang, M. He and Z. Jiang, Recent progress in electrothermal vaporization-inductively coupled plasma atomic emission spectrometry and inductively coupled plasma mass spectrometry, *Appl. Spectrosc. Rev.,* 42, **2007**, 203-234.

[26] D. E. Nixon, V. A. Fassel and R. N. Kniseley, Inductively coupled plasma-optical emission analytical spectroscopy tantalum filament vaporization of microliter samples, *Anal. Chem.*, 46, **1974**, 210-213.

[27] A. M. Gunn, D. L. Millard and G. F. Kirkbright, Optical emission spectrometry with an inductively coupled radiofrequency argon plasma source and sample introduction with a graphite rod electrothermal vaporization device, *Analyst,* 103, **1978**, 1066-1073.

[28] F. Plantikow-VoBgatter and E. Denkhaus, Application of an ETV-ICP system for the determination of elements in human hair, *Spectrochim. Acta, Part B,* 51, **1996**, 261-270.

[29] W. Schron, A. Liebmann and G. Nimmerfall, Direct solid sample analysis of sediments, soils, rocks and advanced ceramics by ETV-ICP-AES and GF-AAS, *Fresenius J. Anal. Chem.*, 366, **2000**, 79-88.

[30] U. Schaffer and V. Krivan, Multielement analysis of graphite and silicon carbide by inductively coupled plasma atomic emission spectrometry using solid sampling and electrothermal vaporization, *Anal. Chem.*, 71, **1999**, 849-854.

[31] A. Asfaw, G. Wibetoe and D. Beauchemin, Solid sampling electrothermal vaporization inductively coupled plasma optical emission spectrometry for discrimination of automotive paint samples in forensic analysis, *J. Anal. At. Spectrom*., 27, **2012**, 1928-1934.

[32] P. R. Perzi, Manual of electrothermal vaporization (ETV-4000c), Spectral System, Germany, October, **2009**.

[33] U. Schaffer and V. Krivan, A graphite furnace electrothermal vaporization system for inductively coupled plasma atomic emission spectrometry, *Anal. Chem.*, 70, **1998**, 482-490.

[34] A. S. Masquelin, F. Kaveh, A. Asfaw, C. J. Oates and D. Beauchemin, Solid sampling ETV-ICP-OES to study the distribution of elements in clay and soil samples for mineral exploration, *Geochem.: Explor., Environ., Anal.*, 13, **2013**, 11-20.

[35] J. Hassler, P. Barth, S. Richter and R. Matschat, Determination of trace elements in high-purity copper by ETV-ICPOES using halocarbons as chemical modifiers, *J. Anal. At. Spectrom*., 26, **2011**, 2404-2418.

[36] T. Voget, D. Bauer, D. Nennstiel and M. Otto, Solid-sampling electrothermal vaporization inductively coupled plasma optical emission spectrometry for direct determination of total oxygen in coal, *Anal. Chem.*, 87, **2015**, 10414-10420.

[37] A. Asfaw and G. Wibetoe, Potential of solid sampling electrothermal vaporization for solving spectral interference in inductively coupled plasma optical emission spectrometry, *Spectrochim. Acta, Part B*, 64, **2009**, 363-368.

[38] G. Zaray, T. Kantor, G. Wolff, Z. Zadgorska and H. Nickel, ICP-AES detection of silicon carbide impurities volatilized in a graphite furnace with the use of carbon tetrachloride vapor, *Mikrochim. Acta*, 107, **1992**, 345-358.

[39] S. Wu, C. Hu, M. He, B. Chen and B. Hu, Capillary microextraction combined with fluorinating assisted electrothermal vaporization inductively coupled plasma optical emission spectrometry for the determination of trace lanthanum, europium, dysprosium and yttrium in human hair, *Talanta*, 115, **2013**, 342-348.

[40] J. Hassler, R. Matschat, S. Richter, P. Barth, A. K. Detcheva and H.-J. Waarlo, Determination of 22 trace elements in high-purity copper including Se and Te by ETV-ICPOES using SF_6, NF_3, CF_4 and H_2 as chemical modifiers, *J. Anal. At. Spectrom*., 31, **2016**, 642-657.

[41] R. E. Sturgeon and J. W. Lam, The ETV as a thermochemical reactor for ICP-MS sample introduction, *J. Anal. At. Spectrom*., 14, **1999**, 785-791.

[42] M. Resano, F. Vanhaecke and M. T. C. de Loos-Vollebregt, Electrothermal vaporization for sample introduction in atomic absorption, atomic emission and plasma mass spectrometry – a critical review with focus on solid sampling and slurry analysis, *J. Anal. At. Spectrom*., 23, **2008**, 1450-1475.

[43] F. Kaveh, C. J. Oates and D. Beauchemin, Direct analysis of soils by ETV-ICP-AES: a powerful tool for mineral exploration, *Geochem.: Explor., Environ., Anal*, 14, **2014**, 305-313.

[44] A. Asfaw, G. Wibetoe and D. Beauchemin, Solid sampling electrothermal vaporization inductively coupled plasma optical emission spectrometry for discrimination of automotive paint samples in forensic analysis, *J. Anal. At. Spectrom*., 27, **2012**, 1928-1934.

[45] L. Hung and D. Beauchemin, Forensic analysis of automotive paint chips for the identification of the vehicle manufacturer, colour and year of production using electrothermal vaporization coupled to inductively coupled plasma optical emission spectrometry, *J. Anal. At. Spectrom*., 32, **2017**, 1601-1607.

[46] F. Kaveh and D. Beauchemin, Improvement of the capabilities of solid sampling ETV-ICP-OES by coupling ETV to a nebulization/pre-evaporation system, *J. Anal. At. Spectrom*., 29, **2014**, 1371-1377.

[47] A. Montaser, R. L. Van Hoven and R. M. Barnes, Mixed-gas, molecular-gas, and helium inductively coupled plasma for analytical atomic spectrometry: a critical review, *Crit. Rev. Anal. Chem.*, 18, **1987**, 45-103.

[48] G. L. Scheffler and D. Pozebon, Advantages, drawbacks and applications of mixed Ar-N_2 sources in inductively coupled plasma-based techniques: an overview, *Anal. Methods*, 6, **2014**, 6170-6182.

[49] W. J. Balsanek, G. Ertas and J. A. Holcombe, The use of concomitant elements to evaluate an Ar-N_2 mixed-gas plasma by electrothermal vaporization inductively coupled plasma orthogonal time-of-flight mass spectrometry, *Spectrochim. Acta, Part B*, 61, **2006**, 732-742.

[50] E. H. Choot and G. Horlick, Evaluation of the analytical performance of mixed gas inductively coupled plasmas, *Spectrochim. Acta, Part B*, 41, **1986**, 925-934.

[51] E. H. Choot and G. Horlick, Spatially resolved electron density measurements in Ar, N_2-Ar and O_2-Ar ICPs using a photodiode array detection, *Spectrochim. Acta, Part B*, 41, **1986**, 935-945.

[52] I. Ishii, D. W. Golightly and A. Montaser, Radial excitation temperatures in argon-nitrogen inductively coupled plasmas, *J. Anal. At. Spectrom*., 3, **1988**, 965-968.

[53] A. Montaser , I. Ishii, B. A. Palmer and L. R. Layman, Line widths and temperatures of Ar-N_2 ICP discharges measured by high-resolution Fourier transform spectrometry, *Spectrochim. Acta, Part B*, 45, **1990**, 603-612.

[54] C. Agatemor and D. Beauchemin, Towards the reduction of matrix effects in inductively coupled plasma mass spectrometry without compromising detection limits: the use of argon-nitrogen mixed-gas plasma, *Spectrochim. Acta, Part B*, 66, **2011**, 1-11.

[55] G. L. Scheffler and D. Pozebon, Straightforward way to enhance robustness in ultrasonic nebulization-axial view inductively coupled plasma optical emission spectrometry via an additional N_2 gas stream, *Spectrochim. Acta, Part B*, 113, **2015**, 84-92.

[56] G. L. Scheffler and D. Pozebon, Advantages and effects of nitrogen doping into the central channel of plasma in axially viewed-inductively coupled plasma optical emission spectrometry, *Anal. Chim. Acta*, 789, **2013**, 33-40.

[57] Z. Hu, S. Gao, Y. Liu, S. Hu, H. Chen and H. Yuan, Signal enhancement in laser ablation ICP-MS by addition of nitrogen in the central channel gas, *J. Anal. At. Spectrom*., 23, **2008**, 1093-1101.

[58] J. P. Matousek and J. M. Mermet, The effect of added hydrogen in electrothermal vaporization inductively coupled plasma atomic emission spectrometry, *Spectrochim. Acta, Part B*, 48, **1993**, 835-850.

[59] N. Shibata, N. Fudagawa and M. Kubota, Effects of hydrogen mixed with argon carrier gas in electrothermal vaporization-inductively coupled plasma-mass spectrometry, *Spectrochim. Acta, Part B*, 47, **1992**, 505-516.

[60] J. W. Olesik and J. C. Fister III, Incompletely desolvated droplets in argon inductively coupled plasmas: their number, original size and effect on emission intensities, *Spectrochim. Acta, Part B*, 46, **1991**, 851-868.

[61] J. C. Fister III and J. W. Olesik, Vertical and radial emission profiles and ion-atom intensity ratios in inductively coupled plasmas: the connection to vaporizing droplets, *Spectrochim. Acta, Part B*, 46 **1991**, 869-883.

[62] J. W. Olesik, Investigating the fate of individual sample droplets in inductively coupled plasmas, *Appl. Spectrosc*., 51, **1997**, 158A-175A.

[63] S. Greenfield and P. B. Smith, The determination of trace metals in microliter samples by torch excitation, *Anal. Chim. Acta*, *59*, **1972**, 341-348.

[64] G. R. Peters and D. Beauchemin, Characterization of an Interface allowing either nebulization or gas chromatography as the sample introduction system in ICPMS, *Anal. Chem*., 65, **1993**, 97-103.

[65] G. R. Peters and D. Beauchemin, Effect of pre-evaporating the solvent on the analytical performance of inductively coupled plasma mass spectrometry, *Spectrochim. Acta, Part B*, 48, 1993, 1481-1494.

[66] S. Liu and D. Beauchemin, The effect of pre-evaporation on ion distributions in inductively coupled plasma mass spectrometry, *Spectrochim. Acta, Part B*, 61, **2006**, 157-163.

[67] S. Liu and D. Beauchemin, Effect of concomitant analytes on As signal during pre-evaporation of the solvent prior to introduction into inductively coupled plasma mass spectrometry, *Spectrochim. Acta, Part, B*, 61, **2006**, 965-970.

[68] A. Asfaw and D. Beauchemin, Improvement of the capabilities of inductively coupled plasma optical emission spectrometry by replacing the desolvation system of an ultrasonic nebulization system with a pre-evaporation tube, *Spectrochim. Acta, Part B*, 65, **2010**, 376-384.

[69] A. Asfaw, W. R. MacFarlane and D. Beauchemin, Ultrasonic nebulization with an infrared heated pre-evaporation tube for sample introduction in ICP-OES: application to geological and environmental samples, *J. Anal. At. Spectrom*. 27, **2012**, 1254-1263.

[70] A. R. Eastgate, R. C. Fry and G. H. Gower, Radiation versus conduction in heated spray chamber desolvation for inductively coupled plasmas, *J. Anal. At. Spectrom*., 8, **1993**, 305-308.

[71] L. Gras, J. Mora, J. L. Todoli, A. Canals and V. Hernandis, Desolvation of acid solutions in inductively coupled plasma atomic emission spectrometry by infrared radiation. Comparison with a system based on microwave radiation, *Spectrochim. Acta, Part B*, 54, **1999**, 1321-1333.

[72] A. Asfaw and D. Beauchemin, Combination of a multimode sample introduction system with a pre-evaporation tube to improve multi-element analysis by ICP-OES, *J. Anal. At. Spectrom*., 27, **2012**, 80-91.

[73] E. Paredes, M. Grotti, J. M. Mermet and J. L. Todoli, Heated-spray chamber-based low sample consumption system for inductively coupled plasma spectrometry, *J. Anal. At. Spectrom*., 24, **2009**, 903-910.

[74] R. Sanchez, J. L. Todoli, C. P. Lienemann and J. M. Mermet, Minimization of the effect of silicon chemical form in xylene matrices on ICP-AES performance, *J. Anal. At. Spectrom*.,24, **2009**, 1382-1388.

[75] J. L. Todoli and J. M. Mermet, New torch design with an in-built chamber for liquid sample analysis by ICP-AES, *J. Anal. At. Spectrom*., 17, **2002**, 345-351.

[76] J. L. Todoli and J. M. Mermet, Influence of the spray chamber design for vapor-based liquid sample introduction at room temperature in ICP-AES, *J. Anal. At. Spectrom*., 17, **2002**, 211-218.

[77] J. M. Mermet and J. L. Todoli, Towards total-consumption pneumatic liquid micro-sample-introduction systems in ICP spectrometry, *Anal Bioanal Chem*., 378, **2004**, 57–59.

[78] R. Sanchez, J. L. Todoli, C. P. Lienemann and J. M. Mermet, Universal calibration for metal determination in fuels and biofuels by inductively coupled plasma atomic emission spectrometry based on segmented flow injection and a 350° C heated chamber, *J. Anal. At. Spectrom*., 27, **2012**, 937-945.

[79] M. Grotti, F. Ardini and J. L. Todoli, Total introduction of microsamples in inductively coupled plasma mass spectrometry by high-temperature evaporation chamber with a sheathing gas stream. *Anal. Chim. Acta*., 767, **2013**, 14– 20.

[80] A. Canabate, E. Gracia-Ruiz, M. Resano and J. L. Todoli, Analysis of whole blood by ICP-MS equipped with a high temperature total sample consumption system, *J. Anal. At. Spectrom*., 32, **2017**, 78-87.

[81] A. Canabate, E. Gracia-Ruiz, M. Resano and J. L. Todoli, Cerebrospinal fluid elemental analysis by using a total sample consumption system operated at high temperature adapted to inductively coupled plasma mass spectrometry, *J. Anal. At. Spectrom*., 32, **2017**, 1916-1924.

[82] K. Jankowski, J. Giersz and M. Paprocka, Improved determination of iodine by sequential (photo) chemical vapor generation and pneumatic nebulization in the programmable temperature spray chamber and inductively coupled plasma optical emission spectrometry, *Microchem. J.*, 113, **2014**, 17-22.

[83] J. Giersz and K. Jankowski, Effect of temperature on direct chemical vapor generation for plasma optical emission spectrometry: An application of programmable temperature spray chamber, *Microchem. J.*, 124, **2016**, 1-8.

[84] J. Giersz, M. Bartosiak and K. Jankowski, Sensitive determination of Hg together with Mn, Fe, Cu, by combined photochemical vapor generation and pneumatic nebulization in the programmable temperature spray chamber and inductively coupled plasma optical emission spectrometry, *Talanta*, 167, **2017**, 279-285.

[85] J. Giersz, M. Bartosiak and K. Jankowski, Spectroscopic diagnostics of axially viewed inductively coupled plasma and microwave induced plasma coupled to photochemical vapor generation with pneumatic nebulization inside a programmable temperature spray chamber, *J. Anal. At. Spectrom*., 32, **2017**, 1885-1892.

[86] Y. Makonnen, J. Burgener and D. Beauchemin, Improvement of analytical performance in inductively coupled plasma optical emission spectrometry without compromising robustness using an infrared-heated sample introduction system with a pneumatic nebulizer, *J. Anal. At. Spectrom*., 30, **2015**, 214-224.

[87] T. K. Anderlini and D. Beauchemin, Improvement of sample introduction to inductively coupled plasma optical emission spectrometry using an ultrasonic nebulizer with an infrared heated pre-evaporation tube, *J. Anal. At. Spectrom*., 33, **2018**, 127-134.

[88] T. K. Anderlini and D. Beauchemin, Improvements to the analytical performance of inductively coupled plasma optical emission spectrometry by coupling a multi-mode sample introduction system to an infrared heated pre-evaporation tube, *J. Anal. At. Spectrom*., 33, **2018**, 1068-1075.

Chapter 2

New Infrared-Heated Sample Introduction System for Enhanced Analytical Performance of Inductively Coupled Plasma Optical Emission Spectrometry[1]

2.1 Introduction

Inductively coupled plasma (ICP) optical emission spectrometry (OES) is widely used for routine trace multi-elemental analysis because of its robustness and low maintenance cost compared to ICP mass spectrometry (MS) [1]. Pneumatic nebulisation with a nebuliser and a spray chamber is the traditional ICPOES sample introduction system. The nebuliser transforms a solution into an aerosol and the spray chamber filters out large droplets that could overload the plasma. Because the sample transport efficiency is typically less than 5%, pneumatic nebulization remains the Achilles' heel of ICP spectrometry [2, 3]. Nonetheless, it is still the standard system for routine elemental analysis because of its stability, simplicity and relatively low cost.

Alternative systems provide enhance sample transport efficiency, such as ultrasonic nebulization [4] and direct injection nebulization [5], but they are susceptible to matrix effects and clogging, respectively. Moreover, they are more expensive and not applicable to a wide range of sample types. A simple approach for enhancing sample transport efficiency of a pneumatic nebulisation system is pre-evaporation of the sample aerosol [6, 7], which involves converting the sample aerosol into vapour prior to its introduction into the plasma, without removing the solvent (usually water) from the system. Water indeed acts as a load buffer, which minimizes matrix effects [8]. It is also the main source

[1] This chapter has been published: A. Al Hejami and D. Beauchemin, *J. Anal. At. Spectrom*., 33, **2018**, 738-744.

of hydrogen in the plasma, which facilitates energy transfer between the bulk plasma and its central channel because of the higher thermal conductivity of hydrogen compared to argon [9].

Pre-evaporation of sample aerosols can be achieved by inserting a heated pre-evaporation tube (PET) between the spray chamber and the ICP torch [10–14], or by direct heating of the spray chamber [6, 7]. For example, replacing the desolvation system (consisting of a heater and condenser) of an ultrasonic nebulisation system with an infrared (IR)-heated PET (PET (IR)) drastically improved analyte sensitivity and detection limit [13, 14]. This was attributed to a reduction of the noise associated with desolvation and vaporization of sample droplets within the plasma as well as to more plasma energy being available for atomization, excitation and ionization processes.

A significant improvement in sensitivity of ICPOES was also reported with the heated torch-integrated sample introduction system (hTISIS) [15, 16]. This was attributed to an increased sample transport efficiency and to a reduction in droplet sizes. The excitation conditions of the plasma were also enhanced, leading to a more robust plasma. The hTISIS, which operates at <20 mL min^{-1}, consists of a pneumatic micro-nebuliser in a single-pass spray chamber that is placed at the torch base [17, 18]. It has been used for the analysis of environmental samples [19], fuels [20, 21], as well as biological and clinical samples [22–24]. However, the analysis speed is limited by the very low sample uptake rate. Additionally, the system is not tolerant of samples with high salt content because the micro-nebuliser is prone to blockage.

In general, convective heating is inefficient, as it relies on heat transfer from the spray chamber wall to the droplets, which may induce deposition of sample droplets on the spray

chamber wall if the primary aerosol is not fine enough, leading to a build-up of sample particles and memory effects [25]. In contrast, IR heating provides uniform and efficient heating, without the necessity to heat the spray chamber wall. As a result, it improved short-term stability while reducing washout time and carry-over effects compared to those observed with a convectively heated system of similar dimensions [25, 26].

In previous work carried out in this laboratory [7], a significant improvement in sensitivity and detection limit of ICPOES was also obtained using different types of spray chambers, such as a flip single-pass spray chamber heated by ceramic block IR heaters, despite the fact that the sample uptake rate was 10 times lower than that for pneumatic nebulisation at room temperature. However, the bulky IR heaters are an impediment for use in routine multi-elemental analysis. The objective of the present work was to design a simple low-cost IR-heated sample introduction system for ICPOES. To achieve this goal, a cyclonic spray chamber was modified to allow the insertion of an IR lamp heater (IR emitter) in its centre for more effective heating. Two IR-heated modified cyclonic spray chambers were tested: one with a regular outlet and another one with a wider outlet that was connected to the long PET previously used in combination with the ultrasonic nebulizer. The new systems were characterised in terms of sensitivity, detection limit, precision, and plasma robustness in comparison to a conventional Scott double-pass spray chamber at room temperature. They were then used for the analysis of two certified reference materials (CRMs).

2.2 Experimental

2.2.1 Instrumentation

A lateral view ARCOS ICPOES instrument (SPECTRO Analytical Instruments, Kleve, Germany) along with a conventional torch (Fassel-type; SCP Science, Baie d'Urfé, Quebec, Canada) and a parallel-flow T 2100 Burgener nebuliser (Burgener Research Inc., Mississauga, Canada) were used throughout. New designs of IR-heated modified cyclonic spray chamber (fabricated by JRV Scientific Glass, Montreal, Canada) with two different female joints were tested (Figure 2.1) and compared to a Scott double-passs pray chamber (SPECTRO Analytical Instruments, Kleve, Germany) at room temperature. The operating parameters for the different systems are summarised in Table 2.1.

Table 2.1 Experimental operating parameters for SPECTRO ARCOS ICPOES with different sample introduction systems.

Parameter	**DP (RT)**[a]	**MC12/5 (RT)**[b]	**MC12/5 (IR)**[c]	**MC28/15 (IR)PET**[d]
R.F. power (kW)	1.7	1.7	1.7	1.7
Plasma gas flow rate (L min^{-1})	14.5	14.5	14.5	14.5
Auxiliary gas flow rate (L min^{-1})	1	1.3	2	2
Nebulizer gas flow rate (L min^{-1})	0.7	0.6	0.6	0.6
Plasma observation height (mm)	10	10	10	10
Sample uptake rate (mL min^{-1})	1	1	1	1
IR temperature (°C)	20	20	150	150

[a] Room temperature Scott double-pass spray chamber. [b] Room temperature modified cyclonic spray chamber with 12 mm/5 mm outlet. [c] IR-heated modified cyclonic spray chamber with 12 mm/5 mm outlet. [d] IR-heated modified cyclonic spray chamber with 28 mm/15 mm outlet connected to a pre-evaporation tube.

2.2.2 IR-heated sample introduction system

A 50 mL cyclonic spray chamber was modified to allow an IR lamp heater (Heraeus Noblelight America LLC, Buford, USA) to be inserted in its centre (Figure 2.1). To this end, the internal diameter (ID) of the baffle was increased from around 7 mm to 17 mm. Two such modified chambers (MCs) were used. The outlet of the first one consisted of a regular 12 mm/5 mm female joint (MC12/5(IR)) that connected directly to the 7 cm long base of the torch. The latter was wrapped with a ceramic beads rope IR heater to prevent condensation in this region (Figure 2.1a). A thermocouple was inserted between the rope IR heater and the surface of the torch base; it was connected to a PL512 Mantle-Minder temperature controller (GLAS-COL Apparatus Company, Terre Haute, USA). A thermocouple was also attached to the surface of the IR lamp heater inside the modified baffle (Figure 2.1) and IR heating was controlled by another PL512 Mantle- Minder temperature controller.

The outlet of the second modified chamber was a 28 mm/15 mm female joint (MC28/15(IR)) to increase transport efficiency and to fit the 28 mm/5 mm glass ball joint at one end of the glass PET (38.1 cm long) (Figure 2.1b), which was previously coupled to an ultrasonic nebulizer [13, 14]. The other end of the PET with a 12 mm/5 mm socket was connected to the base of the ICP torch, which was also wrapped with the ceramic beads rope heater. With this configuration, which allowed more aerosol to be transported to the plasma, the aerosol travelled a 45 cm long IR-heated path between the spray chamber and the torch (Figure 2.1b) to ensure its complete pre-evaporation, as was achieved when the same PET was used with an ultrasonic nebulizer [13, 14]. The total internal volume of the whole system (MC + PET) was 89 cm^3.

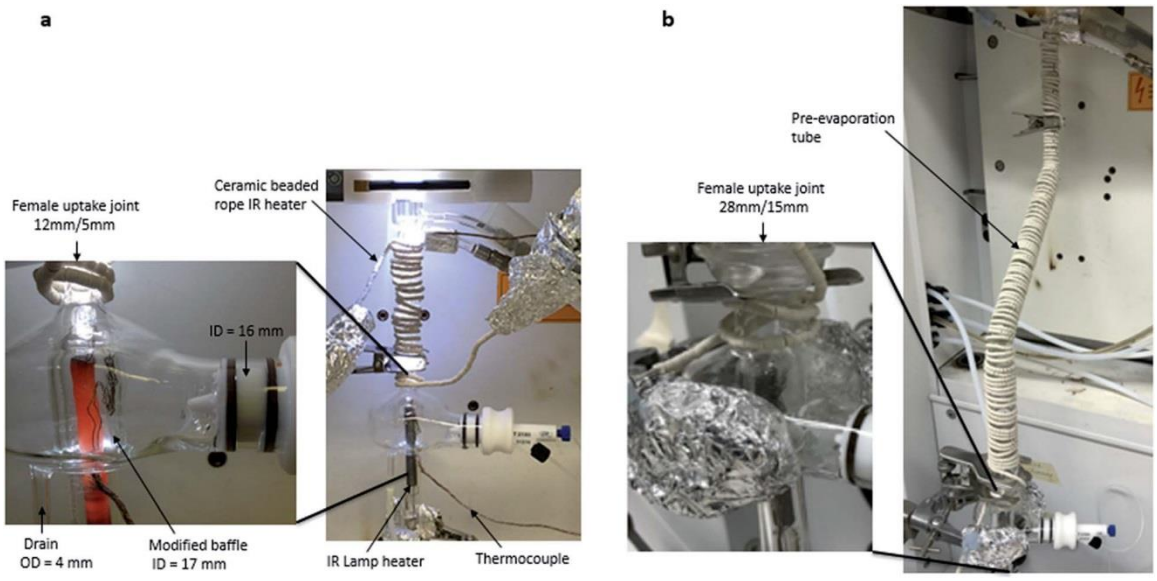

Figure 2.1 IR-heated modified cyclonic spray chambers: (a) with 12 mm/5 mm female joint (MC12/5(IR)); (b) with 28 mm/15 mm female joint coupled to a pre-evaporation tube (MC28/15(IR) PET).

2.2.3 Reagents and certified reference materials

Multi-elemental 100 mg L^{-1} stock solutions were prepared from commercially available 1000 and 10 000 mg L^{-1} individual elemental standard solutions (SCP Science, Baie d'Urfé, Quebec, Canada) in 4% v/v HNO_3. For optimisations, a 5 mg L^{-1} multi-elemental standard solution containing 26 elements in 2% v/v HNO_3 was prepared daily from the100 mg L^{-1} stock solutions, along with the corresponding blank. For calibration purposes, five multi-elemental standard solutions ranging from 0.1–10 mg L^{-1} were prepared from the same100 mg L^{-1} stock solutions. All standard solutions and samples were prepared using 18 MΩ cm doubly deionized water (DDW) (Arium Pro UV/DI System, Sartorius Stedim Biotech, Goettingen, Germany). The HNO_3 and HCl (ACS grade; Fisher Scientific, Ottawa,

Canada) were purified using a DST-1000 sub-boiling distillation system (Savillex, Minnetonka, USA).

For method validation, two certified reference materials, namely drinking water EP-L-3 and contaminated soil SS-2 (SCP Science, Baie d'Urfé, Quebec, Canada) were analysed. Drinking water was analysed directly whereas soil was first digested according to the EPA-3050A method, as recommended by the CRM supplier. In brief, about 0.5 g of soil was placed in a Teflon digestion vessel (Savillex, Minnetonka, USA) and digested in 1:2:0.5 water:HNO_3:HCl and H_2O_2 (30 m/m% in H_2O, ACS reagent, Sigma-Aldrich, Steinhein, Germany) at 95 °C for 2 h. The digest was then diluted to 50 mL with DDW and was filtered (through Whatman no. 541 filter paper) prior to analysis.

2.2.4 Optimisation

Multivariate optimisation of the IR-heating temperature (in the 80–180 °C range), the auxiliary gas flow rate (in the 0.6–2 L min^{-1} range) and the nebulizer gas flow rate (in the 0.6–1 L min^{-1} range), was carried out. A face-centred central composite experimental design was used [7,13,14], with a 5 mg L^{-1} multi-elemental standard solution in 2% v/v HNO_3 and the corresponding blank, to find the best compromise parameters in terms of sensitivity and plasma robustness for multi-elemental analysis. The Mg II (280.270 nm)/Mg I (285.213 nm), ionic to atomic, line emission ratio was monitored to assess robustness, a ratio of at least 10 indicating robust plasma conditions [27], under which improved plasma excitation is not significantly affected by matrix effects [27–29].

2.2.5 Determination of transport efficiency

The transport efficiency of analyte solution into the plasma was measured in triplicate using a mass-based method [30]. A 5 mL micropipette tip filled with a known mass of dry silica gel was placed at the outlet of the spray chamber [31] or of the PET. The micropipette tip was cut so as to match the inner diameter of the outlet. The transport efficiency was simply calculated as the ratio of the mass of a 5 mg L^{-1} solution trapped over that aspirated.

2.2.6 Data analysis

Minitab Release 17 statistical software (Minitab Inc., State College, PA, USA) was utilised to perform experimental designs for multivariate optimizations. Sensitive emission lines (atomic and ionic) free from possible spectroscopic interference were selected for 26 analytes (Smart Analyzer Vision software, SPECTRO Analytical Instruments, Kleve, Germany). Microsoft Excel 2013 was used for all data treatment, including blank subtraction, which was systematically done. Detection limits were computed as three times the standard deviation of the average signal intensity of ten consecutive blanks divided by the sensitivity (*i.e*. the slope of the calibration curve).

2.3 Result and discussion

2.3.1 Selection of operating parameters

The R.F. power was set at 1.7 kW, the maximum provided by the instrument, as high R.F. power increases robustness [32]. This was done for all pneumatic nebulization systems, including those operated at room temperature. The plasma gas flow rate and observation height were kept at 14.5 L min^{-1} and 10 mm, respectively, based on previous

optimisations performed on the same instrument [7]. The sample uptake rate was set to the conventional 1 mL min^{-1} throughout, as the goal was to optimise an efficient IR-heated sample introduction system operating at a regular uptake rate so as to not limit sample throughput.

Multivariate optimisation of the remaining parameters was carried out [7]. Because the plasma became unstable above 180 °C with IR heating and extinguished at more than 200 °C, the maximum IR temperature was set to 180 °C for multivariate optimisations. Increasing the IR-heating temperature from 80 to 180 °C, improved both sensitivity and Mg II/Mg I ratio, which passed through a maximum at around 150 °C and then decreased at higher than 160 °C. An IR temperature of 150 °C was thus selected. At this temperature, transport efficiency was significantly enhanced, as reported previously [7, 15, 22].

Increasing the auxiliary gas flow rate had no significant effect on sensitivity, but had a positive effect on the Mg II/Mg I ratio. A higher auxiliary gas flow rate was required with IR heating than with sample introduction systems at room temperature (Table 2.1). In general, sensitivity and Mg II/Mg I ratio increased upon decreasing the nebulizer gas flow rate. This is consistent with the finding that robust plasma conditions result when high R.F. power was combined with a long residence time [32]. In contrast, increasing the nebulizer gas flow rate above 0.8 L min^{-1} significantly decreased both sensitivity and robustness. This is in agreement with the report by Grotti *et al*. [33] that both the excitation temperature and Mg II/Mg I ratio decreased upon an increase in carrier gas flow rate above 0.85 L min^{-1}.

2.3.2 Sensitivity, detection limit and precision

The sensitivity and detection limit for the MC with a 12 mm/5 mm female joint and the conventional Scott double-pass spray chamber (DP) were comparable at room temperature (RT) according to a 2-tailed paired Student's *t*-test at the 95% confidence level. For all analytes, the average sensitivity ratio (MC(RT)/DP(RT)) and detection limit ratio (DP(RT)/MC(RT)) were 1.3 ± 0.1 and 2.1 ± 1.0, respectively. This is consistent with the similar % transport efficiency measured, of 3.6 ± 0.3 and 3.2 ± 0.2 (n = 3) for MC(RT) and DP(RT) respectively.

Upon IR heating of the MCs, the sensitivity and detection limit were significantly improved compared to those with DP(RT). On average, the improvement in sensitivity was by a factor of 2.6 ± 0.5, and 3.2 ± 0.7 for MC12/5(IR) and MC28/15(IR)PET setups, respectively (Figure 2.2), while the improvement in detection limit was by a factor of 3.6 ± 1.2 and 3.2 ± 1.6 for MC12/5(IR) and MC28/15(IR)PET, respectively (Figure 2.3). These results are consistent with the enhanced % transport efficiency with IR heating, which increased by factors of 3.7 and 4.9 fold to 11.7 ± 0.4 and 15.6 ± 1.0 (n = 3) for MC12/5(IR) and MC28/15(IR)PET, respectively. Similar trends were reported for the hTISIS [15], IR-heated flip single-pass chamber FC(IR) [7], and USN-PET(IR) [13], for which sensitivity and detection limit were improved by 2–15, 2–7, and 5–25, respectively.

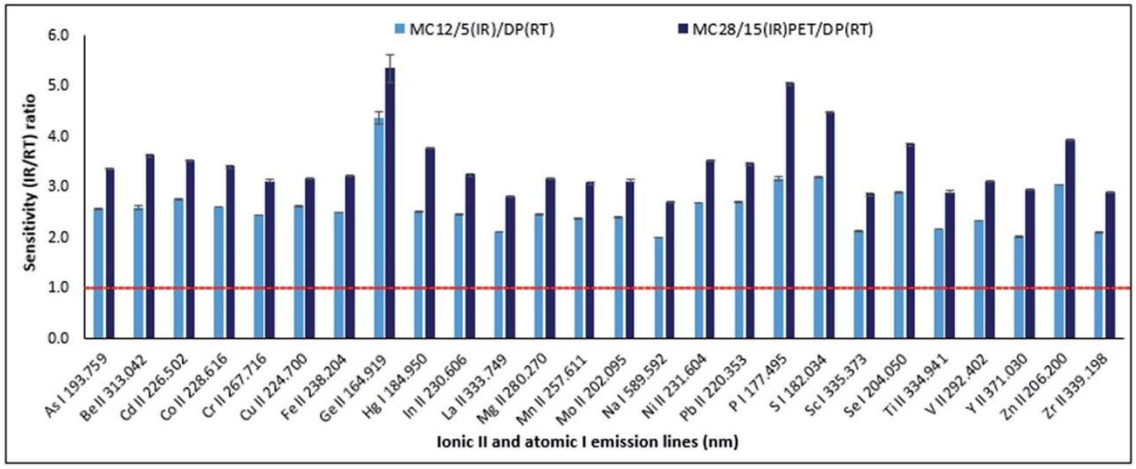

Figure 2.2 Average sensitivity ratio (n = 5) of IR-heated modified cyclonic spray chamber systems over that obtained with a conventional Scott double-pass spray chamber at room temperature, values above 1 (the red bar) constituting improvements.

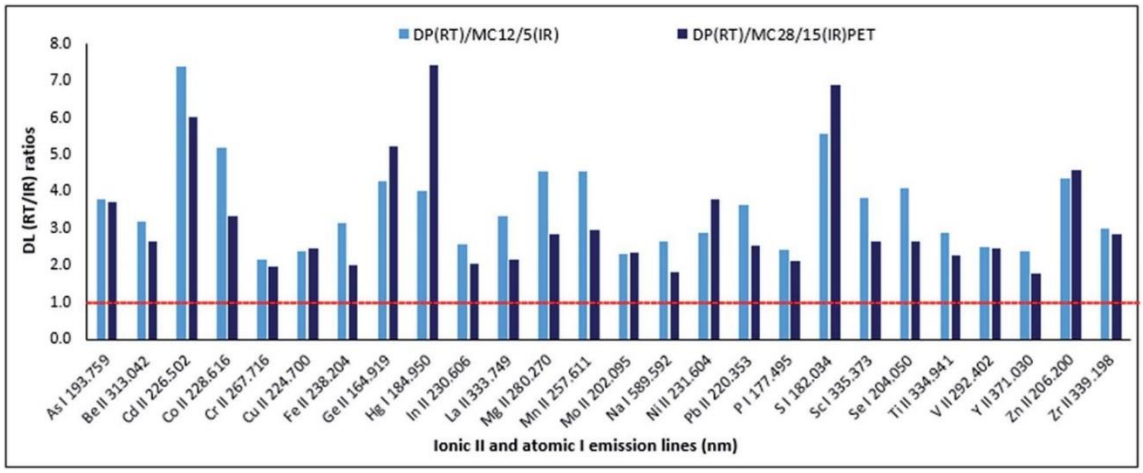

Figure 2.3 Average detection limit (DL) ratio (3s, n = 10) of a conventional Scott double-pass spray chamber at room temperature over that obtained with IR-heated modified cyclonic spray chamber systems, values above 1 (the red bar) constituting improvements.

Converting the sample aerosol into vapour prior to introduction into the plasma minimised the noise associated with the polydisperse nature of the aerosol reaching the plasma [34], which would be expected to result in a larger improvement in detection limit

than in sensitivity. This is indeed observed with the MC12/5(IR) according to a 2-tailed paired Student's t test at the 95% confidence level. However, there is no significant difference between the sensitivity ratios and the detection limit ratios for the MC28/15(IR)PET. Hence, the most compact IR-heated setup appears to be the most efficient, despite the short heated path between the spray chamber and the ICP.

Although the sensitivity of MC28/15(IR)PET was higher than that for MC12/5(IR) (Figure 2.2), the detection limit for both setups were comparable (Figure 2.3) according to a 2-tailed paired Student's *t*-test at the 95% confidence level. In general, the improvement in sensitivity and detection limit was systematically larger for ionic than atomic emission lines. For instance, the improvement in sensitivity when using ionic lines for Cd, Co, Mg and Zn was, on average, 2.1 ± 0.2 and 1.3 ± 0.1 fold that achieved using atomic lines for MC12/5(IR) and MC28/15(IR)PET, respectively. The corresponding improvement in detection limit when using ionic lines was 2.0 ± 0.9 and 1.8 ± 0.6 fold that achieved using atomic lines for MC12/5(IR) and MC28/15(IR)PET, respectively. This is because emission lines with a greater total excitation potential (*i.e.* excitation potentials for atomic lines and sum of ionisation and excitation potentials for ionic lines) are more sensitive to changes in plasma excitation conditions [35].

The instrumental precision, expressed as % relative standard deviation (% RSD) for five replicates of a 5 mg L^{-1} multi-elemental standard solution is reported in Figure 2.4 for the different spray chamber setups. The average % RSD for DP(RT) (1.3 ± 0.4), MC12/5(RT) (1.0 ± 0.7), MC12/5(IR) (0.8 ± 0.2), and MC28/15(IR)PET (0.9 ± 0.5) are comparable. In general, the average % RSD with MC12/5(IR) and MC28/15(IR)PET is

comparable with that for previous IR-heated systems [7,13,14]. However, it is better than that obtained with systems relying on convective heating, such as an earlier USN-PET [36] using heating tape (% RSD = 2.6 ± 0.7) and the hTISIS [6] using heating tape (% RSD ranged from 2 to 5).

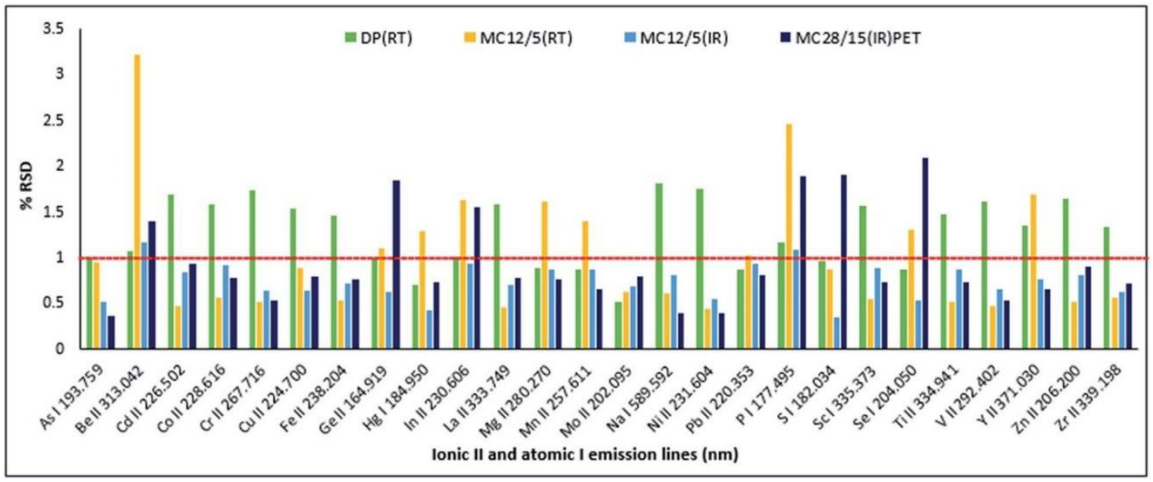

Figure 2.4 Instrumental precision (n = 5) for different sample introduction systems, with 1% RSD indicated by a red bar to facilitate comparisons.

However, two-tailed paired Student's *t* tests at the 95% confidence level indicate that the MC12/5(IR) has a significantly lower RSD than either the DP(RT) and MC12/5(RT). In contrast, there was only a significant difference in RSD between MC28/15(IR)PET and the DP(RT). In fact, a one-tail Student's *t* test at the 95% confidence level between RSD with MC12/5(IR) and MC28/15(IR)PET indicates that there is a significant difference in favour of MC12/5(IR). This confirms that the most compact MC12/5(IR) is the most efficient. In any case, no deposition of sample particles on the modified cyclonic spray chamber's inner surface and the modified baffle was visually observed after several days of operation.

2.3.3 Plasma robustness

The Mg II/Mg I ratio (n = 5) measured using a 5 mg L^{-1} multi-elemental standard solution was 8.3 ± 0.1, 8.5 ± 0.1, 9.8 ± 0.1, and 10.0 ± 0.1 with DP(RT), MC12/5(RT), MC12/5(IR), and MC28/15(IR)PET, respectively. Plasma robustness was clearly improved upon IR heating compared to that achieved at room temperature. This could be attributed to an increase in the amount of water vapour reaching the plasma, which is known to improve plasma characteristics [15]. A Mg II/Mg I ratio of at least 10 was also previously reported upon IR heating of sample introduction systems [7, 13, 14].

2.3.4 Analysis of drinking water and contaminated soil CRMs

To further demonstrate the robustness of the IR-heated modified cyclonic spray chamber setups, two CRMs with different matrices (drinking water and contaminated soil) were analysed. The concentration of major elements in the drinking water CRM is 100 mg L^{-1} Al, 482 mg L^{-1} Ca and 404 mg L^{-1} K whereas that in the final diluted digest of contaminated soil CRM is 133 mg L^{-1} Al and 113 mg L^{-1} Ca. A simple external calibration was used without internal standardization or matrix-matching. The results are summarised in Tables 2.2 and 2.3. They are in good agreement with the certificate values according to a Student's *t* test at the 95% confidence level. This demonstrates the applicability of the new IR-heated sample introduction systems for ICPOES.

Table 2.2 Concentrations in mg L^{-1} (± standard deviation, n = 3) measured for drinking water EP-L-3 CRM by the new IR-heated modified cyclonic spray chambers setups.

Analyte	Certified ± confidence limit	MC12/5(IR)	MC28/15(IR)PET
As	10.6 ± 0.3	10.3 ± 0.2	10.7 ± 0.1
Co	9.75 ± 0.19	9.45 ± 0.36	9.58 ± 0.21
Cr	12.7 ± 0.2	12.7 ± 0.1	12.5 ± 0.3
Cu	15.6 ± 0.3	15.7 ± 0.2	15.7 ± 0.2
Fe	27.9 ± 0.7	27.8 ± 1.0	28.0 ± 0.6
Mg	45.8 ± 0.8	45.9 ± 0.8	45.6 ± 0.7
Mn	5.85 ± 0.09	5.57 ± 0.28	5.72 ± 0.07
Mo	22.6 ± 0.4	22.6 ± 0.4	22.5 ± 0.3
Na	229 ± 6	230 ± 4	231 ± 4
Ni	19.9 ± 0.3	19.2 ± 0.7	19.3 ± 0.4
Se	58.5 ± 1.8	57.8 ± 1.0	58.3 ± 1.0
V	13.6 ± 0.2	13.4 ± 0.6	13.6 ± 0.1
Zn	42.5 ± 0.6	42.1 ± 0.8	42.2 ± 0.5

Table 2.3 Concentrations in mg kg^{-1} (± standard deviation, n = 3) measured for a digest of contaminated soil SS-2 CRM by the new IR-heated modified cyclonic spray chambers setups.

Analyte	Certified ± confidence limit	MC12/5(IR)	MC28/15(IR)PET
As	75 ± 10	85 ± 6	91 ± 6
Cu	191 ± 9	191 ± 5	204 ± 7
Fe	21 046 ± 1449	21 974 ± 571	20 957 ± 1190
Mg	11 065 ± 606	10 461 ± 223	11 077 ± 459
Mn	457 ± 24	461 ± 11	457 ± 19
Ni	54 ± 4	53 ± 2	52 ± 2
P	752 ± 18	769 ± 25	784 ± 20
Ti	850 ± 108	883 ± 20	808 ± 51
V	34 ± 3	36 ± 1	32 ± 2
Zn	467 ± 23	462 ± 14	491 ± 16

2.4 Conclusions

The new modified cyclonic spray chamber with IR lamp heater is a simple approach to significantly improve analytical performance of ICPOES in terms of sensitivity, detection limit, and plasma robustness. In general, 2–7 fold improvement in sensitivity and detection limit were achieved with the most compact system. By improving plasma robustness, accurate multi-elemental analysis of drinking water and soil digest samples can be performed using a simple external calibration without internal standardization or matrix-matching. The new system has many attractive features, such as its portability and simplicity. Hence, it would be a valuable sample introduction system for ICPOES.

Future work will involve designing a more compact IR-heated modified cyclonic spray chamber by trimming the base of the torch and shortening the neck of the modified cyclonic spray chamber so as to allow just the IR lamp heater to heat the entire system without using a ceramic beaded rope IR heater. The new system will also be optimised at low sample uptake rate (<0.1 mL min^{-1} to achieve 100% transport efficiency (total consumption of the sample). It will finally be tested on ICPMS to see if similar improvements are achieved.

2.5 References

[1] G. L. Donati, R. S. Amais and C. B. Williams, Recent advances in inductively coupled plasma optical emission spectrometry, *J. Anal. At. Spectrom*., 32, **2017**, 1283-1296.

[2] R. F. Browner and A. W. Boorn, The Achilles' heel of atomic spectroscopy?, *Anal. Chem*., 56, **1984**, 786A-798A.

[3] N. H. Bings, J. O. Orlandini von Niessen and J. N. Schaper, Liquid sample introduction in inductively coupled plasma atomic emission and mass spectrometry – critical review, *Spectrochim. Acta, Part B*, 100, **2014**, 14-37.

[4] X. Hou and B. T. Jones, Inductively coupled plasma/optical emission spectrometry, in encyclopedia of analytical chemistry, R. A. Meyers, Ed., John Wiley & Sons, Chichester, **2000**.

[5] J. A. McLean, H. Zhang and A. Montaser, A direct injection high-efficiency nebulizer for inductively coupled plasma mass spectrometry, *Anal. Chem.*, 70, **1998**, 1012-1020.

[6] M. Grotti, F. Soggia and J. L. Todoli, Ultratrace analysis of Antarctic snow samples by reaction cell inductively coupled plasma mass spectrometry using a total-consumption micro-sample-introduction system, *Analyst*, 133, **2008**, 1388-1394.

[7] Y. Makonnen, J. Burgener and D. Beauchemin, Improvement of analytical performance in inductively coupled plasma optical emission spectrometry without compromising robustness using an infrared-heated sample introduction system with a pneumatic nebulizer, *J. Anal. At. Spectrom*., 30, **2015**, 214-224.

[8] T. Prohaska, S. Hann, C. Latkoczy and G. Stingeder, Determination of rare earth elements U and Th in environmental samples by inductively coupled plasma double focusing sectorfield mass spectrometry (ICP-SMS), *J. Anal. At. Spectrom*., 14, **1999**, 1-8.

[9] S. E. Long and R. F. Browner, Influence of water on conditions in the inductively coupled argon plasma, *Spectrochim. Acta, Part B*, 43, **1988**, 1461-1471.

[10] G. R. Peters and D. Beauchemin, Effect of pre-evaporating the solvent on the analytical performance of inductively coupled plasma mass spectrometry, *Spectrochim. Acta, Part B*, 48, **1993**, 1481-1494.

[11] S. Liu and D. Beauchemin, Effect of concomitant analytes on As signal during pre-evaporation of the solvent prior to introduction into inductively coupled plasma mass spectrometry, *Spectrochim. Acta, Part B*, 61, **2006**, 965-970.

[12] A. Asfaw and D. Beauchemin, Combination of a multimode sample introduction system with a pre-evaporation tube to improve multi-element analysis by ICP-OES, *J. Anal. At. Spectrom*., 27, **2012**, 80-91.

[13] A. Asfaw, W. R. MacFarlane and D. Beauchemin, Ultrasonic nebulization with an infrared heated pre-evaporation tube for sample introduction in ICP-OES: application to geological and environmental samples, *J. Anal. At. Spectrom*., 27, **2012**, 1254-1263.

[14] T. K. Anderlini and D. Beauchemin, Improvement of sample introduction to inductively coupled plasma optical emission spectrometry using an ultrasonic nebulizer with an infrared heated pre-evaporation tube, *J. Anal. At. Spectrom*., 33, **2018**, 127-134.

[15] E. Paredes, M. Grotti, J. M. Mermet and J. L. Todoli, Heated-spray chamber-based low sample consumption system for inductively coupled plasma spectrometry, *J. Anal. At. Spectrom*., 24, **2009**, 903-910.

[16] R. Sanchez, J. L. Todoli, C. P. Lienemann and J. M. Mermet, Air-segmented, 5-µL flow injection associated with a 200° C heated chamber to minimize plasma loading limitations and difference of behavior between alkanes, aromatic compounds and petroleum products in inductively coupled plasma atomic emission spectrometry, *J. Anal. At. Spectrom*., 25, **2010**, 1888-1894.

[17] J. L. Todoli and J. M. Mermet, Influence of the spray chamber design for vapor-based liquid sample introduction at room temperature in ICP-AES, *J. Anal. At. Spectrom*., 17, **2002**, 211-218.

[18] J. M. Mermet and J. L. Todoli, Towards total-consumption pneumatic liquid micro-sample-introduction systems in ICP spectrometry, *Anal Bioanal Chem*., 378, **2004**, 57–59.

[19] F. Ardini, M. Grotti, R. Sanchez and J. L. Todoli, Improving the analytical performances of ICP-AES by using a high-temperature single-pass spray chamber and segmented-injections micro-sample introduction for the analysis of environmental samples, *J. Anal. At. Spectrom*., 27, **2012**, 1400-1404.

[20] R. Sanchez, J. L. Todoli, C. P. Lienemann and J. M. Mermet, Universal calibration for metal determination in fuels and biofuels by inductively coupled plasma atomic emission spectrometry based on segmented flow injection and a 350 °C heated chamber, *J. Anal. At. Spectrom*., 27, **2012**, 937-945.

[21] C. Sanchez, C. P. Lienemann and J. L. Todoli, Metal and metalloid determination in bioethanol through inductively coupled plasma-optical emission spectroscopy, *Spectrochim. Acta, Part B*, 115, **2016**, 16-22.

[22] M. Grotti, F. Ardini and J. L. Todoli, Total introd2uction of microsamples in inductively coupled plasma mass spectrometry by high-temperature evaporation chamber with a sheathing gas stream, *Anal. Chim. Acta*, 767, **2013**, 14-20.

[23] A. Canabate, E. Garcia-Ruiz, M. Resano and J. L. Todoli, Analysis of whole blood by ICP-MS equipped with a high temperature total sample consumption system, *J. Anal. At. Spectrom*., 32, **2017**, 78-87.

[24] A. Canabate, E. Garcia-Ruiz, M. Resano and J. L. Todoli, Cerebrospinal fluid elemental analysis by using a total sample consumption system operated at high temperature adapted to inductively coupled plasma mass spectrometry, *J. Anal. At. Spectrom.*, 32, **2017**, 1916-1924.

[25] K. O. Douglass, N. Fitzgerald, B. J. Ingebrethsen and J. F. Tyson, Desolvating the sample aerosol with microwave radiation: further theoretical and experimental insight into the significance of such approach, *Spectrochim. Acta, Part B*, 59, **2004**, 261-270.

[26] A. R. Eastgate, R. C. Fry and G. H. Gower, Radiation versus conduction in heated spray chamber desolvation for inductively coupled plasmas, *J. Anal. At. Spectrom*., 8, **1993**, 305-308.

[27] J. M. Mermet, Use of magnesium as a test element for inductively coupled plasma atomic emission spectrometry diagnostics, *Anal. Chim. Acta*, 250, **1991**, 85-94.

[28] A. Fernandez, M. Murillo, N. Carrion and J. M. Mermet, Influence of operating conditions on the effects of acids in inductively coupled plasma atomic emission spectrometry, *J. Anal. At. Spectrom*., 9, **1994**, 217-221.

[29] J. L. Todoli and J. M. Mermet, Minimization of acid effects at low consumption rates in an axially viewed inductively coupled plasma atomic emission spectrometer by using micronebulizer-based sample introduction systems, *J. Anal. At. Spectrom*., 13, **1998**, 727-734.

[30] D. D. Smith and R. F. Browner, Measurement of aerosol transport efficiency in atomic spectrometry, *Anal. Chem*., 54, **1982**, 533-537.

[31] R. P. Lamsal, G. Jerkiewicz and D. Beauchemin, Flow injection single particle inductively coupled plasma mass spectrometry: an original simple approach for the characterization of metal-based nanoparticles, *Anal. Chem*., 88, **2016**, 10552-10558.

[32] X. Romero, E. Poussel and J. M. Mermet, Influence of the operating conditions on the efficiency of internal standardization in inductively coupled plasma atomic emission spectrometry, *Spectrochim. Acta, Part B*, 52, **1997**, 487-493.

[33] M. Grotti, C. Lagomarsino and J. M. Mermet, Effect of operating conditions on excitation temperature and electron number density in axially-viewed ICP-OES with introduction of vapours or aerosols, *J. Anal. At. Spectrom*., 21, **2006**, 963-969.

[34] J. W. Olesik, and J. C. Fister III, Incompletely desolvated droplets in argon inductively coupled plasmas: their number, original size and effect on emission intensities, *Spectrochim. Acta, Part B*, 46, **1991**, 851-868.

[35] I. B. Brenner and A. T. Zander, Axially and radially viewed inductively coupled plasmas – a critical review, *Spectrochim. Acta, Part B*, 55, **2000**, 1195-1240.

[36] A. Asfaw and D. Beauchemin, Improvement of the capabilities of inductively coupled plasma optical emission spectrometry by replacing the desolvation system of an ultrasonic nebulization system with a pre-evaporation tube, *Spectrochim. Acta, Part B*, 65, **2010**, 376-384.

Chapter 3

Infrared heating of commercially available spray chambers to improve the analytical performance of inductively coupled plasma optical emission spectrometry[2]

3.1 Introduction

Inductively coupled plasma optical emission spectrometry (ICPOES) is a powerful simultaneous multi-elemental analysis technique because every sample is atomized and most elements in the periodic table can be ionized in an ICP source. It is usually preferred for major, minor and trace elemental analysis of different types of samples, such as environmental, geological and biological samples [1]. Because of the ease with which liquids can be handled, ICPOES is usually equipped with a pneumatic nebulization system to deliver the sample as small droplets into the ICP [2]. This system consists of a pneumatic nebulizer inserted in a spray chamber that typically filters out 95% of the sample, which is why it is called the Achilles' heel of ICP spectrometry [2, 3]. Sample transport efficiency can be increased using an ultrasonic nebulizer [4] (USN) and direct injection nebulizer [5], which are however susceptible to matrix effects and clogging, respectively.

One way to improve the analytical figures of merit of ICPOES is pre-evaporation of the sample aerosol, without removing the solvent, prior to its introduction into the ICP [6–8]. Water indeed acts as a load buffer in the plasma, which minimizes matrix effects, and is the main source of hydrogen, which facilitates energy transfer between the bulk plasma and its central channel [9, 10]. Moreover, converting the sample aerosol into vapour greatly

[2] This chapter has been published: A. Al Hejami and D. Beauchemin, *J. Anal. At. Spectrom*., 33, **2018**, 2008-2014.

decreases the background noise level that would otherwise be associated with desolvation and vaporization of sample droplets in the plasma [11].

A pre-evaporation tube (PET) installed between the spray chamber and the plasma torch in ICP mass spectrometry (MS) and heated to 400 °C with heating tape improved sensitivity and detection limit [12–15]. This was ascribed to the reduction of noise level resulting from the decrease in mean droplet size of the sample aerosol reaching the plasma. Replacing the whole desolvation system of the USN system by a PET heated to 400 °C using heating tape improved sensitivity, detection limit and plasma robustness in ICPOES [16]. Further improvement with the same USN was obtained by using infrared (IR) heating instead [17]. A PET was also employed in combination with a multimode sample introduction system (MSIS) to improve the analytical performance of ICPOES [18].

The sensitivity of ICPOES significantly improved when the torch integrated sample introduction system (TISIS) was heated to 100 °C, as a result of an increase in sample transport efficiency and a reduction in droplet sizes [19, 20]. The TISIS was developed to minimize analyte washout time without sacrificing sensitivity and detection limit. It consists of a pneumatic micro-nebulizer and a single-pass spray chamber integrated with the base of the torch, providing total consumption of the sample at very low sample uptake rate (<20 mL min^{-1}) [21–23]. The heated TISIS has been applied to the analysis of environmental samples [24], fuels [25–27], as well as biological and clinical samples [28–30]. However, its micro-nebulizer is prone to blockage with high salt content samples, and the sample throughput is limited by the low sample uptake rate.

A significant improvement in analytical performance of ICPOES was also achieved using a non-commercial flip single-pass spray chamber heated by ceramic IR block heaters,

despite its sample uptake rate being a tenth of that used for pneumatic nebulization at room temperature [8]. However, ceramic IR block heaters are bulky and cumbersome. Hence, a new IR-heated modified baffled cyclonic spray chamber was designed, with an IR lamp heater inserted in an enlarged baffle [31]. It too provided a significant improvement in sensitivity and detection limit because of increased transport efficiency and improved plasma excitation conditions.

Compared to IR heating, convective heating, where the wall of the spray chamber or PET is heated and heat is then transferred to the aerosol within it (such as when using heating tape), has drawbacks: inefficient heating, drift, instability in the analyte signal and long washout times [32]. In contrast, IR heating offers: uniform and efficient heating, short-term stability, minimal washout time and reduced carry-over [33, 34]. A flexible alternative to the block heater is the ceramic beaded rope heater, which provides both IR and convective heating because it can be wrapped around. It was utilized to heat the torch base, in combination with a pen heater in a modified cyclonic spray chamber [31], and a PET for USN [35] and MSIS [36] systems. It proved more efficient than a block heater, as similar ICPOES analytical performance was achieved at an even lower heating temperature when the ceramic IR block heater of a USN-PET system was replaced by the ceramic beaded IR rope heater [35].

However, the beaded IR rope heater has so far only been used on a PET [35] and to prevent condensation at the base of the torch [31]. The most compact IR-heated sample introduction system so far is the modified cyclonic chamber mentioned above, which requires modification of the spray chamber by a glass blower. The aim of the present study is to apply the ceramic beaded IR rope heater to two different types of commercially

available spray chambers to improve the analytical performance of ICPOES while making the resulting enhanced sample introduction systems more accessible to ICPOES users. To evaluate the efficiency of the rope heater, the results are compared to those obtained while heating the same spray chambers with ceramic IR block heater(s). The optimized IR-heated systems were then applied to the analysis of a certified reference material of waste water.

3.2 Experimental

3.2.1 Instrumentation

A lateral view SPECTRO ARCOS instrument (SPECTRO Analytical Instruments, Kleve, Germany) and a SeaSpray nebulizer (Glass Expansion, Pocasset, MA, USA) were used for all experiments. Two different spray chambers were IR-heated: a 35 mL baffled cyclonic (BC) spray chamber and a 100 mL Scott double-pass (DP) spray chamber (both SPECTRO Analytical Instruments). They were connected to a torch having an integrated sheathing device (SPECTRO Analytical Instruments). For reference, a double-pass spray chamber was connected to a conventional Fassel-type torch (SCP Science, Baie d'Urfé, QC, Canada), as a sheathing gas is not typically used. The Smart Analyzer Vision software of the ICPOES instrument was utilized to select sensitive atomic and ionic emission lines, which were free from possible spectroscopic interference. Table 3.1 summarizes the operating conditions found by multivariate optimization.

Table 3.1 Operating parameters for SPECTRO ARCOS ICPOES with SeaSpray nebulizer and different spray chambers.*

Parameter	Range tested	DP (RT)	BC (IR rope)	BC (IR block)	DP (IR rope)	DP (IR block)
Radio frequency (RF) power (kW)	—	1.7	1.7	1.7	1.7	1.7
Ar plasma gas flow rate (L min^{-1})	—	14.5	14.5	14.5	14.5	14.5
Ar auxiliary gas flow rate (L min^{-1})	0.6–2	1	1	1.8	1	1.2
Ar nebulizer gas flow rate (L min^{-1})	0.6–1.2	1	0.85	0.9	0.95	1
Ar sheath gas flow rate (L min^{-1})	0–1	0	0.4	0.5	0.4	0.6
Plasma observation height (mm)	—	10	10	10	10	10
Sample uptake rate (mL min^{-1})	0.05–1	1	0.12	0.3	0.1	0.2
Temperature (°C)	20–200	20	200	200	110	200

* DP = Scott double-pass spray chamber; BC = baffled cyclonic spray chamber; RT = room temperature; IR rope = heated with ceramic beaded IR rope heater; IR block = heated with ceramic IR block heater.

3.2.2 IR-heated pneumatic nebulization system

Figure 3.1 shows the two IR-heating setups for each spray chamber. One (for the BC spray chamber) or two (for the DP spray chamber) 6 cm wide and 24.5 cm long ceramic IR block heaters (Process Heaters Inc., Toronto, ON, Canada) were used to heat the spray chambers and the base of the torch (Figure 3.1a and c). Each heater's temperature was controlled by a PL512 Mantle-Minder temperature controller (GLAS-COL Apparatus Company, Terre Haute, IN, USA) connected to a thermocouple located on the inner surface of the heater (facing the spray chamber). The spray chambers were heated through one side because of the rigidity of the IR block heater and its size, compounded with the little room

available within the torch box. In contrast, the ceramic beaded IR rope heater, which is compact and flexible, was wrapped around the spray chamber and the base of the torch (Figure 3.1b and d). A thermocouple was inserted between the IR rope heater and the surface of the spray chamber to enable control of the temperature of the heater by a PL512 Mantle-Minder temperature controller.

3.2.3 Chemicals

Five multi-elemental standard solutions (0.1–10 mg L^{-1}) containing 29 elements in 2% v/v HNO_3 (and the corresponding blank) were prepared from a 100 mg L^{-1} multi-elemental stock solution, itself prepared from commercially available 1000 and 10 000 mg L^{-1} individual elemental standard solutions (SCP Science) in 4% v/v HNO_3, doubly deionized water with 18 MΩ cm resistivity (Arium Pro UV/DI System, Sartorius Stedim Biotech, Goettingen, Germany) and sub-boiled HNO_3. A DST-1000 sub-boiling distillation system (Savillex, Minnetonka, MN, USA) was used to purify ACS grade HNO_3 (Fisher Scientific, Ottawa, ON, Canada). A certified reference material of waste water EU-L-3 (SCP Science) was directly analysed to validate the method.

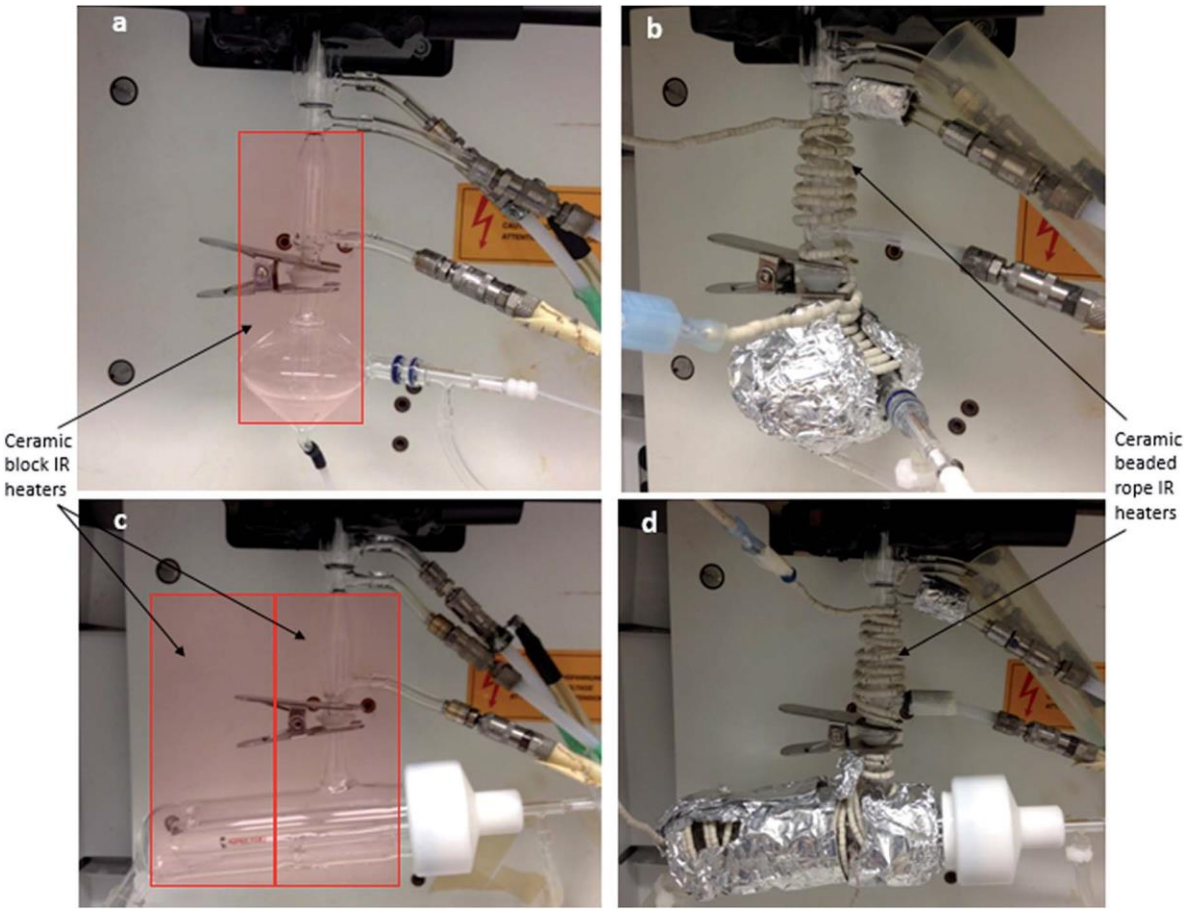

Figure 3.1 IR-heated systems for SPECTRO ARCOS ICPOES: (a & b) IR-heated baffled cyclonic spray chamber and (c & d) IR-heated Scott double- pass spray chamber. Two types of ceramic IR heaters were used (block and rope types).

3.2.4 Optimization

A face-centred central composite experimental design [8, 12, 31, 35] was used for multivariate optimization of auxiliary gas flow rate, nebulizer gas flow rate, sheath gas flow rate, IR heating temperature, and sample uptake rate (in the range of mL min^{-1}), along with a 5 mg L^{-1} multi-elemental standard solution in 2% v/v HNO_3 and its corresponding blank, to find the best compromise conditions in terms of sensitivity and plasma robustness. To maximize robustness, the plasma power was kept at the maximum (1.7 kW). The ionic

emission to atomic emission intensity ratio of Mg II (280.270 nm)/Mg I (285.213 nm) was measured to estimate the robustness, a value of 10 indicating robust plasma conditions [37]. Under these conditions, plasma excitation is not significantly affected by matrix effect and/or small changes in operating parameters [37–39].

3.2.5 Data analysis

Minitab Release 17 statistical software (Minitab Inc., State College, PA, USA) generated all experimental designs for multivariate optimization. Blank subtraction of the signal intensity of standards and samples, and other data treatment, were done using Microsoft Excel 2013. Detection limit were measured as three times the standard deviation of the average signal intensity of ten consecutive blanks divided by the slope of the calibration curve (*i.e.*, sensitivity).

3.3 Results and discussion

3.3.1 Selection of operating conditions

Based on previous optimizations performed on the same instrument [8, 31], the RF power, plasma gas flow rate, and observation height were set at 1.7 kW, 14.5 L min^{-1}, and 10 mm, respectively. The maximum IR heating temperature was set to 200 °C for multivariate optimizations of the remaining parameters to avoid damaging the Teflon fitting of the spray chambers. The IR heating temperature that provided maximum sensitivity and plasma robustness (200 °C in most cases) was selected (Table 3.1). A maximum of 1 L min^{-1} nebulizer gas flow rate had to be used because sensitivity and plasma robustness significantly decreased at higher values from a concurrent reduction in analyte residence time [40, 41]. The auxiliary gas flow rate of 1–1.8 L min^{-1} (Table 3.1)

for the IR-heated systems is higher than that reported for IR heating of other types of spray chambers with ceramic block heaters, although the sheath gas flow rate is similar [8].

No waste was noticed with the ceramic beaded IR rope heater, suggesting complete pre-evaporation. This limited the sample uptake rate to around 0.1 mL min^{-1}, as in the previous work with non-commercial spray chambers, where complete pre-evaporation appeared to be achieved with IR block heaters [8]. At the higher sample uptake rate selected with the ceramic IR block heater in this work, pre-evaporation was not complete.

3.3.2 Analytical figures of merit

A Scott DP spray chamber at room temperature (RT) being standard on the SPECTRO ARCOS ICPOES instrument, all IR-heated systems were compared to it. Tables 3.2 and 3.3, where a ratio above 1 indicates improvement, show that, in agreement with the literature [8, 31], sensitivity and detection limit significantly improved upon IR heating of the pneumatic nebulization system compared to those with a DP (RT). This was confirmed with a paired Student's *t* test at the 95% confidence level. The average improvement factors with each spray chamber for all analytes are summarised in Table 3.4. Similar trends were reported for the heated TISIS [19], USN-PET (IR) [17], and other IR- heated spray chambers [8, 31]. Sensitivity with the BC (RT) was 1.2 fold that with the DP (RT) and is significantly higher according to a paired Student's *t* test at the 95% confidence level. However, there is no significant difference in detection limit with the two spray chambers according to the same test.

Table 3.2 Sensitivity ratio (IR-heated spray chamber/double-pass spray chamber at room temperature) for two different spray chambers with two different IR heaters.

Emission line, nm	Baffled cyclonic		Double-pass	
	IR rope	IR block	IR rope	IR block
As I 189.042	2.4	1.6	3.4	1.9
Be II 313.107	2.6	2.3	4.0	2.8
Be I 234.861	2.1	1.8	3.3	2.3
Cd II 226.502	3.4	2.3	5.1	1.9
Cd I 228.802	2.5	1.9	3.9	1.9
Ce II 413.765	3.6	3.5	6.2	6.1
Co II 228.616	2.8	1.9	4.1	1.8
Cr II 267.716	4.8	3.4	6.3	3.3
Cr I 302.156	3.1	2.4	4.4	4.4
Cu II 224.700	2.2	2.1	4.6	2.3
Eu II 381.967	3.0	3.0	5.3	5.3
Fe II 238.204	2.8	2.1	4.1	2.0
Ga I 287.424	3.0	2.4	4.0	3.8
In II 230.606	2.1	1.9	3.7	2.2
K I 766.491	3.1	2.5	5.0	5.5
La II 333.749	4.0	3.6	6.3	4.9
Li I 670.780	2.8	2.7	5.2	7.3
Mg I 285.123	2.4	2.1	3.8	3.5
Mn II 257.611	3.0	2.4	4.5	2.6
Mo II 202.095	3.5	2.7	6.1	2.9
Ni II 221.648	3.7	2.5	5.2	2.1
Pb II 220.353	3.7	2.2	5.2	1.8
P I 177.495	4.4	3.0	6.6	3.7
S I 182.034	2.6	1.7	3.6	2.0
Sb I 206.833	2.0	1.2	2.6	1.1
Sc I 335.373	3.5	3.2	5.5	4.6
Se I 204.050	3.3	2.1	4.6	2.6
Sr II 421.552	2.9	2.7	4.9	4.8
Ti II 334.941	3.6	3.2	5.6	4.7
V II 292.402	3.9	3.3	5.9	3.9
Y II 324.228	3.1	2.7	5.8	3.6
Zr II 339.198	4.4	4.1	7.8	6.0

Table 3.3 Detection limit (3σ, n = 10) ratio (double-pass spray chamber at room temperature/IR-heated spray chamber) for two different spray chambers with two different IR heaters.

Element, nm	Baffled cyclonic		Double-pass	
	IR rope	IR block	IR rope	IR block
As I 189.042	3.3	3.9	4.1	4.2
Be II 313.107	2.6	3.5	1.8	11
Be I 234.861	1.0	1.6	0.9	6.6
Cd II 226.502	3.8	2.8	2.6	7.1
Cd I 228.802	3.2	3.3	1.9	6.9
Ce II 413.765	1.6	3.0	1.3	17
Co II 228.616	3.6	3.1	2.2	7.8
Cr II 267.716	4.6	10	4.1	16
Cr I 302.156	2.6	4.1	1.5	11
Cu II 224.700	1.5	6.6	2.9	7.8
Eu II 381.967	1.2	3.9	1.1	16
Fe II 238.204	4.4	5.9	2.4	5.2
Ga I 287.424	2.4	5.0	1.6	9.6
In II 230.606	2.0	2.2	2.0	8.5
K I 766.491	2.8	4.2	1.9	25
La II 333.749	4.7	4.5	2.4	11
Li I 670.780	2.4	1.9	1.4	12
Mg I 285.123	2.8	6.5	1.8	4.3
Mn II 257.611	2.9	4.4	2.2	11
Mo II 202.095	1.5	9.2	5.7	7.8
Ni II 221.648	2.3	4.8	1.5	7.5
Pb II 220.353	4.3	6.3	2.6	7.8
P I 177.495	5.7	6.9	6.8	26
S I 182.034	1.3	4.0	2.2	2.9
Sb I 206.833	3.0	4.6	1.6	6.4
Sc I 335.373	8.1	6.0	3.2	14
Se I 204.050	5.3	5.0	3.1	5.5
Sr II 421.552	1.0	2.7	0.9	11
Ti II 334.941	3.9	4.3	2.2	16
V II 292.402	2.6	3.2	1.9	8.2
Y II 324.228	4.9	3.9	2.5	9.2
Zr II 339.198	2.5	3.0	2.0	8.1

For a given spray chamber, the improvement in sensitivity for the ceramic beaded rope heater was significantly better than with the ceramic block heater (Table 3.2) according to a paired Student's *t* test. The flexibility of the IR rope heater allowed the whole system including the spray chamber and the sheathing device to be covered, resulting in 100% solvent transport efficiency, as no waste was seen. On the other hand, the improvement in detection limit with the block heater was significantly better than that with the rope heater according to a paired Student's *t* test. This is likely because heating with the block heater is mostly through IR radiation whereas both IR heating and convective heating (through physical contact with the sample introduction system) are involved with the rope heater. Thus, using solely IR heating seems to result in more efficient and uniform heating than a combination of convective and IR heating [35]. In general, a larger improvement in detection limit than in sensitivity resulted with the IR block heater (Table 3.4), in agreement with previous works with ceramic IR block heaters [17, 31]. This is consistent with both an increase in sample introduction efficiency (which improves sensitivity and detection limit) and a reduction in noise (which further improves detection limit). In contrast, the improvement was larger in sensitivity than in detection limit with the rope heater (Table 3.4). This indicates that the increase in sample introduction efficiency was accompanied by an even greater increase in noise as a result of the less uniform heating than with the block heater.

Table 3.4 Effect of IR heating on analytical figures of merit (n = 32 emission lines unless otherwise specified) compared to those with a double- pass spray chamber at room temperature.

Spray chamber	Sample uptake rate (mL min^{-1})	Washout time (s)	Average sensitivity improvement	Average detection limit improvement	Average % RSD	Average Mg II/Mg I (n = 7)
DP (RT)	1.00	16 ± 3	—	—	1.5 ± 0.5	8.6 ± 0.1
BC (RT)	1.00	13 ± 5	1.25 ± 0.02	0.9 ± 0.2	1.3 ± 0.5	8.4 ± 0.1
BC (IR rope)	0.12	41 ± 11	3.1 ± 0.7	3.1 ± 1.6	2.6 ± 0.7	12.6 ± 0.4
BC (IR block)	0.30	33 ± 11	2.5 ± 0.7	4.5 ± 1.9	2.3 ± 0.3	12.0 ± 0.1
DP (IR rope)	0.10	49 ± 10	4.9 ± 1.1	2.4 ± 1.3	2.2 ± 0.5	12.1 ± 0.1
DP (IR block)	0.20	45 ± 11	3.4 ± 1.5	10.2 ± 5.3	1.3 ± 0.4	12.5 ± 0.1

As reported previously [8, 17, 31, 35], sensitivity and detection limit improvements were, in general, greater for ionic emission lines than atomic emission lines (Tables 3.2 and 3.3) because emission lines with a higher total excitation potential (*i.e*. excitation potentials for atomic emission lines and sum of ionization and excitation potentials for ionic emission lines) are more susceptible to changes in plasma excitation conditions [42]. For example, the detection limit improvement when using ionic emission lines was, on average, 1.8 ± 0.6, 1.8 ± 0.9, 2.0 ± 0.7 and 1.4 ± 0.3 fold that obtained using atomic emission lines for BC (IR rope), BC (IR block), DP (IR rope) and DP (IR block), respectively.

Table 3.5 summarizes the instrumental precision, in term of % relative standard deviation (% RSD), obtained for seven replicates of a 5 mg L^{-1} multi-elemental standard solution with the different systems. The average % RSD for all analytes is compiled in Table 3.4. As can be seen, the % RSD is comparable for DP (RT) and DP (IR block). The

% RSD with DP (IR block) is significantly better than that for the other IR-heated systems according to a paired Student's *t*-test. In general, for a given spray chamber, the precision with the IR block heater was significantly better than that with the rope heater according to a paired Student's *t* test. The precision with the DP (IR block) is comparable to that reported for other IR heated systems [8, 17, 31].

The washout time, *i.e*. the time taken for the steady-state signal to return to baseline when the analyte solution was no longer aspirated, was measured using a 5 mg L^{-1} multi-elemental standard solution containing 29 elements. The average values of the washout time for all analytes for different systems are included in Table 3.4. As expected, the washout time increased with a decrease in sample uptake rate, the longest washout time being observed with the IR rope heater because the sample uptake rate was the lowest. However, it did not increase proportionately to the decrease in sample uptake rate. For example, with DP (IR rope), the sample uptake rate was a tenth of that with DP (RT) and one might have expected ten times the washout time. Yet, 49 s were required instead of 160 s. Similarly, the sample uptake rate with DP (IR block) being a fifth of that with DP (RT), one might have expected 80 s washout time, but 45 s were required. This further demonstrates the beneficial effect of pre-evaporation.

The best results in terms of detection limit and precision were thus obtained with the Scott double-pass spray chamber using two IR block heaters. This is in contrast to the previous study comparing IR rope and IR block heaters for heating the PET of a USN, where the IR rope heater was found to be more efficient [35]. However, only the fine aerosol exiting the spray chamber was heated and a narrow PET was wrapped with IR rope

heater in the latter case. In this work, the poly-disperse aerosol generated by the nebulizer was heated and the IR rope was wrapped around a spray chamber. Although there was no aerosol wasted with the IR-heater, unlike with the IR block heater, the resulting pre-evaporation was evidently not as uniform as that achieved with the IR block heater.

Table 3.5 Instrumental precision (% RSD for 5 mg L^{-1}, n = 7) for different spray chambers

Element, nm	Double-pass	Baffled cyclonic		Double-pass	
	RT	IR rope	IR block	IR rope	IR block
As I 189.042	1.7	2.8	1.9	2.1	1.7
Be II 313.107	1.2	3.2	2.9	2.0	1.4
Be I 234.861	1.1	3.1	2.7	2.0	1.5
Cd II 226.502	0.9	2.0	2.4	3.0	2.2
Cd I 228.802	0.7	1.7	2.2	2.8	1.7
Ce II 413.765	1.4	2.7	2.1	1.3	1.3
Co II 228.616	1.5	1.8	2.4	2.9	2.0
Cr II 267.716	1.8	2.5	2.0	2.9	1.5
Cr I 302.156	2.6	3.4	2.0	1.4	0.8
Cu II 224.700	1.4	3.3	2.0	2.1	1.2
Eu II 381.967	1.1	1.5	2.6	1.9	1.3
Fe II 238.204	1.3	1.9	2.4	2.9	1.7
Ga I 287.424	1.7	2.4	1.7	1.6	0.7
In II 230.606	2.2	2.5	2.0	1.6	1.2
K I 766.491	2.0	2.9	2.0	1.2	1.5
La II 333.749	1.4	2.9	2.2	2.5	1.1
Li I 670.780	1.5	1.6	2.7	1.5	1.6
Mg I 285.123	1.4	2.6	2.2	2.4	1.1
Mn II 257.611	1.0	1.7	2.3	2.9	1.6
Mo II 202.095	1.5	3.1	2.2	2.2	1.8
Ni II 221.648	1.4	2.0	2.1	3.1	1.5
Pb II 220.353	1.8	2.9	1.9	2.4	0.6
P I 177.495	3.3	3.0	2.4	1.8	0.9
S I 182.034	2.2	3.8	2.3	2.0	0.8
Sb I 206.833	1.6	4.2	1.9	2.2	1.2
Sc I 335.373	1.2	1.8	2.4	2.5	1.3
Se I 204.050	1.6	3.8	2.0	1.9	0.6
Sr II 421.552	1.1	3.5	2.7	1.8	1.3
Ti II 334.941	1.1	1.7	2.4	2.5	1.3
V II 292.402	1.4	2.5	2.2	2.7	1.1
Y II 324.228	1.1	2.0	2.7	2.6	1.6
Zr II 339.198	1.3	2.0	2.7	2.6	1.4

3.3.3 Plasma robustness

Upon IR heating, the plasma robustness significantly improved compared to that at room temperature (Table 3.4) according to a Student's *t* test at the 95% confidence level. Plasma excitation characteristics are indeed improved by an increase in the amount of water vapour reaching the plasma [10, 19]. Similar results were previously reported for other IR-heated sample introduction systems on the same instrument [8, 17, 31, 35].

3.3.4 Analysis of certified reference material of waste water

Plasma robustness was further checked through direct analysis of a certified reference material of waste water. A simple external calibration without internal standardization or matrix- matching was performed. The results in Table 3.6 fall within the tolerance limits of the certified values. This further demonstrates the robustness of the IR-heated systems.

3.4 Conclusions

Pre-evaporation of the sample aerosol using IR heating is a simple approach to significantly improve sensitivity, detection limit and plasma robustness in ICPOES, in addition to reducing sample waste. Under the compromise operating conditions for multi-elemental analysis, the greatest improvement in detection limit, which ranged from 3-fold for S I 182.034 nm to 25- fold for K I 766.491 nm, was achieved using a double-pass spray chamber with two IR block heaters. This is because a ceramic block IR heater provides uniform and mostly IR heating. In contrast, the IR rope heater, which provided the greatest improvement in sensitivity and is less cumbersome than the block heater, did not improve detection limit as much, indicating that the combination of convective and IR heating was not as uniform. Nonetheless, because of the resulting robust plasma conditions, all IR-

heated systems allowed the accurate multi-elemental analysis of waste water by a simple external calibration, without internal standardization or matrix- matching. Future work will look into better thermal insulation along the IR-heated system to further improve detection limit. The sample introduction system of ICPMS will also be IR-heated to check if comparable improvements can be obtained.

Table 3.6 Concentrations in mg L^{-1} (± standard deviation, n = 7) measured for Waste Water EU-L-3 certified reference material with different spray chambers at room temperature or IR heated.

Analyte	Certified ± tolerance limit	BC (RT)	DP (RT)	BC (IR rope)	BC (IR block)	DP (IR rope)	DP (IR block)
As	8.40 ± 0.98	7.74 ± 0.09	8.01 ± 0.06	7.68 ± 0.21	8.20 ± 0.24	7.52 ± 0.16	7.80 ± 0.12
Cd	2.28 ± 0.42	1.99 ± 0.01	2.03 ± 0.02	2.49 ± 0.05	2.20 ± 0.06	1.99 ± 0.06	2.16 ± 0.02
Co	8.25 ± 0.63	8.33 ± 0.06	8.46 ± 0.04	8.29 ± 0.22	8.39 ± 0.26	8.02 ± 0.23	8.27 ± 0.12
Cr	6.26 ± 1.39	6.13 ± 0.06	6.15 ± 0.04	6.21 ± 0.11	6.27 ± 0.17	5.80 ± 0.17	6.25 ± 0.06
Fe	5.80 ± 0.76	6.31 ± 0.06	6.34 ± 0.03	6.13 ± 0.17	6.48 ± 0.19	6.01 ± 0.19	6.29 ± 0.10
K	207 ± 39	231 ± 2	210 ± 7	204 ± 6	219 ± 7	205 ± 3	225 ± 4
Mg	93.8 ± 18.5	99.9 ± 0.5	103.3 ± 0.3	97.3 ± 2.3	104.1 ± 2.4	96.6 ± 1.9	107.6 ± 1.8
Mn	12.2 ± 1.5	12.3 ± 0.1	12.4 ± 0.1	12.3 ± 0.3	12.5 ± 0.4	11.8 ± 0.3	12.2 ± 0.2
Mo	3.97 ± 0.70	4.04 ± 0.02	4.07 ± 0.04	4.02 ± 0.11	4.15 ± 0.11	3.95 ± 0.10	4.09 ± 0.03
Ni	8.34 ± 1.03	8.5 ± 0.1	8.55 ± 0.04	8.35 ± 0.23	8.37 ± 0.22	8.00 ± 0.26	8.36 ± 0.08
Pb	4.18 ± 0.57	3.88 ± 0.06	4.30 ± 0.03	4.25 ± 0.12	4.24 ± 0.11	3.99 ± 0.11	4.19 ± 0.07
P	99.0 ± 11.5	93.5 ± 1.1	102.3 ± 0.7	95.3 ± 2.6	98.9 ± 3.1	93.2 ± 2.4	100.8 ± 1.7
Se	2.79 ± 1.42	2.61 ± 0.12	3.05 ± 0.07	2.02 ± 0.08	3.25 ± 0.04	1.88 ± 0.13	2.71 ± 0.03
Sr	14.0 ± 3.7	14.3 ± 0.1	14.7 ± 0.1	14.0 ± 0.3	15.0 ± 0.3	13.8 ± 0.2	14.6 ± 0.2
V	4.95 ± 0.61	4.81 ± 0.02	5.06 ± 0.03	4.89 ± 0.14	5.19 ± 0.13	4.74 ± 0.11	5.04 ± 0.04

3.5 References

[1] G. L. Donati, R. S. Amais and C. B. Williams, Recent advances in inductively coupled plasma optical emission spectrometry, *J. Anal. At. Spectrom*., 32, **2017**, 1283-1296.

[2] N. H. Bings, J. O. Orlandini von Niessen and J. N. Schaper, Liquid sample introduction in inductively coupled plasma atomic emission and mass spectrometry – critical review, *Spectrochim. Acta, Part B*, 100, **2014**, 14-37.

[3] R. F. Browner and A. W. Boorn, The Achilles' heel of atomic spectroscopy?, *Anal. Chem*., 56, **1984**, 786A-798A.

[4] J. Borkowska-Burnecka, A. Lesniewicz and W. Zyrnicki, Comparison of pneumatic and ultrasonic nebulizations in inductively coupled plasma atomic emission spectrometry – matrix effects and plasma parameters, *Spectrochim. Acta, Part B*, 61, **2006**, 579-587.

[5] J. A. McLean, H. Zhang and A. Montaser, A direct injection high-efficiency nebulizer for inductively coupled plasma mass spectrometry, *Anal. Chem*., 70, **1998**, 1012-1020.

[6] S. Greenfield and P. B. Smith, The determination of trace metals in microliter samples by plasma torch excitation, *Anal. Chim. Acta*, 59, **1972**, 341-348.

[7] M. Grotti, F. Soggia and J. L. Todoli, Ultratrace analysis of Antarctic snow samples by reaction cell inductively coupled plasma mass spectrometry using a total-consumption micro-sample-introduction system, *Analyst*, 133, **2008**, 1388-1394.

[8] Y. Makonnen, J. Burgener and D. Beauchemin, Improvement of analytical performance in inductively coupled plasma optical emission spectrometry without

compromising robustness using an infrared-heated sample introduction system with a pneumatic nebulizer, *J. Anal. At. Spectrom*., 30, **2015**, 214-224.

[9] I. Novotny, J. C. Farinas, W. Jia-Liang, E. Poussel and J.M. Mermet, Effect of power and carrier gas flow rate on the tolerance to water loading in inductively coupled plasma atomic emission spectrometry, *Spectrochim. Acta, Part B*, 51, **1996**, 1517-1526.

[10] S. E. Long and R. F. Browner, Influence of water on conditions in the inductively coupled argon plasma, *Spectrochim. Acta, Part B*, 43, **1988**, 1461-1471.

[11] J. W. Olesik, and J. C. Fister III, Incompletely desolvated droplets in argon inductively coupled plasmas: their number, original size and effect on emission intensities, *Spectrochim. Acta, Part B*, 46, **1991**, 851-868.

[12] G. R. Peters and D. Beauchemin, Characterization of an interface allowing either nebulization or gas chromatography as the sample introduction system in ICPMS, *Anal. Chem*., 65, **1993**, 97-103.

[13] G. R. Peters and D. Beauchemin, Effect of pre-evaporating the solvent on the analytical performance of inductively coupled plasma mass spectrometry, *Spectrochim. Acta, Part B*, 48, **1993**, 1481-1494.

[14] S. Liu and D. Beauchemin, The effect of pre-evaporating on ion distributions in inductively coupled plasma mass spectrometry, *Spectrochim. Acta, Part B*, 61, **2006**, 157-163.

[15] S. Liu and D. Beauchemin, Effect of concomitant analytes on As signal during pre-evaporation of the solvent prior to introduction into inductively coupled plasma mass spectrometry, *Spectrochim. Acta, Part B*, 61, **2006**, 965-970.

[16] A. Asfaw and D. Beauchemin, Improvement of the capabilities of inductively coupled plasma optical emission spectrometry by replacing the desolvation system of an ultrasonic nebulization system with a pre-evaporation tube, *Spectrochim. Acta, Part B*, 65, **2010**, 376-384.

[17] A. Asfaw, W. R. MacFarlane and D. Beauchemin, Ultrasonic nebulization with an infrared heated pre-evaporation tube for sample introduction in ICP-OES: application to geological and environmental samples, *J. Anal. At. Spectrom.*, 27, **2012**, 1254-1263.

[18] A. Asfaw and D. Beauchemin, Combination of a multimode sample introduction system with a pre-evaporation tube to improve multi-element analysis by ICP-OES, *J. Anal. At. Spectrom.*, 27, **2012**, 80-91.

[19] E. Paredes, M. Grotti, J. M. Mermet and J. L. Todoli, Heated-spray chamber-based low sample consumption system for inductively coupled plasma spectrometry, *J. Anal. At. Spectrom.*, 24, **2009**, 903-910.

[20] R. Sanchez, J.L. Todoli, C. P. Lienemann and J. M. Mermet, Minimization of the effect of silicon chemical form in xylene matrices on ICP-AES performance, *J. Anal. At. Spectrom.*, 24, **2009**, 1382-1388.

[21] J. L. Todoli and J. M. Mermet, New torch design with an in-built chamber for liquid sample analysis by ICP-AES, *J. Anal. At. Spectrom.*, 17, **2002**, 345-351.

[22] J. L. Todoli and J. M. Mermet, Influence of the spray chamber design for vapor-based liquid sample introduction at room temperature in ICP-AES, *J. Anal. At. Spectrom.*, 17, **2002**, 211-218.

[23] J. M. Mermet and J. L. Todoli, Towards total-consumption pneumatic liquid micro-sample-introduction systems in ICP spectrometry, *Anal Bioanal Chem*., 378, **2004**, 57–59.

[24] F. Ardini, M. Grotti, R. Sanchez and J. L. Todoli, Improving the analytical performances of ICP-AES by using a high-temperature single-pass spray chamber and segmented-injections micro-sample introduction for the analysis of environmental samples, *J. Anal. At. Spectrom*., 27, **2012**, 1400-1404.

[25] R. Sanchez, J. L. Todoli, C. P. Lienemann and J. M. Mermet, Air-segmented, 5-µL flow injection associated with a 200° C heated chamber to minimize plasma loading limitations and difference of behavior between alkanes, aromatic compounds and petroleum products in inductively coupled plasma atomic emission spectrometry, *J. Anal. At. Spectrom*., 25, **2010**, 1888-1894.

[26] R. Sanchez, J. L. Todoli, C. P. Lienemann and J. M. Mermet, Universal calibration for metal determination in fuels and biofuels by inductively coupled plasma atomic emission spectrometry based on segmented flow injection and a 350° C heated chamber, *J. Anal. At. Spectrom*., 27, **2012**, 937-945.

[27] C. Sanchez, C. P. Lienemann and J. L. Todoli, Metal and metalloid determination in bioethanol through inductively coupled plasma-optical emission spectroscopy, *Spectrochim. Acta, Part B*, 115, **2016**, 16-22.

[28] M. Grotti, F. Ardini and J. L. Todoli, Total introduction of microsamples in inductively coupled plasma mass spectrometry by high-temperature evaporation chamber with a sheathing gas stream, *Anal. Chim. Acta*, 767, **2013**, 14-20.

[29] A. Canabate, E. Garcia-Ruiz, M. Resano and J. L. Todoli, Analysis of whole blood by ICP-MS equipped with a high temperature total sample consumption system, *J. Anal. At. Spectrom*., 32, **2017**, 78-87.

[30] A. Canabate, E. Garcia-Ruiz, M. Resano and J. L. Todoli, Cerebrospinal fluid elemental analysis by using a total sample consumption system operated at high temperature adapted to inductively coupled plasma mass spectrometry, *J. Anal. At. Spectrom*., 32, **2017**, 1916-1924.

[31] A. Al Hejami and D. Beauchemin, New infrared-heated sample introduction system for enhanced analytical performance of inductively coupled plasma optical emission spectrometry, *J. Anal. At. Spectrom*., 33, **2018**, 738-744.

[32] L. Gras, J. Mora, J. L. Todoli, A. Canals and V. Hernandis, Desolvation of acid solutions in inductively coupled plasma atomic emission spectrometry by infrared radiation. Comparison with a system based on microwave radiation, *Spectrochim. Acta, Part B*, 54, **1999**, 1321-1333.

[33] A. R. Eastgate, R. C. Fry and G. H. Gower, Radiation versus conduction in heated spray chamber desolvation for inductively coupled plasmas, *J. Anal. At. Spectrom*., 8, **1993**, 305-308.

[34] K. O. Douglass, N. Fitzgerald, B. J. Ingebrethsen and J. F. Tyson, Desolvating the sample aerosol with microwave radiation: further theoretical and experimental insight into the significance of such approach, *Spectrochim. Acta, Part B*, 59, **2004**, 261-270.

[35] T. K. Anderlini and D. Beauchemin, Improvement of sample introduction to inductively coupled plasma optical emission spectrometry using an ultrasonic nebulizer with an infrared heated pre-evaporation tube, *J. Anal. At. Spectrom*., 33, **2018**, 127-134.

[36] T. K. Anderlini and D. Beauchemin, Improvements to the analytical performance of inductively coupled plasma optical emission spectrometry by coupling a multi-mode sample introduction system to an infrared heated pre-evaporation tube, *J. Anal. At. Spectrom.*, 33, **2018**, 1068-1075.

[37] J. M. Mermet, Use of magnesium as a test element for inductively coupled plasma atomic emission spectrometry diagnostics, *Anal. Chim. Acta*, 250, **1991**, 85-94.

[38] A. Fernandez, M. Murillo, N. Carrion and J. M. Mermet, Influence of operating conditions on the effects of acids in inductively coupled plasma atomic emission spectrometry, *J. Anal. At. Spectrom.*, 9, **1994**, 217-221.

[39] J. L. Todoli and J. M. Mermet, Minimization of acid effects at low consumption rates in an axially viewed inductively coupled plasma atomic emission spectrometer by using micronebulizer-based sample introduction systems, *J. Anal. At. Spectrom.*, 13, **1998**, 727-734.

[40] X. Romero, E. Poussel and J. M. Mermet, Influence of the operating conditions on the efficiency of internal standardization in inductively coupled plasma atomic emission spectrometry, *Spectrochim. Acta, Part B*, 52, **1997**, 487-493.

[41] M. Grotti, C. Lagomarsino and J. M. Mermet, Effect of operating conditions on excitation temperature and electron number density in axially-viewed ICP-OES with introduction of vapours or aerosols, *J. Anal. At. Spectrom.*, 21, **2006**, 963-969.

[42] I. B. Brenner and A. T. Zander, Axially and radially viewed inductively coupled plasmas – a critical review, *Spectrochim. Acta, Part B*, 55, **2000**, 1195-1240.

Chapter 4

Infrared Heating of the Top Surface of a Cyclonic Spray Chamber to Improve the Analytical Performance of Inductively Coupled Plasma Optical Emission Spectrometry[3]

4.1 Introduction

Pneumatic nebulization consisting of a spray chamber and pneumatic nebulizer is a traditional sample introduction system for inductively coupled plasma (ICP) optical emission spectrometry (OES) and mass spectrometry (MS). The main drawback of this system is its low sample transport efficiency (typically less than 5%), which is why it is considered as the weakest link of ICP spectrometry. However, it is still a standard system for routine multi-elemental analysis by ICP-based techniques because of its simplicity, stability and relatively low cost [1-4]. Different systems have been used to enhance sample transport efficiency, for instance ultrasonic nebulization (USN) [5] and direct injection nebulization [6], but they have limited applications because of associated matrix effects and clogging issues, respectively.

Pre-evaporation of the analyte aerosol, without removing the solvent (usually water), prior to its introduction into the plasma is an alternative approach to significantly improve analytical performance of ICP spectrometry by enhancing sample transport efficiency [7-9]. Preserving water vapour has many advantages. Water acts as a load buffer in the plasma, which helps to minimize matrix effects [10]. Moreover, it is the main source of hydrogen,

[3] This chapter has been published: A. Al Hejami and D. Beauchemin, *J. Anal. At. Spectrom.*, 34, **2019**, 232-238.

which can facilitate energy transfer between the surrounding plasma and the central channel [11]. In addition, converting the sample aerosol into vapour greatly decreases the background noise associated with desolvation and vaporization of sample droplets in the plasma [12].

Greenfield and Smith [13] were the first to perform pre-evaporation, for the determination of trace elements in oil, organic compounds and blood. They heated a spray chamber by convective heating, thereby achieving total consumption of microliter samples, which improved the sensitivity of ICPOES by up to one order of magnitude. Peters and Beauchemin [14, 15] installed a pre-evaporation tube (PET) between the spray chamber and ICP torch, which was wrapped with heating tape and maintained at 400 °C. This improved sensitivity and detection limit for ICPMS, as a result of the reduction of noise arising from the decrease in average droplet size of the sample aerosol entering the plasma. Replacing the whole desolvation system of a USN system by a PET (400 °C) wrapped with heating tape also improved sensitivity, detection limit and plasma robustness for ICPOES [16]. Switching from a heating tape to infrared (IR) heating further improved the analytical performance achieved with the same USN system [17]. The combination of a PET with a multimode sample introduction system (MSIS) also improved the analytical figures of merit of ICPOES [18].

The so-called heated torch integrated sample introduction system (hTISIS), which consists of a pneumatic micro-nebuliser and single-pass spray chamber, has been used to improve sensitivity of ICPOES [19, 20] and ICPMS [8] by increasing sample transport efficiency. A variety of samples have been analysed by the hTISIS including

environmental, fuel, biological and environmental samples [21-28]. However, the hTISIS operates at very low sample uptake rate (*i.e*. 20 µL min^{-1}), which limits the analysis speed and consequently the sample throughput. Moreover, the micro-nebuliser precludes the applications of the hTISIS to samples with high salt content because of the ensuing blockage problems. A pneumatic nebulization in programmable temperature spray chamber (PN-PTSC) system combined with chemical vapour generation, where the spray chamber was heated to 40 °C – 60 °C significantly improved ICPOES sensitivity and detection limit without degradation in plasma thermal characteristics [29-32].

Because IR heating provides uniform and more efficient heating as well as better short-term stability, shorter washout time and less carry-over than convective heating with heating tape [33-35], which was nonetheless used in most of the above applications, it was employed to enhance transport efficiency for PN. Using ceramic block IR heaters to heat a non-commercial flip single-pass spray chamber improved the analytical performance of ICPOES although the sample uptake rate was an order of magnitude less than that used for PN at room temperature [9]. Sensitivity, detection limit and plasma robustness were also significantly improved for ICPOES using a new IR-heated modified cyclonic (MC) spray chamber with an IR lamp heater inserted in its centre [36]. The bulky block IR heater was replaced by a more flexible ceramic beaded rope IR heater, which provides both IR and convective heating [7]. The later was utilized to heat the entire spray chambers [37], the torch base for the MC [36], as well as a PET for USN [7] and MSIS [38] systems.

In the previous study performed in this laboratory [37], different spray chambers were entirely heated with IR rope heaters to achieve total sample consumption at low sample

uptake rate (*i.e*. 0.1 mL min^{-1}), which may affect the analysis time. The aim of the present work was to improve the analytical performance of ICPOES at a sample uptake rate close to 1 mL min^{-1} by using the IR rope heater to heat only the top of a quartz baffled cyclonic (BC) spray chamber along with its side arm, the elbow connection to the torch and the torch base. The outlet of the BC spray chamber in this work, which is normally used with ICPMS, is bent so as to connect to a horizontal torch, in contrast to those used previously, whose outlet is vertical so as to connect to a vertical torch. The resulting sensitivity, detection limit, precision and plasma robustness were compared with those obtained at room temperature with the same system and with previous IR-heated BC systems with vertical outlets. Certified reference materials of drinking and waste water were then analysed to verify the accuracy of the optimized system.

4.2 Experimental

4.2.1 Instrumentation

All measurements were made using a lateral view ARCOS ICPOES instrument (SPECTRO Analytical Instruments, Kleve, Germany) equipped with a Fassel-type torch (SCP Science, Baie d'Urfé, QC, Canada), a 50 mL quartz baffled cyclonic spray chamber and PFA nebulizer (both ESI Elemental Scientific, Omaha, NE, USA). To avoid melting by IR heating, the Teflon adapter outlet of the spray chamber (Figure 4.1) was replaced by a 12 mm/5 mm female quartz joint (by JRV Scientific Glass, Montreal, QC, Canada). The top surface of the spray chamber was heated by a ceramic beaded IR rope heater along with its side arm (7 cm long), elbow glass connection to the torch (7 cm long) and torch base (7 cm long, Figure 4.2). In total, the aerosol travelled a 21 cm IR-heated path between the spray chamber and the torch injector. The IR heating temperature was controlled by a

PL512 Mantle-Minder temperature controller (GLAS-COL Apparatus Company, Terre Haute, USA) connected to a thermocouple, which was inserted between the surface of the spray chamber and the IR rope heater.

Figure 4.1 Quartz baffled cyclonic spray chamber with Teflon adapter outlet (left) and 12 mm/5 mm female quartz joint (right).

Figure 4.2 Experimental set-up for IR-heated quartz baffled cyclonic spray chamber using ceramic beaded IR rope heater to heat from the top of the spray chamber to the base of the torch.

4.2.2 Chemicals

Individual elemental standard solutions of 1000 and 10000 mg L^{-1} (SCP Science) were diluted to prepare all multi-elemental standard solutions in 2% v/v HNO_3. Doubly deionized water 18 MΩ cm (Arium Pro UV/DI System, Sartorius Stedim Biotech, Goettingen, Germany) and sub-boiled HNO_3 were used to prepare all standard solutions. HNO_3 (ACS grade; Fisher Scientific, Ottawa, Canada) was purified using a DST-1000 sub-boiling distillation system (Savillex, Minnetonka, USA). Two certified reference materials of water, namely drinking water EP-L3 and waste water EU-L-3 (both SCP Science) were directly analysed to verify method accuracy.

4.2.3 Measurements of transport efficiency and washout time

The transport efficiency was measured in triplicate as the ratio of the mass of a 5 mg L^{-1} multi-elemental standard solution trapped by dry silica gel (in a 5 mL micropipette tip placed at the outlet of the spray chamber) over that aspirated [36,39]. The washout time, defined as the time taken for the steady-state signal from a 5 mg L^{-1} multi-elemental standard solution to return to baseline, was measured for the 14 emission lines that did not saturate the detector.

4.2.4 Optimization

The ICPOES instrumental operating parameters are listed in Table 4.1, along with those used in previous works [36, 37] on IR heating of cyclonic spray chambers. The R.F. power was set at 1.6 kW to prevent plasma extinction while the transport efficiency was increased upon IR heating of the sample aerosol. The plasma gas flow rate and observation height

were selected based on previous optimizations carried out on the same instrument [9]. The sample uptake rate was set at 0.9 mL min^{-1} for a good sample throughput. A 5 mg L^{-1} multi-elemental standard solution in 2% v/v HNO_3 along with the corresponding blank were used to perform multivariate optimization of the remaining parameters. A face-centred central composite experimental design [7, 9, 36-38] was utilized to optimize of the nebulizer gas flow rate (in the range of 0.6 – 1.2 L min^{-1}), the auxiliary gas flow rate (in the range of 0.6 – 2 L min^{-1}) and the IR heating temperature (in the range of 20 – 200 °C) as the goal was to find the best compromise parameters providing improved sensitivity for all analytes and robust plasma conditions. Plasma robustness was assessed by measuring the ionic to atomic emission intensity ratio of Mg II (280.270 nm)/ Mg I (285.213 nm). Plasma excitation under robust plasma conditions (when the Mg II / Mg I ratio is at least 10) is not remarkably affected by small changes in operating conditions and/or matrix effect [40-42].

4.2.5 Data analysis

The Smart Analyzer Vision software (SPECTRO Analytical Instruments) was utilized to select emission (atomic and ionic) lines free from potential spectroscopic interference for 21 elements. Minitab Release 17 statistical software (Minitab Inc., State College, PA, USA) was used to carry out all experimental designs for multivariate optimizations. All data processing, starting with blank subtraction, was done using Microsoft Excel 2013. Detection limit was computed as three times the standard deviation corresponding to the average emission signal intensity of 10 consecutive blanks divided by the calibration slope (*i.e.*, sensitivity).

Table 4.1 Experimental ICPOES operating conditions for the present work with BC spray chamber at room temperature (RT) or IR-heated using ceramic beaded rope IR heater (IR rope) along with conditions used in previous works with other cyclonic spray chamber designs.

Parameter	**Present work**		**Previous work** [37]		**Previous work** [36]
	RT	**IR rope**	**IR rope**	**IR block**	**IR lamp in the baffle**
Nebulizer	PFA nebulizer		SeaSpray nebulizer		Burgener nebulizer
Baffled cyclonic spray chamber design	With bent outlet		With straight outlet		With straight outlet and enlarged baffle
R.F. power (kW)	1.6	1.6	1.7	1.7	1.7
Plasma gas flow rate (L min^{-1})	14.5	14.5	14.5	14.5	14.5
Auxiliary gas flow rate (L min^{-1})	1	1.2	1	1.8	2
Nebulizer gas flow rate (L min^{-1})	1	0.9	0.85	0.9	0.6
Sheath gas flow rate (L min^{-1})	0	0	0.4	0.5	0
Plasma observation height (mm)	10	10	10	10	10
Sample uptake rate (mL min^{-1})	0.9	0.9	0.12	0.3	1
IR temperature (°C)	---	150	200	200	150

4.3 Results and discussion

4.3.1 Sensitivity, detection limit and precision

As reported in the literature [9, 17, 36, 37], sensitivity and detection limit were significantly improved (according to a paired Student's *t*-test at the 95% confidence level) upon IR heating the quartz BC spray chamber compared to those with the same system at room temperature (Tables 4.2 and 4.3). The improvement in sensitivity and detection limit

for BC(IR) with bent outlet used in this work was higher than that obtained with the previous BC (IR rope and block) [37] with straight outlet and MC(IR) [36] (Tables 4.2 and 4.3). The average (n = 26) factors of improvement in sensitivity and detection limit with the present set-up were 3.7 ± 0.6 and 7.6 ± 2.6, respectively. Moreover, the noise associated with droplet desolvation and vaporization [12] was clearly reduced with IR heating because a greater improvement in detection limit than in sensitivity was achieved, as was also previously observed with other IR-heated spray chambers [36, 37] and USN-PET(IR) [17].

The improvement in sensitivity is consistent with the significant enhancement in transport efficiency by 3.5 fold upon IR heating, from 4.5% (± 0.1) at room temperature to 15.7% (± 0.5) with IR heating. The latter is slightly better than the 11.7% (± 0.4) transport efficiency with MC(IR) [36] but less than the essentially 100% achieved when a whole BC was heated with IR rope [37]. Yet, despite the lower transport efficiency than in the latter case, similar detection limits were achieved in this work. This suggests that pre-evaporation of the whole aerosol, including the primary aerosol, with IR heating of a whole BC chamber, led to an aerosol with a broader size distribution, which translated into a noisier signal in the ICP than when mostly pre-evaporating the tertiary aerosol, as performed in the present work.

Table 4.2 Sensitivity ratio (IR-heated/room temperature) for different cyclonic spray chambers.

Analyte, nm	**BC (bent outlet; IR rope)**	**BC** [37] **(straight outlet)**		**MC** [36] **(straight outlet; IR lamp)**
		IR rope	**IR block**	
Al II 167.078	4.9			
As I 189.042	4.0	2.4	1.6	
Be II 313.107	3.9	2.6	2.3	
Be I 234.861	3.1	2.1	1.8	
Cd II 226.502	4.3	3.4	2.3	2.8
Cd I 228.802	3.0	2.5	1.9	
Ce II 413.765	3.2	3.6	3.5	
Co II 228.616	3.9	2.8	1.9	2.6
Cr II 267.716	3.8	4.8	3.4	2.4
Cr I 302.156	3.0	3.1	2.4	
Cu II 224.700	3.4	2.2	2.1	2.6
Fe II 238.204	3.8	2.8	2.1	2.5
K I 766.491	3.0	3.1	2.5	
La II 333.749	3.4	4.0	3.6	2.1
Mg II 280.270	3.7			2.5
Mg I 285.213	3.1	2.4	2.1	
Mn II 257.611	3.7	3.0	2.4	2.4
Ni II 221.648	4.1	3.7	2.5	
Pb II 220.353	4.0	3.7	2.2	2.7
P I 178.287	4.3			
S I 182.034	4.3	2.6	1.7	3.2
Se I 204.050	4.5	3.3	2.1	2.9
Sr II 421.552	3.2	2.9	2.7	
V II 292.402	3.5	3.9	3.3	2.3
Zn II 206.200	4.6			3.1
Zn I 213.856	3.2			

Table 4.3 Detection limit (3σ, n = 10; μg L^{-1}) for different spray chambers.

Element, nm	**BC (bent outlet)**		**DP*** [37] **(RT)**	**BC** [37] **(straight outlet)**		**DP** [36] **(RT)**	**MC** [36] **(straight outlet; IR lamp)**
	RT	**IR rope**		**IR rope**	**IR block**		
Al II 167.078	0.6	0.09					
As I 189.042	20	2	10	3	3		
Be II 313.107	1	0.1	0.3	0.1	0.09		
Be I 234.861	0.6	0.08	0.2	0.2	0.09		
Cd II 226.502	3	0.5	1	0.3	0.4	7	1
Cd I 228.802	3	0.8	2	0.6	0.6		
Ce II 413.765	306	70	116	72	39		
Co II 228.616	7	1	3	1	1	10	2
Cr II 267.716	11	1	10	2	1	12	6
Cr I 302.156	394	43	126	48	31		
Cu II 224.700	17	3	13	9	2	19	8
Fe II 238.204	6	1	3	0.7	0.5	6	2
K I 766.491	429	115	234	85	56		
La II 333.749	24	2	10	2	2	39	12
Mg II 280.270	0.6	0.09				0.9	0.2
Mg I 285.123	6	1	3	1	0.5		
Mn II 257.611	2	0.2	0.8	0.3	0.2	3	0.6
Ni II 221.648	9	1	3	1	0.6		
Pb II 220.353	46	5	29	7	5	81	22
P I 177.495	29	5					
S I 182.034	37	4	19	15	5	43	8
Se I 204.050	111	12	45	9	9	118	29
Sr II 421.552	3	0.7	0.8	0.8	0.3		
V II 292.402	12	1	6	2	2	15	6
Zn II 206.200	3	0.3				3	0.7
Zn I 213.856	2	0.5					

* Scott double-pass spray chamber used as a reference in previous works.

The percent relative standard deviation (%RSD) was used to assess the instrumental precision and is summarized in Table 4.4. The average %RSD for the partially heated BC was 1.0 ± 0.3 and 2.7 ± 0.4 at room temperature and with IR heating, respectively. Precision was systematically degraded upon IR heating with a ceramic beaded IR rope heater as

reported previously [37]. Nonetheless, consistent with the observed detection limits, the precisions of BC(IR) with bent outlet and BC(IR rope) with straight outlet are comparable, whereas the precisions of BC(IR block) and MC(IR) (both with straight outlet) are better than that of BC(IR) with bent outlet according to a paired Student's *t*-test at the 95% confidence level. This likely stems from the IR rope heater providing both convective and IR heating [7], whereas mostly IR heating is generated by the IR block heater [9, 17, 37] and the IR lamp heater [36]. Furthermore, heating the top of the spray chamber likely induced temperature gradients in the spray chamber.

The average (n = 14 elements) washout time was 17 ± 4 and 21 ± 5 for BC(RT) and BC(IR), respectively. Although the sample uptake rate was identical in both cases, the washout time with IR heating was significantly longer than that without heating according to a paired Student`s *t* test at the 95% confidence level. This is likely because of the temperature gradient induced by IR heating the top of the spray chamber, as well as the convective heating from the ceramic beads in contact with the spray chamber, which may favour analyte deposition on the walls during evaporation.

4.3.2 Plasma robustness

The Mg II/ Mg I ratio (n = 7) was 9.4 ± 0.1 and 11.1 ± 0.2 without and with IR heating, respectively. According to a Student's *t*-test at the 95% confidence level, IR heating significantly improved plasma robustness because increasing water vapour loading improves plasma excitation conditions [11, 20]. A ratio larger than 10 was also reported with IR-heated spray chambers [37] and USN-PET(IR) [17] on the same ICPOES instrument as well as with hTISIS [20].

Table 4.4 Precision (% RSD for 5 mg L^{-1}, n = 7) for different IR-heated cyclonic spray chambers.

Analyte, nm	BC (bent outlet)		**BC** [37] (straight outlet)		**MC** [36] (straight outlet; IR lamp)
	RT	**IR rope**	**IR rope**	**IR block**	
Al II 167.078	1.1	2.6			
As I 189.042	0.6	3.4	2.8	1.9	
Be II 313.107	1.4	3.2	3.2	2.9	
Be I 234.861	1.2	3.1	3.1	2.7	
Cd II 226.502	1.0	2.1	2.0	2.4	0.8
Cd I 228.802	0.9	2.1	1.7	2.2	
Ce II 413.765	1.2	3.1	2.7	2.1	
Co II 228.616	1.0	2.2	1.8	2.4	0.9
Cr II 267.716	1.0	3.1	2.5	2.0	0.6
Cr I 302.156	0.5	2.8	3.4	2.0	
Cu II 224.700	1.0	2.4	3.3	2.0	0.6
Fe II 238.204	0.9	2.3	1.9	2.4	0.7
K I 766.491	0.6	2.9	2.9	2.0	
La II 333.749	0.9	3.3	2.9	2.2	0.7
Mg II 280.270	1.4	3.0			0.9
Mg I 285.213	0.9	2.2	2.6	2.2	
Mn II 257.611	1.4	2.5	1.7	2.3	0.9
Ni II 221.648	1.1	3.0	2.0	2.1	
Pb II 220.353	0.8	2.8	2.9	1.9	0.9
P I 178.287	1.0	2.8			
S I 182.034	0.7	2.9	3.8	2.3	0.4
Se I 204.050	1.4	2.8	3.8	2.0	0.5
Sr II 421.552	1.3	3.0	3.5	2.7	
V II 292.402	0.9	3.3	2.5	2.2	0.7
Zn II 206.200	1.2	1.8			0.8
Zn I 213.856	0.9	2.2			

4.3.3 Analysis of water certified reference materials

Two certified reference materials of water were analysed using a simple external calibration without internal standardization or matrix-matching to assess the accuracy with the IR-heated BC spray chamber. The results, summarized in Table 4.5, fall within the

tolerance limits of the certified values. Hence, the IR-heated spray chamber is suitable as a sample introduction system for ICPOES.

Table 4.5 Concentrations in mg L^{-1} (± standard deviation, n = 3) measured for drinking water EP-L-3 and waste water EU-L3 certified reference materials with the baffled cyclonic spray chamber at room temperature or IR heated.

Analyte	CRM Drinking Water EP-L-3			CRM Waste Water EU-L-3		
	Certified ± tolerance limit	BC(RT)	BC(IR)	Certified ± tolerance limit	BC(RT)	BC(IR)
Al	100 ± 10	97.5 ± 4.2	107 ± 13	6.28 ± 1.50	7.51 ± 0.14	6.79 ± 0.31
As	10.6 ± 1.8	10.59 ± 0.02	10.4 ± 0.2	8.40 ± 0.98	7.71 ± 0.07	7.43 ± 0.09
Cd	1.97 ± 0.22	1.98 ± 0.02	1.89 ± 0.07	2.28 ± 0.42	2.24 ± 0.03	2.09 ± 0.01
Co	9.75 ± 1.22	10.08 ± 0.05	9.84 ± 0.23	8.25 ± 0.63	8.07 ± 0.09	7.78 ± 0.04
Cr	12.7 ± 1.0	13.3 ± 0.1	13.5 ± 0.3	6.26 ± 1.39	6.08 ± 0.10	6.04 ± 0.06
Fe	27.9 ± 3.7	27.95 ± 0.02	28.8 ± 0.6	5.80 ± 0.76	6.33 ± 0.09	6.38 ± 0.06
K	404 ± 42	411 ± 1	405 ± 5	207 ± 39	210 ± 2	205 ± 1
Mg	45.8 ± 4.3	47.2 ± 0.4	46.7 ± 0.6	93.8 ± 18.5	103.0 ± 0.9	102 ± 1
Mn	5.85 ± 0.58	5.82 ± 0.01	5.71 ± 0.11	12.2 ± 1.5	12.0 ± 0.1	11.9 ± 0.1
Ni	19.9 ± 2.0	20.5 ± 0.1	20.1 ± 0.5	8.34 ± 1.03	8.22 ± 0.09	7.96 ± 0.05
Sr	141 ± 10	141 ± 1	134.0 ± 0.4	14.0 ± 3.7	14.2 ± 0.08	13.1 ± 0.07
V	13.6 ± 1.1	14.4 ± 0.1	14.5 ± 0.2	4.95 ± 0.61	4.98 ± 0.08	4.80 ± 0.04
Zn	42.5 ± 3.6	43.00 ± 0.02	44.7 ± 1.2	3.05 ± 1.79	2.75 ± 0.04	2.67 ± 0.02

4.4 Conclusions

Infrared heating of the top surface of a cyclonic spray chamber improves sensitivity, detection limit and plasma robustness in ICPOES. The increased transport efficiency and reduction in noise lead to, in general, 3 – 12 fold improvement in sensitivity and detection limit compared to those obtained at room temperature at the same sample uptake rate. Moreover, accuracy was not jeopardized with IR heating, as very similar results were obtained with and without IR heating for the multi-elemental analysis of waters with a simple external calibration without internal standardization or matrix-matching. Future

work will include using the optimized system to improve the analytical performance of ICPMS.

4.5 References

[1] J. Mora, S Maestre, V. Hernandis and J. L. Todoli, Liquid-sample introduction in plasma spectrometry, *Trends Anal. Chem*., 22, **2003**, 123-132.

[2] N. H. Bings, J. O. Orlandini von Niessen and J. N. Schaper, Liquid sample introduction in inductively coupled plasma atomic emission and mass spectrometry – critical review, *Spectrochim. Acta, Part B,* 100, **2014**, 14-37.

[3] G. L. Donati, R.S. Amais and C. B. Williams, Recent advances in inductively coupled plasma optical emission spectrometry, *J. Anal. At. Spectrom*., 32, **2017**, 1283-1296.

[4] R. F. Browner and A. W. Boorn, The Achilles' heel of atomic spectroscopy?, *Anal. Chem*., 56, **1984**, 786A-798A.

[5] J. Borkowska-Burnecka, A. Lesniewicz and W. Zyrnicki, Comparison of pneumatic and ultrasonic nebulizations in inductively coupled plasma atomic emission spectrometry – matrix effects and plasma parameters, *Spectrochim. Acta, Part B,* 61, **2006**, 579-587.

[6] J. A. McLean, H. Zhang and A. Montaser, A direct injection high-efficiency nebulizer for inductively coupled plasma mass spectrometry, *Anal. Chem.*, 70, **1998**, 1012-1020.

[7] T. K. Anderlini and D. Beauchemin, Improvement of sample introduction to inductively coupled plasma optical emission spectrometry using an ultrasonic nebulizer with an infrared heated pre-evaporation tube, *J. Anal. At. Spectrom*., 33, **2018**, 127-134.

[8] M. Grotti, F. Soggia and J. L. Todoli, Ultratrace analysis of Antarctic snow samples by reaction cell inductively coupled plasma mass spectrometry using a total-consumption micro-sample-introduction system, *Analyst*, 133, **2008**, 1388-1394.

[9] Y. Makonnen, J. Burgener and D. Beauchemin, Improvement of analytical performance in inductively coupled plasma optical emission spectrometry without compromising robustness using an infrared-heated sample introduction system with a pneumatic nebulizer, *J. Anal. At. Spectrom*., 30, **2015**, 214-224.

[10] I. Novotny, J.C. Farinas, W. Jia-Liang, E. Poussel and J. M. Mermet, Effect of power and carrier gas flow rate on the tolerance to water loading in inductively coupled plasma atomic emission spectrometry, *Spectrochim. Acta, Part B*, 51, **1996**, 1517-1526.

[11] S. E. Long and R.F. Browner, Influence of water on conditions in the inductively coupled argon plasma, *Spectrochim. Acta, Part B*, 43, **1988**, 1461-1471.

[12] J. W. Olesik, and J. C. Fister III, Incompletely desolvated droplets in argon inductively coupled plasmas: their number, original size and effect on emission intensities, *Spectrochim. Acta, Part B*, 46, **1991**, 851-868.

[13] S. Greenfield and P.B. Smith, The determination of trace metals in microliter samples by plasma torch excitation, *Anal. Chim. Acta*, 59, **1972**, 341-348.

[14] G. R. Peters and D. Beauchemin, Characterization of an interface allowing either nebulization or gas chromatography as the sample introduction system in ICPMS, *Anal. Chem*., 65, **1993**, 97-103.

[15] G. R. Peters and D. Beauchemin, Effect of pre-evaporating the solvent on the analytical performance of inductively coupled plasma mass spectrometry, *Spectrochim. Acta, Part B*, 48, **1993**, 1481-1494.

[16] A. Asfaw and D. Beauchemin, Improvement of the capabilities of inductively coupled plasma optical emission spectrometry by replacing the desolvation system of an ultrasonic nebulization system with a pre-evaporation tube, *Spectrochim. Acta, Part B*, 65, **2010**, 376-384.

[17] A. Asfaw, W. R. MacFarlane and D. Beauchemin, Ultrasonic nebulization with an infrared heated pre-evaporation tube for sample introduction in ICP-OES: application to geological and environmental samples, *J. Anal. At. Spectrom.*, 27, **2012**, 1254-1263.

[18] A. Asfaw and D. Beauchemin, Combination of a multimode sample introduction system with a pre-evaporation tube to improve multi-element analysis by ICP-OES, *J. Anal. At. Spectrom.*, 27, **2012**, 80-91.

[19] R. Sanchez, J. L. Todoli, C. P. Lienemann and J. M. Mermet, Minimization of the effect of silicon chemical form in xylene matrices on ICP-AES performance, *J. Anal. At. Spectrom.*, 24, **2009**, 1382-1388.

[20] E. Paredes, M. Grotti, J. M. Mermet and J. L. Todoli, Heated-spray chamber-based low sample consumption system for inductively coupled plasma spectrometry, *J. Anal. At. Spectrom.*, 24, **2009**, 903-910.

[21] F. Ardini, M. Grotti, R. Sanchez and J. L. Todoli, Improving the analytical performances of ICP-AES by using a high-temperature single-pass spray chamber and segmented-injections micro-sample introduction for the analysis of environmental samples, *J. Anal. At. Spectrom.*, 27, **2012**, 1400-1404.

[22] R. Sanchez, J. L. Todoli, C. P. Lienemann and J. M. Mermet, Air-segmented, 5-µL flow injection associated with a 200 °C heated chamber to minimize plasma loading limitations and difference of behavior between alkanes, aromatic compounds and

petroleum products in inductively coupled plasma atomic emission spectrometry, *J. Anal. At. Spectrom*., 25, **2010**, 1888-1894.

[23] R. Sanchez, J. L. Todoli, C. P. Lienemann and J. M. Mermet, Universal calibration for metal determination in fuels and biofuels by inductively coupled plasma atomic emission spectrometry based on segmented flow injection and a 350 °C heated chamber, *J. Anal. At. Spectrom*., 27, **2012**, 937-945.

[24] C. Sanchez, C. P. Lienemann and J. L. Todoli, Metal and metalloid determination in bioethanol through inductively coupled plasma-optical emission spectroscopy, *Spectrochim. Acta, Part B*, 115, **2016**, 16-22.

[25] C. Sanchez, C. P. Lienemann and J. L. Todoli, Analysis of bioethanol samples through inductively coupled plasma mass spectrometry with a total sample consumption system, *Spectrochim. Acta, Part B*, 124, **2016**, 99-108.

[26] M. Grotti, F. Ardini and J. L. Todoli, Total introduction of microsamples in inductively coupled plasma mass spectrometry by high-temperature evaporation chamber with a sheathing gas stream, *Anal. Chim. Acta*, 767, **2013**, 14-20.

[27] A. Canabate, E. Garcia-Ruiz, M. Resano and J. L. Todoli, Analysis of whole blood by ICP-MS equipped with a high temperature total sample consumption system, *J. Anal. At. Spectrom*., 32, **2017**, 78-87.

[28] A. Canabate, E. Garcia-Ruiz, M. Resano and J. L. Todoli, Cerebrospinal fluid elemental analysis by using a total sample consumption system operated at high temperature adapted to inductively coupled plasma mass spectrometry, *J. Anal. At. Spectrom*., 32, **2017**, 1916-1924.

[29] K. Jankowski, J. Giersz and M. Paprocka, Improved determination of iodine by sequential (photo) chemical vapor generation and pneumatic nebulization in the programmable temperature spray chamber and inductively coupled plasma optical emission spectrometry *Microchem. J.*, 113, **2014**, 17-22.

[30] J. Giersz and K. Jankowski, Effect of temperature on direct chemical vapor generation for plasma optical emission spectrometry: An application of programmable temperature spray chamber, *Microchem. J.*, 124, **2016**, 1-8.

[31] J. Giersz, M. Bartosiak and K. Jankowski, Sensitive determination of Hg together with Mn, Fe, Cu, by combined photochemical vapor generation and pneumatic nebulization in the programmable temperature spray chamber and inductively coupled plasma optical emission spectrometry, *Talanta*, 167, **2017**, 279-285.

[32] J. Giersz, M. Bartosiak and K. Jankowski, Spectroscopic diagnostics of axially viewed inductively coupled plasma and microwave induced plasma coupled to photochemical vapor generation with pneumatic nebulization inside a programmable temperature spray chamber, *J. Anal. At. Spectrom*., 32, **2017**, 1885-1892.

[33] K. O. Douglass, N. Fitzgerald, B. J. Ingebrethsen and J. F. Tyson, Desolvating the sample aerosol with microwave radiation: further theoretical and experimental insight into the significance of such approach, *Spectrochim. Acta, Part B*, 59, **2004**, 261-270.

[34] L. Gras, J. Mora, J. L. Todoli, A. Canals and V. Hernandis, Desolvation of acid solutions in inductively coupled plasma atomic emission spectrometry by infrared radiation. Comparison with a system based on microwave radiation, *Spectrochim. Acta, Part B*, 54, **1999**, 1321-1333.

[35] A. R. Eastgate, R. C. Fry and G. H. Gower, Radiation versus conduction in heated spray chamber desolvation for inductively coupled plasmas, *J. Anal. At. Spectrom*., 8, **1993**, 305-308.

[36] A. Al Hejami and D. Beauchemin, New infrared-heated sample introduction system for enhanced analytical performance of inductively coupled plasma optical emission spectrometry, *J. Anal. At. Spectrom*., 33, **2018**, 738-744.

[37] A. Al Hejami and D. Beauchemin, Infrared heating of commercially available spray chambers to improve analytical performance of inductively coupled plasma optical emission spectrometry, *J. Anal. At. Spectrom*., 33, **2018**, 2008-2014.

[38] T. K. Anderlini and D. Beauchemin, Improvements to the analytical performance of inductively coupled plasma optical emission spectrometry by coupling a multi-mode sample introduction system to an infrared heated pre-evaporation tube, *J. Anal. At. Spectrom*., 33, **2018**, 1068-1075.

[39] R. P. Lamsal, G. Jerkiewicz and D. Beauchemin, Flow injection single particle inductively coupled plasma mass spectrometry: an original simple approach for the characterization of metal-based nanoparticles, *Anal. Chem*., 88, **2016**, 10552-10558.

[40] J. M. Mermet, Use of magnesium as a test element for inductively coupled plasma atomic emission spectrometry diagnostics, *Anal. Chim. Acta*, 250, **1991**, 85-94.

[41] A. Fernandez, M. Murillo, N. Carrion and J. M. Mermet, Influence of operating conditions on the effects of acids in inductively coupled plasma atomic emission spectrometry, *J. Anal. At. Spectrom*., 9, **1994**, 217-221.

[42] J. L. Todoli and J. M. Mermet, Minimization of acid effects at low consumption rates in an axially viewed inductively coupled plasma atomic emission spectrometer by using

micronebulizer-based sample introduction systems, *J. Anal. At. Spectrom.*, 13, **1998**, 727-734.

Chapter 5

Effect of Sheathing the Sample Aerosol with Hydrogen, Nitrogen or Water Vapour on the Analytical Performance of Solid Sampling Electrothermal Vaporisation Coupled to Inductively Coupled Plasma Optical Emission Spectrometry[4]

5.1 Introduction

Solid sampling (SS) electrothermal vaporisation (ETV) is an attractive alternative sample introduction system to pneumatic nebulisation, which is the Achilles' heel of inductively coupled plasma (ICP) optical emission spectrometry (OES) and mass spectrometry (MS). Indeed, ETV-ICP spectrometry has several interesting features, such as high sample transport efficiency (up to 100%), direct analysis of a variety of sample types, very low sample mass requirement, easy removal of organic matrix during the pyrolysis step and low detection limit [1, 2]. The versatility of ETV for sample introduction into the ICP stems from its ability to accommodate non-aqueous solutions, samples with high dissolved salt or acid concentration, slurries and especially solid samples [3]. As a result, SS-ETV-ICPOES has been used for the analysis of biological [4–7], environmental [8, 9], high-purity materials [10, 11] and forensic samples [12, 13].

On the other hand, ETV-ICP spectrometry may experience severe matrix effects [14] as a result of the high transport efficiency. Fortunately, this can be reduced by judicious selections of ETV temperature programs and chemical modifiers [15, 16]. However, because of the sudden introduction of a large sample amount into the ICP at different rates, plasma load in ETV-ICP spectrometry can be considerably high, especially if no venting

[4] This chapter has been published: A. Al Hejami and D. Beauchemin, *J. Anal. At. Spectrom*., **2019**, DOI: 10.1039/c8ja00266e.

of the solvent and/or matrix is done, as with the commercially available SS-ETV system that connects directly to the base of the torch, and if temporal separation of the analyte and the matrix through judicious selection of the temperature program is not possible. This may deteriorate plasma robustness and stability by changing plasma temperature and electron number density [1]. An argon emission line can be used as an internal standard to minimise the effect of changing plasma conditions in ETV-ICPOES [7, 9, 12, 13]. A mixed-gas (Ar–N_2 or Ar–H_2) plasma, where N_2 or H_2 is introduced into any gas flow (outer, auxiliary, carrier gas) of the ICP torch, may be used to improve ICP stability and robustness [17, 18]. For instance, matrix effects were mitigated by addition of 2% N_2 to the outer plasma gas in ETV-ICPMS, at the expense of sensitivity however [17]. Addition of N_2 to the outer plasma gas enhances sample–plasma interactions from the narrower central channel diameter and overall smaller plasma volume that result, leading to increase plasma temperatures and electron densities [19–24].

No attempt has been made to study the effect of adding N_2 to the central channel of a dry Ar plasma in ETV-ICP spectrometry. Yet, plasma robustness was remarkably improved, without degradation of analytical performance, by adding 20 mL min^{-1} N_2 to the central channel of the plasma in ICPOES with pneumatic nebulisation using an aerosol desolvation system [25] and ultrasonic nebulization [26]. The resulting improvement in energy transfer between the bulk plasma and the central channel mitigated matrix effects. Moreover, the addition of 5–10 mL min^{-1} N_2 to the central channel gas flow in laser ablation ICPMS enhanced sensitivity by a factor of 2–3 for most of the 65 analytes investigated [27]. Similar results would be expected from N_2 addition to the central ICP channel in SS-ETV-ICPOES.

The analytical performance of ETV-ICPOES was also improved when adding a small amount of H_2 to the carrier gas flow [18]. This was explained by increased plasma excitation temperature and electron number density stemming from the high thermal conductivity of H_2 relative to Ar, which enhances energy transfer between the surrounding plasma and the central channel where the sample is injected. Similar results were found upon adding 20–100 mL min^{-1} H_2 to the carrier gas in ETV-ICPMS [28].

Coupling SS-ETV-ICPOES to a nebulisation/pre-evaporation system also enhanced plasma robustness and stability [29]. The water aerosol exiting the spray chamber was pre-evaporated and continuously introduced into the plasma through a sheathing device, which was infrared (IR) heated to 400 °C along with the base of the torch. The analyte aerosol from the ETV unit was introduced via the side arm of the sheathing device allowing the introduction of more than twice the amount of solid sample without extinguishing the plasma. As a result, sensitivity and detection limit were significantly improved. SS-ETV-ICPOES coupled to a nebulisation/pre-evaporation system was recently applied to direct multi-elemental analysis of glutinous rice flour samples [30].

The aim of this study was to evaluate the analytical performance of SS-ETV-ICPOES with a sheathing device for the introduction of H_2, N_2 or water vapour. In the latter case, the wet aerosol exiting a pneumatic nebulisation system was pre- evaporated using IR heating prior to its introduction into the device. Addition of H_2, N_2 or water vapour into the central gas flow of the ICP torch was done through the side arm of a sheathing device, whereas the analyte aerosol exiting the ETV unit was introduced through its base. Sensitivity, detection limit and percent relative standard deviation (% RSD) were compared under almost the same set of operating conditions, using conventional SS-ETV-ICPOES

as reference. To the best of the Authors' knowledge, this is the first attempt to study the effect of N_2 addition to the central channel of the plasma on the analytical performance of SS-ETV-ICPOES.

5.2 Experimental

5.2.1 Instrumentation

All experiments were carried out using a lateral view ARCOS ICPOES instrument (SPECTRO Analytical Instruments, Kleve, Germany) equipped with a conventional Fassel-type torch (SCP Science, Baie d'Urfé, QC, Canada). A 1 m long Teflon tube with 5 mm internal diameter connected the ETV unit (ETV 4000C, Spectral Systems, Furstenfeldbruck, Germany) outlet to the ICP torch injector for the conventional SS-ETV-ICPOES system or to the base of a sheathing device in all other cases. Pyrolytically coated graphite boats (Meinhard, Golden, CO, USA) containing solid samples were manually inserted into the graphite furnace using tweezers. A mass flow controller (MCR-Series, Alicat Scientific, Tucson, AZ, USA) controlled the flow rate of ultra-high purity N_2 or H_2 to the central channel of the plasma through the side arm of the sheathing device (Figure 5.1a).

To introduce water vapour (Figure 5.1b), doubly deionised water (DDW) with 18 Ω cm resistivity (Arium Pro UV/DI System, Sartorius Stedim Biotech, Goettingen, Germany) was continuously nebulised by a SeaSpray nebuliser (Glass Expansion, Pocasset, MA, USA) into a Scott double-pass spray chamber (SPECTRO Analytical Instruments, Kleve, Germany) that was connected to the side arm of the sheathing device. Two 6.0 cm wide and 24.5 cm long ceramic block IR heaters (Process Heaters Inc.,

Toronto, Canada) heated the outlet of the spray chamber, sheathing device and bottom of the torch to 400 °C. The temperature for each IR heater was controlled by a PL512 Mantle-Minder temperature controller (GLAS-COL Apparatus Company, Terre Haute, IN, USA) connected to a thermocouple located on the inner surface of the heater (facing the sheathing device).

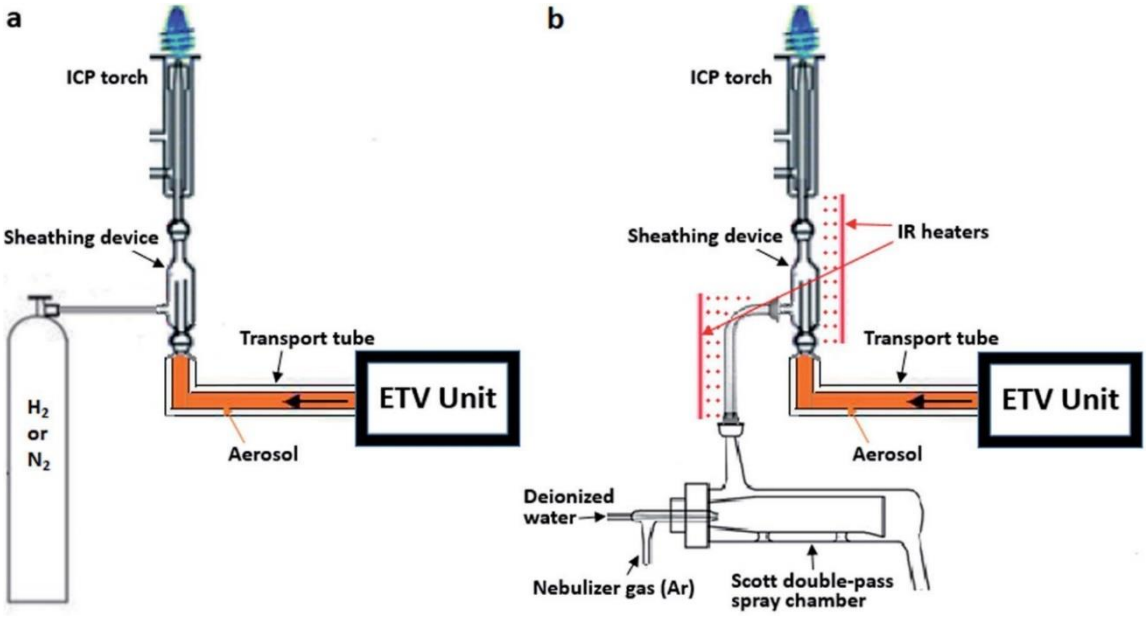

Figure 5.1 SS-ETV-ICPOES set-ups with different sheaths: (a) H_2 or N_2 sheath; (b) water vapour sheath.

5.2.2 Optimisation of SS-ETV-ICPOES operating conditions

Instrumental operating conditions for SS-ETV-ICPOES are summarised in Table 5.1. The ICPOES operating parameters were selected based on previous optimisations carried out on the same instrument [9, 29-31]. The temperature program was adopted from previous optimisations for soil analysis [9, 29, 31]. Because the reaction gas (CCl_2F_2) previously used was no longer available in Canada, it was replaced by CF_4. Multivariate

optimisation of the bypass gas (in the 0.3–0.6 L min^{-1} range), the carrier gas (in the 0.1–0.3 L min^{-1} range) and the reaction gas (in the 1–10 mL min^{-1} range) flow rates was thus performed to find the best compromise ETV conditions in terms of sensitivity with each SS-ETV-ICPOES setup. Minitab Release 17 statistical software (Minitab Inc., State College, PA, USA) was used to this end.

Table 5.1 Operating conditions for SS-ETV-ICPOES.

	No sheath	N_2 sheath	H_2 sheath	Water vapour sheath
ICPOES parameter				
Radio frequency power (kW)	1.4	1.4	1.4	1.4
Ar plasma gas flow rate (L min^{-1})	13	13	13	13
Ar auxiliary gas flow rate (L min^{-1})	2	2	2	2
Ar nebulizer gas flow rate (L min^{-1})	—	—	—	0.4
Sheath gas flow rate (mL min^{-1})	—	45	30	—
Observation height above the load coil (mm)	10	10	10	10
Sample uptake rate (mL min^{-1})	—	—	—	1.5
IR heating temperature (°C)	—	—	—	400
ETV parameter				
Ar carrier gas flow rate (L min^{-1})	0.12	0.12	0.12	0.12
Ar bypass gas flow rate (L min^{-1})	0.5	0.5	0.5	0.25
CF_4 flow rate (mL min^{-1})	9	9	9	9

ETV temperature program

Step	T (°C)	Ramp (s)	Hold (s)	Step	T (°C)	Ramp (s)	Hold (s)
1	400	0	20	2	20	0	15
3	2200	0	30	4	20	0	20

N_2 and H_2 sheath gas flow rates (in the 0–50 mL min^{-1} range) were optimised for maximum analyte sensitivity and compromise conditions for multi-elemental analysis were selected. For the nebulisation/pre-evaporation set-up, the nebuliser gas flow rate was set to 0.4 L min^{-1}, which is the minimum recommended by the manufacturer. The bypass gas

flow rate was then re-optimised to keep the total injector gas flow rate (*i.e*. nebuliser gas, bypass gas, carrier gas and reaction gas flow rates) as low as possible (around 0.8 L min^{-1}) so as to achieve acceptable residence time to maximise analyte sensitivity.

5.2.3 Chemicals

Carbon tetrafluoride (CF_4, MEGS Gages, Ottawa, ON, Canada) was added to the carrier gas as a reaction gas (chemical modifier) to enhance analyte volatility [32, 33]. Standard reference materials (SRMs) obtained from the National Institute for Standards and Technology (Gaithersburg, MD, USA) consisted of: urban particulate matter SRM 1648a, for optimisation of SS-ETV- ICPOES parameters, Montana Soil SRM 2710 for external calibration and comparison purposes, and Montana soil SRM 2711 and coal fly ash SRM 1633c to verify the accuracy of multi-elemental determinations.

Multi-elemental standard solutions in 2% v/v HNO_3 were prepared by serial dilution of 10000 mg L^{-1} individual elemental standard solutions (SCP Science) with doubly deionized water and sub-boiled HNO_3. The HNO_3 (ACS grade; Fisher Scientific, Ottawa, ON, Canada) was purified using a DST-1000 sub-boiling distillation system (Savillex, Minnetonka, MN, USA).

5.2.4 External calibration

Five-point multi-elemental calibrations were conducted using 1–5 mg aliquots of SRM 2710. For external calibration with standard solutions, 15 mL aliquots of standard solutions were placed onto graphite boats and dried with an IR heater before their introduction into the ETV furnace.

5.2.5 Data analysis

Transient signals were acquired by the Smart Analyses Vision software of the ICPOES instrument and exported to Microsoft Excel 2013 for data processing. Before integration of peak area, the analyte signal was normalised using an Ar emission line (763.511 nm) by computing the point-by-point ratio of analyte signal intensity over Ar signal intensity to compensate forsample loading effects under dry plasma conditions [9, 12, 13, 29]. For external calibration, peak area of the blank-subtracted internally standardised signal was plotted as a function of the absolute analyte content in the SRM. Internal standardisation with Ar improved the linearity of calibration curves [7, 29]. Empty graphite boats were used as blanks. Detection limit was computed as three times the standard deviation of the signal of ten consecutive blanks divided by sensitivity (*i.e*. the slope of the calibration curve).

5.3 Result and discussion

5.3.1 Effect of internal standardisation

Figure 5.2 shows the effect of internal standardisation with an Ar emission line on the analyte emission signal profile. It not just compensated for sample loading effects, thereby improving the linearity of calibration curves [9, 12, 13, 29], but also improved the Gaussian shape of the transient temporal peak. Whereas a robust plasma can withstand a greater amount of sample [29], a maximum of 5 mg was introduced, as it can be handled by the conventional setup and thus enables direct comparison of the results with sheath to those without sheath.

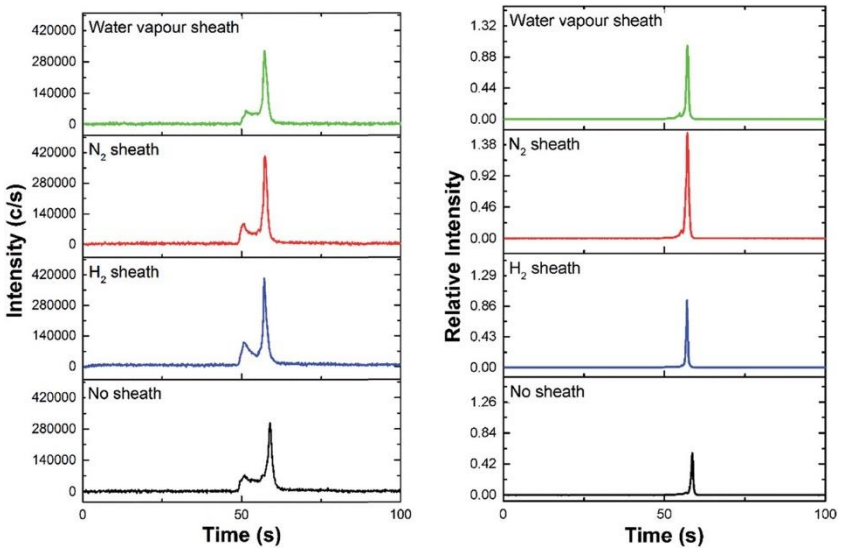

Figure 5.2 Effect of internal standardization on the Mo II emission signal profile at 202.095 nm resulting from 3 mg of Montana soil SRM 2710. Left-hand side: without, right-hand side: with Ar-based internal standardization.

5.3.2 Sensitivity and detection limit

The parameters of each calibration curve, *i.e.*, the slope and intercept, with and without sheath can be found in Table A1 (see Appendix). Detection limits are compiled in Table A2 (see Appendix). Tables 5.2 and 5.3 show that sensitivity and detection limit were significantly improved (according to a paired Student's *t* test at the 95% confidence level) compared to those with conventional SS-ETV-ICPOES upon adding H_2, N_2 or water vapour as a sheath around the sample aerosol. For all analytes, the average improvement in sensitivity was 1.4 ± 0.4, 2.9 ± 0.7 and 2.0 ± 0.5 with H_2, N_2 and water vapour sheaths, respectively, with corresponding average improvements in detection limit of 2.1 ± 1.5, 5.0 ± 3.1 and 3.4 ± 1.6. These results support previous reports of significant improvement in excitation and ionisation energies of the ICP with the addition of H_2, N_2 or water vapour to its central channel [18, 27, 29].

Table 5.2 Sensitivity ratios (with/without sheathing) for SS-ETV-ICPOES, values above 1 indicating improvements with sheathing.

Analyte, nm	E_{sum}* **(eV)** [34]	H_2 **sheath**	N_2 **sheath**	**Water vapour sheath**
Al II 167.078	13.41	2.4	2.4	2.4
Al I 176.641	7.03	1.1	2.3	2.1
Cd II 226.502	14.46	1.7	3.3	2.3
Cd I 228.802	5.42	1.3	2.8	2.5
Co II 228.616	13.7	1.7	3.2	2.4
Cr II 205.618	12.8	1.6	3.6	1.6
Cu II 224.700	15.96	0.7	1.2	1.2
Mn I 403.076	3.08	0.9	3	1.8
Mo II 202.095	13.23	1.4	4.1	1.4
Ni II 174.828	14.72	1.4	3.6	2.1
P I 178.287	6.95	1.3	2.5	1.8
V II 292.402	11.37	1.8	2.4	2.9
Zn II 206.200	15.4	0.9	3.1	1.7

* Excitation energy for atomic emission lines and sum of the ionization and excitation energies for ionic emission lines.

Table 5.3 Detection limit (3s, n = 10) ratios (without/with sheathing) for SS-ETV-ICPOES, values above 1 indicating improvements with sheathing.

Analyte, nm	E_{sum} **(eV)** [34]	H_2 **sheath**	N_2 **sheath**	**Water vapour sheath**
Al II 167.078	13.41	5.6	3.5	5.9
Al I 176.641	7.03	0.5	2.5	1.7
Cd II 226.502	14.46	3.5	10	3.5
Cd I 228.802	5.42	3	3	3
Co II 228.616	13.7	1.7	3.3	2.5
Cr II 205.618	12.8	4	13	6.7
Cu II 224.700	15.96	1	2	2
Mn I 403.076	3.08	1.3	4.4	4
Mo II 202.095	13.23	1.3	5	2.5
Ni II 174.828	14.72	1	4	2
P I 178.287	6.95	1.3	5	2.5
V II 292.402	11.37	2	4	5
Zn II 206.200	15.4	1.7	5	2.5

The sensitivity improvements differ from those in a previous study where water vapour was introduced along with the ETV effluent [29], because of several important differences. Several emission lines (notably for Cd, Cu and Mn) were different than in the present work. A valve was previously used to vent pyrolysis products whereas everything was introduced in the plasma in this study. Furthermore, the ETV effluent entered through the side arm of the sheathing device while water vapour was introduced through its base. This led to a significant loss of aerosol within the sheathing device. In this work, introducing water vapour through the side arm (as for H_2 or N_2) enabled the introduction of the ETV effluent in its centre, which drastically reduced aerosol loss within the sheathing device.

The improvements in sensitivity and detection limit follow the order N_2 sheath > water vapor sheath > H_2 sheath. Similarly, when a small amount of H_2 or N_2 was added to the main plasma gas inlet in ICPMS, the signal enhancement was greater with N_2 than with H_2 [35]. This is likely because an addition of N_2 to the central channel significant increases the excitation temperature of the plasma [2, 36].

The improvements in sensitivity and detection limit with H_2 stem from the beneficial effect of its higher thermal conductivity than that of Ar on plasma characteristics [18]. However, the introduction of water vapour, which would dissociate into hydrogen and oxygen in the plasma, resulted in similar or improved sensitivity and detection limit compared to a sole addition of H_2. Water is known to act as a load buffer in the plasma [37, 38], which enables the introduction of a greater quantity of sample, thereby improving sensitivity and detection limit, as reported previously [29].

In some cases, the improvement in sensitivity and especially in detection limit was greater for ionic than atomic emission lines, as exemplified by Al and Cd in Tables 5.2 and 5.3 [29]. This might stem from emission lines with high excitation potentials (for atomic lines) and high sum of ionisation and excitation potentials (for ionic lines) being more susceptible to changes in plasma excitation conditions [39]. However, the sensitivity and detection limit improvement factors did not correlate with the corresponding E_{sum}. The Mn I 403.076 nm emission signal was monitored because the Mn II 257.610 nm emission signal saturated the detector. The fact that the Mn emission at 403.076 nm nearly saturated the detector may explain the apparently anomalous behaviour of this line.

5.3.3 Effect of sheathing gas or water vapour on background emission

Average background signals for different SS-ETV-ICPOES conditions can be found in Table A3 (see Appendix). Addition of H_2 and N_2 into the central flow of the ICP torch not only increased the analyte emission signal but also the background. This is in agreement with previous works that reported an increase in background signal upon addition of H_2 [18] or N_2 [25] to the carrier gas. The increase in background signal follows the order H_2 sheath > N_2 sheath > no sheath > water vapour sheath. The enhancement with H_2 sheath, which was on average 2.6 ± 0.6 fold that without sheath, was higher than the enhancement in sensitivity. In contrast, the enhancement in background signal with N_2 sheath, which was on average 1.3 ± 0.2 fold that without sheath, was lower than the enhancement in sensitivity. However, the relative standard deviation (% RSD) of the background signal (for all analytes, n = 13) was 8.7 ± 10.0, 2.6 ± 2.4, 4.2 ± 4.8 and 7.9 ± 6.3 with no sheath, H_2 sheath, N_2 sheath and water vapour sheath, respectively. Hence, the background signal

with H_2 and N_2 sheaths increases concurrently with an improvement in RSDs. The lowest background signal with water vapour sheath may be a result of the higher total central gas flow rate in the ICP torch (the sum of nebuliser, carrier and bypass gas flow rates) versus that without sheath. The background signal indeed decreases as the carrier gas flow rate increases [39–41].

5.3.4 Plasma robustness

The Mg II (280.270 nm)/Mg I (285.213 nm) ratio is commonly used to assess plasma robustness, a ratio of at least 8 indicating robust plasma conditions under which plasma excitation is not remarkably affected by matrix effects [42, 43]. The Mg II/Mg I ratio (n = 3) determined using a 1 mg L^{-1} standard solution was 6.13 ± 0.02, 7.4 ± 0.3, 7.9 ± 0.1 and 6.9 ± 0.1 with no sheath, H_2 sheath, N_2 sheath and water vapour sheath respectively. Plasma excitation characteristics are apparently improved by addition of H_2 [18], N_2 [25, 36] or water vapour [38, 44] into the plasma. This is supported by the improvement in sensitivity and detection limit obtained with H_2, N_2 and water vapour sheaths. In fact, the order of improvement in sensitivity and detection limit is similar to that in plasma robustness. The greatest Mg II/Mg I ratios with N_2 indicate that the best excitation conditions were obtained with a N_2 sheath, in agreement with a previous study [36].

5.3.5 Accuracy and precision

Method accuracy was verified by analysing Montana soil SRM 2711 as a sample with Montana soil SRM 2710 for external calibration and using Ar 763.511 nm emission line for internal standardisation. The results in Table 5.4 show good agreement with the certified values for all sheaths (which was verified using a Student's *t* test at the 95%

confidence level). The instrumental precision (expressed as % relative standard deviation, % RSD) when analysing five replicate 3 mg aliquots of SRM 2711 with the different set-ups are also comparable. The average % RSD for conventional SS-ETV-ICPOES (8.7 ± 2.7), H_2 sheath (7.8 ± 3.7), N_2 sheath (11.9 ± 4.9) and water vapour sheath (11.3 ± 3.9) are comparable with those previously reported for SS-ETV- ICPOES [6, 29, 31, 45].

Table 5.4 Concentrations (mean ± standard deviation, n = 5) measured by SS-ETV-ICPOES with and without sheathing gas or water vapour in Montana soil SRM 2711 using Montana soil SRM 2710 for external calibration and Ar 763.511 nm for internal standardisation.

Analyte	**Certified (indicative) ± confidence limit**	**No sheath**	**H_2 sheath**	**N_2 sheath**	**Water vapour sheath**
Al (%)	6.53 ± 0.09	6.59 ± 0.43	6.17 ± 0.41	6.61 ± 0.42	6.31 ± 0.32
Co (mg kg^{-1})	(10)	10.2 ± 1.2	10.7 ± 1.2	9.2 ± 1.1	10.7 ± 1.7
Cr (mg kg^{-1})	(47)	50.4 ± 4.9	43.8 ± 3.0	43.6 ± 8.9	48.0 ± 5.8
Ni (mg kg^{-1})	20.6 ± 1.1	21.2 ± 2.5	20.9 ± 2.1	20.7 ± 2.2	19.2 ± 1.6
P (%)	0.086 ± 0.007	0.091 ± 0.005	0.088 ± 0.009	0.087 ± 0.011	0.092 ± 0.012
V (mg kg^{-1})	81.6 ± 2.9	81.5 ± 6.4	80.4 ± 1.1	81.4 ± 7.2	80 ± 11

To assess matrix effects, Montana soil SRM 2711 was re-analysed using multi-elemental standard solutions for external calibration. The results are summarised in Table 5.5. Except for P, all the results obtained with H_2 or N_2 sheath are in good agreement with the certified values according to a Student's t test at the 95% confidence level. In contrast, most of the results without sheath do not agree with the certified or information values. This demonstrates that matrix effects could be mitigated using a H_2 or N_2 sheath. The water vapour sheath was not as effective at alleviating matrix effects. To further verify the accuracy and applicability of SS-ETV-ICPOES, coal fly ash SRM 1633c was analysed using urban particulate matter SRM 1648a for external calibration and Ar 763.511 nm

emission line for internal calibration. The results in Table 5.6 are in good agreement with the certified values.

Table 5.5 Concentrations (mean ± standard deviation, n = 5) measured by SS-ETV-ICPOES with and without sheathing gas or water vapour in Montana soil SRM 2711 using multi-elemental standard solutions for external calibration and Ar 763.511 nm for internal standardization.

Analyte	**Certified (indicative) ± confidence limit**	**No sheath**	**H_2 sheath**	**N_2 sheath**	**Water vapour sheath**
Al (%)	6.53 ± 0.09	**8.43 ± 0.47***	6.6 ± 0.91	6.01 ± 0.93	7.58 ± 0.96
Co (mg g^{-1})	(10)	**7 ± 1.4**	11.4 ± 1.6	10.4 ± 1.5	**12.8 ± 1.1**
Cr (mg g^{-1})	(47)	44.6 ± 8.2	42 ± 10	44.9 ± 5.9	55.2 ± 7.2
Ni (mg g^{-1})	20.6 ± 1.1	**9.87 ± 2.08**	17.5 ± 3.2	21.2 ± 3.4	18.1 ± 2.5
P (%)	0.086 ± 0.007	**0.143 ± 0.015**	**0.120 ± 0.013**	**0.273 ± 0.039**	**0.198 ± 0.015**
V (mg g^{-1})	81.6 ± 2.9	90 ± 11	75 ± 13	73.3 ± 6.9	**64.5 ± 3.7**

* Boldface values are not in agreement with the certified (or information) values according to a Student's *t* test at the 95% confidence limit.

Table 5.6 Concentrations in mg kg^{-1} (mean ± standard deviation, n = 5) measured by SS-ETV-ICPOES with and without sheathing gas or water vapour in coal fly ash SRM 1633c using urban particulate matter SRM 1648a for external calibration and Ar 763.511 nm for internal standardization.

Analyte	**Certified ± confidence limit**	**No sheath**	**H_2 sheath**	**N_2 sheath**	**Water vapour sheath**
Co	42.9 ± 3.5	48.7 ± 6.5	43.2 ± 5.0	39.9 ± 6.5	38.5 ± 5.5
Cr	258 ± 6	223 ± 48	267 ± 42	267 ± 34	276 ± 44
Cu	173.7 ± 6.4	186 ± 18	185 ± 13	174 ± 15	164 ± 16
Ni	132 ± 10	128 ± 18	131 ± 15	135 ± 23	129 ± 16
V	286.2 ± 7.9	282 ± 46	264 ± 32	275 ± 82	268 ± 39

5.4 Conclusions

Addition a small amount of H_2, N_2 or water vapour as a sheath around the aerosol in the central gas flow remarkably improves the analytical performance of SS-ETV-ICPOES. The greatest improvement in sensitivity and detection limit (by 1.2–13 fold, depending on the element) was obtained with N_2. The use of a sheathing gas or water vapour enabled the accurate multi- elemental analysis of a soil sample using a simple external calibration with increasing amounts of a soil SRM and an Ar emission line as internal standard. The substantial alleviation of matrix effects with a H_2 or N_2 sheath even enabled the accurate determination of several elements in a soil SRM using external calibration with standard solutions. Given that up to 13 mg of soil sample could be introduced in the plasma without overloading it while simultaneously introducing water vapour [29], future work will check if an even greater amount of sample can be introduced with a N_2 or H_2 sheath, as this would further improve the detection limit. Future work will also include studying the effect of adding H_2 or N_2 to the main plasma gas flow of the ICP on the analytical performance of SS-ETV-ICPOES.

5.5 References

[1] A. Limbeck, M. Bonta and W. Nischkauer, Improvements in the direct analysis of advanced materials using ICP-based measurement techniques, *J. Anal. At. Spectrom*., 32, **2017**, 212-232.

[2] G. L. Donati, R. S. Amais and C. B. Williams, Recent advances in inductively coupled plasma optical emission spectrometry, *J. Anal. At. Spectrom*., 32, **2017**, 1283-1296.

[3] B. Hu, S. Li, G. Xiang, M. He and Z. Jiang, Recent progress in electrothermal vaporization-inductively coupled plasma atomic emission spectrometry and inductively coupled plasma mass spectrometry, *Appl. Spectrosc. Rev.*, 42, **2007**, 203-234.

[4] A. Detcheva, P. Barth and J. Hassler, Application of an ETV-ICP system for the determination of elements in human hair, *Spectrochim. Acta, Part B*, 51, **1996**, 261-270.

[5] F. Plantikow-VoBgatter and E. Denkhaus, Calibration possibilities and modifier use in ETV ICP OES determination of trace and minor elements in plant materials, *Anal. Bioanal. Chem.*, 394, **2009**, 1485-1495.

[6] C. M. M. Santos, M. A. G. Nunes, A. B. Costa, D. Pozebon, F. A. Duarte and V. L. Dressler, Multielement determination in medicinal plants using electrothermal vaporization coupled to ICP OES, *Anal. Methods*, 9, **2017**, 3497-3504.

[7] N. Sadiq and D. Beauchemin, Optimization of the operating conditions of solid sampling electrothermal vaporization coupled to inductively coupled plasma optical emission spectrometry for the sensitive direct analysis of powdered rice, *Anal. Chim. Acta*, 851, **2014**, 23–29.

[8] W. Schron, A. Liebmann and G. Nimmerfall, Direct solid sample analysis of sediments, soils, rocks and advanced ceramics by ETV-ICP-AES and GF-AAS, *Fresenius J. Anal. Chem.*, 366, **2000**, 79-88.

[9] F. Kaveh, C. J. Oates and D. Beauchemin, Direct analysis of soils by ETV-ICP-AES: a powerful tool for mineral exploration, *Geochem.: Explor., Environ., Anal*, 14, **2014**, 305-313.

[10] U. Schaffer and V. Krivan, Multielement analysis of graphite and silicon carbide by inductively coupled plasma atomic emission spectrometry using solid sampling and electrothermal vaporization, *Anal. Chem.*, 71, **1999**, 849-854.

[11] J. Hassler, P. Barth, S. Richter and R. Matschat, Determination of trace elements in high-purity copper by ETV-ICPOES using halocarbons as chemical modifiers, *J. Anal. At. Spectrom*., 26, **2011**, 2404-2418.

[12] A. Asfaw, G. Wibetoe and D. Beauchemin, Solid sampling electrothermal vaporization inductively coupled plasma optical emission spectrometry for discrimination of automotive paint samples in forensic analysis, *J. Anal. At. Spectrom*., 27, **2012**, 1928-1934.

[13] L. Hung and D. Beauchemin, Forensic analysis of automotive paint chips for the identification of the vehicle manufacturer, colour and year of production using electrothermal vaporization coupled to inductively coupled plasma optical emission spectrometry, *J. Anal. At. Spectrom*., 32, **2017**, 1601-1607.

[14] S. Maestre and M. T. C. de Loos-Vollebregt, Plasma behavior during electrothermal vaporization sample introduction in inductively coupled plasma atomic emission spectrometry, *Spectrochim. Acta, Part B*, 56, **2001**, 1209-1217.

[15] R. E. Sturgeon and J. W. Lam, The ETV as a thermochemical reactor for ICP-MS sample introduction, *J. Anal. At. Spectrom*., 14, **1999**, 785-791.

[16] M. Resano, F. Vanhaecke and M. T. C. de Loos-Vollebregt, Electrothermal vaporization for sample introduction in atomic absorption, atomic emission and plasma mass spectrometry – a critical review with focus on solid sampling and slurry analysis, *J. Anal. At. Spectrom*., 23, **2008**, 1450-1475.

[17] W. J. Balsanek, G. Ertas and J. A. Holcombe, The use of concomitant elements to evaluate an Ar-N_2 mixed-gas plasma by electrothermal vaporization inductively coupled plasma orthogonal time-of-flight mass spectrometry, *Spectrochim. Acta, Part B*, 61, **2006**, 732-742.

[18] J. P. Matousek and J. M. Mermet, The effect of added hydrogen in electrothermal vaporization inductively coupled plasma atomic emission spectrometry, *Spectrochim. Acta, Part B*, 48, **1993**, 835-850.

[19] A. Montaser, R. L. Van Hoven and R. M. Barnes, Mixed-gas, molecular-gas, and helium inductively coupled plasma for analytical atomic spectrometry: a critical review, *Crit. Rev. Anal. Chem.*, 18, **1987**, 45-103.

[20] E. H. Choot and G. Horlick, Evaluation of the analytical performance of mixed gas inductively coupled plasmas, *Spectrochim. Acta, Part B*, 41, **1986**, 925-934.

[21] E. H. Choot and G. Horlick, Spatially resolved electron density measurements in Ar, N_2-Ar and O_2-Ar ICPs using a photodiode array detection, *Spectrochim. Acta, Part B*, 41, **1986**, 935-945.

[22] I. Ishii, D. W. Golightly and A. Montaser, Radial excitation temperatures in argon-nitrogen inductively coupled plasmas, *J. Anal. At. Spectrom.*, 3, **1988**, 965-968.

[23] A. Montaser , I. Ishii, B. A. Palmer and L. R. Layman, Line widths and temperatures of Ar-N_2 ICP discharges measured by high-resolution Fourier transform spectrometry, *Spectrochim. Acta, Part B*, 45, **1990**, 603-612.

[24] C. Agatemor and D. Beauchemin, Towards the reduction of matrix effects in inductively coupled plasma mass spectrometry without compromising detection limits: the use of argon-nitrogen mixed-gas plasma, *Spectrochim. Acta, Part B*, 66, **2011**, 1-11.

[25] G. L. Scheffler and D. Pozebon, Advantages and effects of nitrogen doping into the central channel of plasma in axially viewed-inductively coupled plasma optical emission spectrometry, *Anal. Chim. Acta,* 789, **2013**, 33-40.

[26] G. L. Scheffler and D. Pozebon, Straightforward way to enhance robustness in ultrasonic nebulization-axial view inductively coupled plasma optical emission spectrometry via an additional N_2 gas stream, *Spectrochim. Acta, Part B,* 113, **2015**, 84-92.

[27] Z. Hu, S. Gao, Y. Liu, S. Hu, H. Chen and H. Yuan, Signal enhancement in laser ablation ICP-MS by addition of nitrogen in the central channel gas, *J. Anal. At. Spectrom*., 23, **2008**, 1093-1101.

[28] N. Shibata, N. Fudagawa and M. Kubota, Effects of hydrogen mixed with argon carrier gas in electrothermal vaporization-inductively coupled plasma-mass spectrometry, *Spectrochim. Acta, Part B,* 47, **1992**, 505-516.

[29] F. Kaveh and D. Beauchemin, Improvement of the capabilities of solid sampling ETV-ICP-OES by coupling ETV to a nebulization/pre-evaporation system, *J. Anal. At. Spectrom*., 29, **2014**, 1371-1377.

[30] N. Sadiq, L. Huang, F. Kaveh and D. Beauchemin, Solid sampling ETV-ICPOES coupled to a nebulization/pre-evaporation system for direct elemental analysis of glutinous rice by external calibration with standard solutions, *Food Chem*., 237, **2017**, 1-6.

[31] A. S. Masquelin, F. Kaveh, A. Asfaw, C. J. Oates and D. Beauchemin, Solid sampling ETV-ICP-OES to study the distribution of elements in clay and soil samples for mineral exploration, *Geochem.: Explor., Environ., Anal,* 13, **2013**, 11-20.

[32] L. Duester, D. Rakcheev, J. V. Bayer, P. M. Abraham, A. Dabrunz, R. Schulz and G. E. Schaumann, A robust, particle size independent, method for quantifying metal(loid oxide) nanoparticles and their agglomerates in complex environmental matrices by electrothermal vaporization coupled to ICP-MS, *J. Anal. At. Spectrom*., 26, **2011**, 450-455.

[33] J. Hassler, R. Matschat, S. Richter, P. Barth, A. K. Detcheva and H.-J. Waarlo, Determination of 22 trace elements in high-purity copper including Se and Te by ETV-ICPOES using SF_6, NF_3, CF_4 and H_2 as chemical modifiers, *J. Anal. At. Spectrom*., 31, **2016**, 642-657.

[34] A. Kramida, Y. Ralchenko and J. Reader, NIST Atomic Spectra Database, *ver. 5.5.6, http://physics.nist.gov/asd*.

[35] H. Louie and S. Y.-P. Soo, Use of nitrogen and hydrogen in inductively coupled plasma mass spectrometry, *J. Anal. At. Spectrom*., 7, **1992**, 557-564.

[36] G. L. Scheffler and D. Pozebon, Effect of N_2 on the emission profile and excitation temperature in axially viewed plasma-ICP OES, *J. Anal. At. Spectrom.*, 30, **2015**, 468-478.

[37] I. Novotny, J. C. Farinas, W. Jia-Liang, E. Poussel and J. M. Mermet, Effect of power and carrier gas flow rate on the tolerance to water loading in inductively coupled plasma atomic emission spectrometry, *Spectrochim. Acta, Part B*, 51, **1996**, 1517-1526.

[38] S. E. Long and R. F. Browner, Influence of water on conditions in the inductively coupled plasma, *Spectrochim. Acta, Part B*, 43, **1988**, 1461-1471.

[39] I. B. Brenner and A. T. Zander, Axially and radially viewed inductively coupled plasmas – a critical review, *Spectrochim. Acta, Part B*, 55, **2000**, 1195-1240.

[40] I. B. Brenner, A. Zander, M. Cole and A. Wiseman, Comparison of axially and radially viewed inductively coupled plasmas for multi-element analysis: effect of sodium and calcium, *J. Anal. At. Spectrom*., 12, **1997**, 897-906.

[41] H. P. Longerich, Effect of nitric acid, acetic acid and ethanol on inductively coupled plasma mass spectrometry ion signals as a function of nebuliser gas flow, with implications on matrix suppression and enhancements, *J. Anal. At. Spectrom*., 4, **1989**, 665-667.

[42] A. Fernandez, M. Murillo, N. Carrion and J. M. Mermet, Influence of operating conditions on the effects of acids in inductively coupled plasma atomic emission spectrometry, *J. Anal. At. Spectrom*., 9, **1994**, 217-221.

[43] J. L. Todoli and J. M. Mermet, Minimization of acid effects at low consumption rates in an axially viewed inductively coupled plasma atomic emission spectrometer by using micronebulizer-based sample introduction systems, *J. Anal. At. Spectrom*., 13, **1998**, 727-734.

[44] E. Paredes, M. Grotti, J. M. Mermet and J. L. Todoli, Heated-spray chamber-based low sample consumption system for inductively coupled plasma spectrometry, *J. Anal. At. Spectrom*., 24, **2009**, 903-910.

[45] P. Masson, Direct phosphorus determination on solid plant samples by electothermal vaporization-inductively coupled plasma atomic emission spectrometry, *J. Anal. At. Spectrom*., 26, **2011**, 1290-1293.

Chapter 6

Summary and Future Work

6.1 Summary of chapters and general conclusions

This thesis has explored and assessed a number of new and improved methods for enhancing the analytical performance of ICPOES with pneumatic nebulization or electrothermal vaporization.

In Chapter 2, a new IR-heated MC spray chamber system combined with a Burgener nebulizer was established for ICPOES. A cyclonic spray chamber was modified to allow the insertion of an IR lamp heater at its center for more effective heating. Two versions of the MC(IR) were used, with a regular 12mm/5mm female joint (MC12/5(IR)) and a 28mm/15mm female joint connected to a PET (MC28/15(IR)PET). To find operating conditions for ICPOES, multivariate optimizations were carried out by monitoring analyte sensitivity and plasma robustness. Upon IR heating (up to 150 °C) and under optimized conditions, a 2-5 fold improvement in sensitivity and 2-7 fold improvement in detection limit were obtained for 26 elements using MC12/5(IR) and MC28/15(IR)PET. This was ascribed to an increase in sample transport efficiency and to the conversion of the sample aerosol into vapour. The most compact system (*i.e.* MC12/5(IR)) would be a good alternative to the conventional pneumatic nebulization for ICPOES because of its simplicity and the increased sample throughput that it enables. This was proved through the accurate multi-elemental analysis of certified reference materials of drinking water and soil digest using a simple external calibration without internal standardization or matrix-matching.

In Chapter 3, a ceramic beaded IR rope heater was evaluated for improving analytical performance of ICPOES. Two spray chambers (Scott double-pass and baffled cyclonic spray chambers) were entirely heated up to 200 °C by the rope heaters. The results of sensitivity, detection limit and plasma robustness were compared with IR-heated spray chambers using ceramic IR block heaters. Under compromise optimum conditions, the greatest improvement in sensitivity was obtained with the double-pass spray chamber and IR rope heater, whereas the highest improvement in detection limit was achieved with the same spray chamber and the IR block heaters. This stems from the solely IR heating which is provided by the block heater resulting in more uniform heating than a combination of convective and IR heating, which is offered by the IR rope heater. For a given spray chamber, the improvement in detection limit was significantly higher than that in sensitivity with the IR block heater. On average, an order of magnitude improvement in detection limit was attained with a double-pass spray chamber and the IR block heaters, without degradation in precision.

In Chapter 4, the effect of IR heating the top surface of a cyclonic spray chamber on analytical figures of merit of ICPOES was investigated. The ceramic IR rope heater was utilized to heat the top area of a quartz baffled cyclonic spray chamber, side arm of the spray chamber, elbow connection to the torch and base of the torch up to 150 °C. Under optimum operating conditions, which were selected using multivariate optimizations for 21 elements, and upon IR heating, sensitivity and detection limit were improved by 3-12 fold compared to those with the same pneumatic nebulization system at room temperature. This was attributed to a significant enhancement in transport efficiency (3 fold upon IR heating compared to the same system at room temperature) and reduction in noise (due to

converting the sample aerosol into vapour). The plasma robustness was enhanced as well, which simplified calibration for accurate multi-elemental analysis of waters without the need for internal standardization or matrix-matching.

In general, Chapters 2, 3 and 4 focused on using different sorts of IR-heated systems for improving the transport efficiency of the pneumatic nebulization system, which typically wastes 95% of sample solutions and is thus the Achilles' heel of ICP spectrometry. Pre-evaporation of the sample aerosol using IR heating is a simple approach to significantly enhance transport efficiency of the conventional pneumatic nebulization and concurrently improve sensitivity, detection limit and plasma robustness of ICPOES. Preserving water vapour plays an important role in decreasing matrix effects because it acts as a load buffer in the plasma. Moreover, water vapour facilitates energy transfer between the plasma bulk and its central channel because water is a main source of hydrogen. Thus, the IR-heated pneumatic nebulization system can be a valuable sample introduction system for ICPOES to perform accurate multi-elemental analysis. Table 6.1 summarizes the features and limitations of the different IR-heated spray chambers that were described in this work. The most compact design is the MC12/5(IR). However, the best improvement in detection limit was achieved with the DP (IR block) setup. One apparent outlier is the BC with bent outlet and IR rope heater, where the improvement in detection limit is higher than that obtained with a BC with straight outlet and IR block heater and almost as large as that with the DP with IR block heater. This stems from the fact that a quartz spray chamber was used in this case, whereas glass spray chambers were used in all other cases. Quartz is more transparent to IR radiation than glass.

Table 6.1 Summary of the features and limitations of different IR-heated spray chamber systems presented in Chapter 2, 3 and 4 with selected operating conditions.

Spray chamber	Operating conditions	Average sensitivity improvement	Average detection limit improvement	Average %RSD	Limitations
MC12/5 (IR) straight outlet	• Burgener nebulizer • 1 mL min^{-1} sample uptake rate • 150 °C	2.6 ± 0.5 n = 26	3.6 ± 1.2 n = 26	0.8 ± 0.2 n = 26	Using two different types of IR heaters
MC28/15 (IR)PET straight outlet	• Burgener nebulizer • 1 mL min^{-1} sample uptake rate • 150 °C	3.5 ± 0.7 n = 26	3.2 ± 1.6 n = 26	0.9 ± 0.5 n = 26	Cumbersome due to PET
BC (IR rope) straight outlet	• SeaSpray nebulizer • 0.12 mL min^{-1} sample uptake rate • 200 °C	3.1 ± 0.7 n = 32	3.1 ± 1.6 n = 32	2.6 ± 0.7 n = 32	Cumbersome due to sheathing device
BC (IR block) straight outlet	• SeaSpray nebulizer • 0.3 mL min^{-1} sample uptake rate • 200 °C	2.5 ± 0.7 n = 32	4.5 ± 1.9 n = 32	2.3 ± 0.3 n = 32	Cumbersome due to sheathing device and bulky IR heater
DP (IR rope) straight outlet	• SeaSpray nebulizer • 0.1 mL min^{-1} sample uptake rate • 110 °C	4.9 ± 1.1 n = 32	2.4 ± 1.3 n = 32	2.2 ± 0.5 n = 32	Cumbersome due to sheathing device
DP (IR block) straight outlet	• SeaSpray nebulizer • 0.2 mL min^{-1} sample uptake rate • 200 °C	3.4 ± 1.5 n = 32	10.2 ± 5.3 n = 32	1.3 ± 0.4 n = 32	Cumbersome due to sheathing device and bulky IR heater
BC (IR rope) bent outlet	• PFA nebulizer • 0.9 mL min^{-1} sample uptake rate • 150 °C	3.7 ± 0.6 n = 26	7.6 ± 2.6 n = 26	2.7 ± 0.4 n = 26	Cumbersome due to elbow connection

Chapter 5 compared the effect of addition a small amount of H_2, N_2 or water vapour to the central channel of the plasma on the analytical performance of SS-ETV-ICPOES. A sheathing device was used to introduce H_2, N_2 or water vapour around the sample aerosol. The water vapour was generated by pre-evaporation of water aerosol exiting the spray

chamber of a pneumatic nebulization system using IR heating of the sheathing device and the base of the torch to 400 °C. Upon sheathing the sample aerosol with H_2, N_2 or water vapour, sensitivity and detection limit were significantly improved for 11 elements compared to those with conventional SS-ETV-ICPOES. The N_2 sheath setup showed the greatest improvement in sensitivity (improved 1.2-4 fold) and detection limit (improved 2-13 fold). Improving plasma excitation characteristics with H_2, N_2 or water vapour enabled an accurate multi-elemental analysis of a standard reference material (SRM) of soil using external calibration with another soil SRM and internal standardization with Ar 763.511 nm emission line to compensate for sample loading effects on plasma. However, an attempt to use standard solutions as external calibration revealed that matrix effects were not completely mitigated with the water vapour sheath, whereas substantial mitigation of matrix effects was achieved with the H_2 or N_2 sheath. To the best of the author's knowledge, Chapter 5 is the first published study of the effect of adding a small amount of N_2 to the central channel of the ICP on the analytical performance of SS-ETV-ICPOES.

This thesis further demonstrated that promoting pre-evaporation is a simple and powerful way to improve the analytical performance of ICPOES with PN or ETV. The introduction of water vapour in the plasma substantially increases robustness, as demonstrated with the developed IR-heated PN (Chapters 2, 3 and 4) and SS-ETV (Chapter 5) systems. This allows the accurate multi-elemental analysis of samples with different matrices, such as water samples and soil digests, by external calibration without matrix-matching or internal standardization using the developed IR-heated PN systems. In the case of SS-ETV, because most of the sample is introduced into the plasma, internal standardization with an Ar emission line is required to compensate for sample loading

effects on the plasma. External calibration with increasing amounts of SRM allows the accurate multi-elemental analysis of soil, urban particulate matter and coal fly ash samples using the developed SS-ETV system. However, using a N_2 sheath may enable the analysis of solid samples using standard solutions for external calibration, as accurate results were obtained for several elements in soil, which is inherently inhomogeneous. The developed systems should be applicable to multi-elemental analysis of variety of samples with different matrices, such as environmental, geological, biological and clinical samples.

Additionally, the developed systems overcome some drawbacks of the current commercially-available systems (Table 6.2). For example, the transport efficiency is significantly improved for the developed IR-heated PN systems compared with the conventional PN at room temperature. In fact, the improvement in detection limit achieved in this work with IR heating of conventional sample introduction systems is comparable to that obtained with an ultrasonic nebulizer equipped with a desolvation system without any of the drawbacks of the latter (in particular, the loss of B and Hg in the desolvation system, important memory effects, and restriction to samples that are compatible with the membrane covering the piezoelectric crystal).

Moreover, pre-evaporation enhances sample throughput because IR heating reduces the washout time. Table 6.3 summarizes the washout times measured with the different IR-heated spray chamber systems used in this work. Of course, the washout time increased with a decrease in sample uptake rate. However, the increase was less than expected. For example, when the sample uptake was reduced from 1 mL min^{-1} for DP (RT) to 0.1 mL min^{-1} for DP (IR rope), the washout time with DP (IR rope) should have been 10 times that

Table 6.2 Sample introduction systems for ICPOES with their applications, features and limitations.

Sample introduction system	Sample type	Analytes	Features	Limitations
MC12/5(IR) Straight outlet [Chapter 2]	Drinking water and soil	26 elements	• 0.1-130 µg L^{-1} detection limit • 1 mL min^{-1} sample uptake	• Using two different types of IR heaters
DP(IR block) straight outlet [Chapter 3]	Waste water	29 elements	• 0.02-12 µg L^{-1} detection limit • 0.2 mL min^{-1} sample uptake	• Cumbersome due to sheathing device and bulky IR heater
BC(IR rope) bent outlet [Chapter 4]	Drinking and waste water	21 elements	• 0.08-70 µg L^{-1} detection limit • 0.9 mL min^{-1} sample uptake	• Cumbersome due to elbow connection
SS-ETV (N_2 sheath) [Chapter 5]	Urban particulate matter, soil and coal fly ash	Al, Cd, Co, Cr, Cu, Mn, Mo, Ni, P, V, Zn	• Low sample consumption (3 mg) • Minimum sample preparation • 0.007-2 mg kg^{-1} detection limit	• Low precision (%RSD = 6-21)
PN [1]	Sea water	Cd, Co, Cr, Cu, Fe, Mn, Ni, Pb, V, Zn	• 2-84 µg L^{-1} detection limit • 1.8 mL min^{-1} sample uptake	• Low transport efficiency (<5%) • Standard additions calibration
USN [1]	Sea water	Cd, Co, Cr, Cu, Fe, Mn, Ni, Pb, V, Zn	• 1-20 µg L^{-1} detection limit • 2.8 mL min^{-1} sample uptake	• Some elements (Hg, B) may get lost through desolvation • Standard additions calibration • Expensive
PN with desolvation system [2]	Orchard and tomato leaves	Ba, Cd, Co, Cr, Cu, Mn, Ni, Pb, Sr, V, Zn	• 0.02-4 µg L^{-1} detection limit • 0.65 mL min^{-1} sample uptake	• Some elements (Hg, B) may get lost through desolvation • Internal standard calibration
Direct injection nebulization [3]	Shale oil, solvent refined coal and crude oil	As, Cd, Co, Cr, Cu, Ni, S, Se, Zn	• 1-100 µg L^{-1} detection limit • Total sample consumption • 0.12 mL min^{-1} sample uptake	• Clogging issue with high salt content • Fragile
SS-ETV [4]	Sediments, soils, rocks and advanced ceramics	Cd, Cr, Cu, Ni, Pb, Zn	• Low sample consumption (3 mg) • Minimum sample preparation • 0.7-6 mg kg^{-1} detection limit	• Low precision (%RSD = 5-8) • Matrix-matched calibration

with DP (RT), i.e. 160 s, but it was 49 s, i.e. three times shorter than expected. Hence, pre-evaporation with IR heating would reduce the washout time and thus enhance the sample throughput compared to that without pre-evaporation at the same sample uptake rate. Furthermore, one might expect the washout time to increase with an increase in sample transport efficiency. Yet, when the sample transport efficiency increased from 4.5% to 15.7% upon IR rope heating of part of a BC with bent outlet, the washout time was only slightly higher than that for BC (RT) with bent outlet instead of about 3 times the latter (Table 6.3). This further demonstrates the efficiency of pre-evaporation at reducing the washout time and concurrently enhancing the sample throughput.

Table 6.3 Washout time with sample uptake rate for different IR-heated spray chamber systems and their reference systems presented in Chapter 3 and 4.

Spray chamber	Sample uptake rate (mL min^{-1})	Washout time (s)
DP (RT) straight outlet	1.00	16 ± 3 (n = 32)
DP (IR rope) straight outlet	0.10	49 ± 10 (n = 32)
DP (IR block) straight outlet	0.20	45 ± 5 (n = 32)
BC (RT) straight outlet	1.00	13 ± 5 (n = 32)
BC (IR rope) straight outlet	0.12	41 ± 11 (n = 32)
BC (IR block) straight outlet	0.30	33 ± 11 (n = 32)
BC (RT) bent outlet	0.90	17 ± 4 (n = 14)
BC (IR rope) bent outlet	0.90	21 ± 5 (n = 14)

6.2 Future work

Although numerous research works have been devoted to the sample introduction system, it is still referred to as the weakest part in ICP spectrometry [5, 6]. This is essentially because, with PN, typically more than 95% of the sample goes to the drain, thereby affecting sensitivity and detection limit. The pre-evaporation technique used in the

Beauchemin lab [7, 8] and Todoli's lab [9, 10] can significantly improve the analytical performance of ICPOES. So far, the results from the previous works and the current work are promising. Therefore, future work will chiefly be focused on designing a simple low-cost IR-heated integrated sample introduction system for ICP spectrometry that can be commercialized for routine multi-elemental analysis, while providing more accurate and precise results at lower detection limit. The system will be more compact so as to fit easily in the torch box of different instruments. The system should significantly improve the sample transport efficiency (up to 100%), leading to enhancement in sensitivity, detection limit and plasma robustness. To this end, the IR-heated MC spray chamber system described in Chapter 2 will be re-designed to create a more compact system heated with only the IR lamp heater without using the ceramic IR rope heater by trimming the base of the torch and shrinking the neck of the modified cyclonic spray chamber, which will be entirely made of quartz. However, the resulting shortened sample aerosol path may not be long enough to enable complete pre-evaporation of the aerosol before its introduction into the plasma. To achieve total consumption of the sample (*i.e.* 100% transport efficiency), the new system will be optimized at low sample uptake rate (<0.1 mL min^{-1}). This would provide a greener approach in which no sample waste would be produced, thereby reducing or eliminating hazardous waste, such as corrosive and toxic materials. The new system will also be optimized and tested to improve the analytical performance of ICPMS. It will also be optimized at 1 mL min^{-1} to provide a high sample throughput enhanced system.

The new IR-heated system will also be coupled with flow injection (FI) to analyze samples with complex matrices, such as samples with high salt content and samples not compatible with the conventional liquid sample introduction systems (usually made of

glass), such as basic samples. The FI has several features, for example small sample consumption, high sample throughout and ease of automation [11]. The air-segmented FI technique, where the sample is injected into air bubbles in a continuous water carrier stream [12, 13], will be modified and optimized as well. To facilitate reproducible injection into air bubbles, instead of using an air-segmented carrier flow, each injection will be made within an air sandwich using a sandwich injection manifold [14]. Injection into air significantly reduces the dispersion of the sample (associated with the regular FI) along the flow path, which would further increase the sample throughput (as more injections can be done during the same time) while improving the sample introduction efficiency [12-13].

On the other hand, addition of N_2 to the outer gas flow of the plasma significantly improved plasma robustness of ETV-ICPMS [15]. Therefore, future work will also involve improving the analytical performance of SS-ETV-ICPOES by simultaneously adding N_2 into both the outer and central gas flows of the plasma. Moreover, increasing the sample mass up to 13 mg without extinction of the plasma was achieved by adding water vapour at 400 °C into the central channel of the plasma [16]. Thus, the future work will examine if the sample mass could be increased, while adding N_2 or H_2 into the central channel of the plasma, as this would further improve the detection limit and precision of SS-ETV-ICPOES.

6.3 References

[1] S. S. Berman, J. W. McLaren and S. N. Willie, Simultaneous determination of five trace metals in seawater by inductively coupled plasma atomic emission spectrometry with ultrasonic nebulization, *Anal. Chem*., 52, **1980**, 488-492.

[2] G. L. Scheffler and D. Pozebon, Internal standardization in axially viewed inductively coupled plasma optical emission spectrometry (ICP OES) combined with pneumatic nebulization and aerosol desolvation, Anal. Methods, 5, **2013**, 4371-4377.

[3] K. E. LaFreniere, V. A. Fassel and D. E. Eckels, Elemental speciation via high-performance liquid chromatography combined with inductively coupled plasma atomic emission spectroscopic detection: application of a direct injection nebulizer, *Anal. Chem*., 59, **1987**, 879-887.

[4] W. Schron, A. Liebmann and G. Nimmerfall, Direct solid sample analysis of sediments, soils, rocks and advanced ceramics by ETV-ICP-AES and GF-AAS, *Fresenius J. Anal. Chem.*, 366, **2000**, 79-88.

[5] J. L. Todoli and J. M. Mermet, Liquid sample introduction in ICP spectrometry: a practical guide. Elsevier: Oxford, **2008**.

[6] N. H. Bings, J. O. Orlandini von Niessen and J. N. Schaper, liquid sample introduction in inductively coupled plasma atomic emission and mass spectrometry – critical review, *Spectrochim. Acta B.*, 100, **2014**, 14-37.

[7] A. Asfaw, W.R. MacFarlane and D. Beauchemin, Ultrasonic nebulization with an infrared heated pre-evaporation tube for sample introduction in ICP-OES: application to geological and environmental samples, *J. Anal. At. Spectrom*. 27, **2012**, 1254-1263.

[8] Y. Makonnen, J. Burgener and D. Beauchemin, Improvement of analytical performance in inductively coupled plasma optical emission spectrometry without compromising robustness using an infrared-heated sample introduction system with a pneumatic nebulizer, *J. Anal. At. Spectrom.*, 30, **2015**, 214-224.

[9] E. Paredes, M. Grotti, J.M. Mermet and J.L. Todoli, Heated-spray chamber-based low sample consumption system for inductively coupled plasma spectrometry, *J. Anal. At. Spectrom*., 24, **2009**, 903-910.

[10] R. Sanchez, J.L. Todoli, C.P. Lienemann and J.M. Mermet, Minimization of the effect of silicon chemical form in xylene matrices on ICP-AES performance, *J. Anal. At. Spectrom*.,24, **2009**, 1382-1388.

[11] D. Beauchemin, Preliminary characterization of inductively coupled plasma mass spectrometry with flow injection into a gaseous (air) carrier, *Anal. Chem*., 118, **1993**. 815-819.

[12] J. M. Craig and D. Beauchemin, Characterization of inductively coupled plasma mass spectrometry with segmented-flow injection, *Anal*yst, 119, **1994**. 1677-1682.

[13] Y. Hsieh and S. R. Crouch, Air-segmented flow injection: a hybrid technique for automated, low dispersion determinations, *Anal. Chim. Acta*, 303, **1995**, 231-239.

[14] R. P. Lamsal, G. Jerkiewicz and D. Beauchemin, Enhancement of the capabilities of inductively coupled plasma mass spectrometry using monosegmented flow analysis, *Anal. Chem*., 90, **2018**, 13842-13847.

[15] W. J. Balsanek, G. Ertas and J. A. Holcomb, The use of concomitant elements to evaluate an Ar-N_2 mixed-gas plasma by electrothermal vaporization inductively coupled plasma orthogonal time-of-flight mass spectrometry, *Spectrochim. Acta, Part B,* 61, **2006**, 732-742.

[16] F. Kaveh and D. Beauchemin, Improvement of the capabilities of solid sampling ETV-ICP-OES by coupling ETV to a nebulization/pre-evaporation system, *J. Anal. At. Spectrom*., 29, **2014**, 1371-1377.

Appendix

Table A1 Slope and intercept of each SS-ETV-ICPOES calibration curve obtained with increasing amounts of Montana soil SRM 2710, using Ar 763.511 nm for internal standardization, with and without sheathing gas or water vapour.

Aanalyte, nm	No sheath		H_2 sheath		N_2 sheath		Water vapour sheath	
	Slope (μg^{-1})	Intercept	Slope (μg^{-1})	Intercept	Slope (μg^{-1})	Intercept	Slope (μg^{-1})	Intercept
Al II 167.078	0.041 ± 0.003	0.9 ± 0.5	0.10 ± 0.02	2.2 ± 3.6	0.10 ± 0.01	0.9 ± 0.9	0.10 ± 0.01	0.3 ± 2.3
Al I 176.641	0.89 ± 0.03	-8.3 ± 5.6	1.02 ± 0.07	-14 ± 14	2.0 ± 0.1	-42 ± 28	1.87 ± 0.05	-12 ± 10
Cd II 226.502	96 ± 3	-0.1 ± 0.2	164 ± 13	-0.2 ± 0.9	319 ± 20	-1.9 ± 1.3	222 ± 21	-1.5 ± 1.4
Cd I 228.802	242 ± 10	-1.1 ± 0.7	303 ± 34	-2.0 ± 2.3	670 ± 69	-4.4 ± 4.5	607 ± 72	-7.2 ± 5.0
Co II 228.616	59 ± 4	0.03 ± 0.13	102 ± 7	-0.08 ±0.22	186 ± 12	-0.47 ± 0.36	139 ± 7	-0.2 ± 0.2
Cr II 205.618	49 ± 4	-0.3 ± 0.5	78 ± 18	-1.3 ± 2.1	176 ± 14	-2.9 ± 1.6	80 ± 11	0.5 ± 1.3
Cu II 224.700	23.0 ± 0.5	-7.9 ± 4.2	17 ± 4	19 ± 34	28 ± 1	0 ± 11	27 ± 1	-15 ± 9
Mn I 403.076	22 ± 2	-63 ± 44	20 ± 4	-80 ± 110	66 ± 7	-330 ± 210	40 ± 2	-71 ± 50
Mo II 202.095	100 ± 11	-0.8 ± 0.6	140 ± 53	-1.4 ± 3.1	411 ± 38	-3.8 ± 2.2	137 ± 47	0.5 ± 2.8
Ni II 174.828	28 ± 3	-0.2 ± 0.1	40 ± 13	-0.4 ± 0.5	102 ± 11	-0.8 ± 0.5	58 ± 8	-0.07 ± 0.37
P I 178.287	10 ± 1	-3.9 ± 3.3	13 ± 1	-5.4 ± 4.7	25 ± 3	-16 ± 10	18 ± 2	-8.5 ± 6.8
V II 292.402	16 ± 4	1.0 ± 0.9	28 ± 8	0.8 ± 1.9	39 ± 5	0.5 ± 1.1	47 ± 5	-0.2 ± 1.3
Zn II 206.200	15 ± 1	4 ± 22	14 ± 1	0.4 ± 22.5	47 ± 5	-150 ± 100	26 ± 4	28 ± 80

Table A2 Detection limits (3σ, n = 10) in mg kg^{-1} by SS-ETV-ICPOES based on 3-mg sample aliquots.

Analyte, nm	No sheath	H_2 sheath	N_2 sheath	Water vapour sheath
Al II 167.078	200	40	60	40
Al I 176.641	5	10	2	3
Cd II 226.502	0.07	0.02	0.007	0.02
Cd I 228.802	0.03	0.01	0.01	0.01
Co II 228.616	0.1	0.06	0.03	0.04
Cr II 205.618	0.4	0.1	0.03	0.06
Cu II 224.700	0.4	0.4	0.2	0.2
Mn I 403.076	0.4	0.3	0.09	0.1
Mo II 202.095	0.05	0.04	0.01	0.02
Ni II 174.828	0.2	0.2	0.05	0.1
P I 178.287	0.5	0.4	0.1	0.2
V II 292.402	0.4	0.2	0.1	0.08
Zn II 206.200	0.5	0.3	0.1	0.2

Table A3 Average background emission signals in counts per second (± standard deviation, n = 10) for SS-ETV- ICPOES with and without sheathing gas or water vapour.

Analyte, nm	No sheath	H_2 sheath	N_2 sheath	Water vapour sheath
Al II 167.078	830 ± 270	1710 ± 110	840 ± 160	660 ± 110
Al I 176.641	1380 ± 140	4493 ± 340	2140 ± 130	740 ± 150
Cd II 226.502	4440 ± 180	13600 ± 110	6187 ± 64	2880 ± 120
Cd I 228.802	7300 ± 170	21590 ± 120	9890 ± 190	4610 ± 190
Co II 228.616	7600 ± 170	21900 ± 200	10250 ± 190	5070 ± 160
Cr II 205.618	3050 ± 880	5600 ± 210	3090 ± 130	1780 ± 140
Cu II 224.700	3990 ± 240	11430 ± 180	5290 ± 130	3400 ± 170
Mn I 403.076	40000 ± 280	129550 ± 200	52360 ± 180	35620 ± 180
Mo II 202.095	3350 ± 140	7970 ± 190	4410 ± 130	2220 ± 110
Ni II 174.828	3950 ± 170	5800 ± 180	5210 ± 150	2980 ± 190
P I 178.287	2060 ± 160	3900 ± 160	2000 ± 96	870 ± 150
V II 292.402	4910 ± 170	16620 ± 140	6800 ± 140	3800 ± 110
Zn II 206.200	3150 ± 240	9350 ± 140	4420 ± 190	1580 ± 160